THE CUTTING BEHAVIOR OF BANDSAWS

By

BRUCE FREDRIK LEHMANN

B.A.Sc, The University of British Columbia, 1983
M.A.Sc, The University of British Columbia, 1985

A THESIS SUBMITTED AS PARTIAL FULFILLMENT OF

THE REQUIREMENTS FOR THE DEGREE OF

DOCTOR OF PHILOSOPHY

in

THE FACULTY OF GRADUATE STUDIES

Department of Mechanical Engineering

We accept this thesis as conforming
to the required standard

THE UNIVERSITY OF BRITISH COLUMBIA

September 1993

© Bruce Fredrik Lehmann, 1993

In presenting this thesis in partial fulfilment of the requirements for an advanced degree at the University of British Columbia, I agree that the Library shall make it freely available for reference and study. I further agree that permission for extensive copying of this thesis for scholarly purposes may be granted by the head of my department or by his or her representatives. It is understood that copying or publication of this thesis for financial gain shall not be allowed without my written permission.

Department of Mechanical Engineering
The University of British Columbia
Vancouver, Canada

October 7, 1993

The Cutting Behavior of Bandsaws

Bruce F. Lehmann

Abstract

A model of a bandsaw, subjected to lateral cutting forces on the teeth and restrained by the sawn surfaces of the wood, has been developed. The blade model includes the effects of blade dimensions, bandmill strain, in-plane stresses, tooth (gullet) depth, tooth bending stiffness, blade speed, strain system parameters, and the span between the guides. The lateral cutting forces along the length of the cut were found to have dominant low frequency components and are modelled by functions having spectra that are inversely proportional to the frequency.

The results of the model simulation show that when there is little or no contact between the body of the blade and the sawn surfaces, the sawing accuracy is governed by the tooth-tip stiffness and the magnitude of the lateral cutting forces. When the clearance gap is small compared to the blade deflection, the contact forces dominate and poor cutting accuracy results because the blade cannot recover quickly from disturbances. The clearance gap between the blade and a sawn surface is shown to be less than the side clearance of the teeth because of sawdust spillage and surface roughness. A formula is developed that defines how blade stiffness, the clearance gap, and the cutting forces affect sawing deviation. It is found that the tooth-tip stiffness is the blade parameter that most significantly affects cutting accuracy. An example of determining the optimal side clearance and some practical implications of the results are presented.

TABLE OF CONTENTS

ABSTRACT ii

TABLE OF CONTENTS iii

LIST OF FIGURES v

LIST OF TABLES vii

NOMENCLATURE viii

ACKNOWLEDGMENTS xii

1. INTRODUCTION 1

Objectives
Method and Scope
Background and Previous Research

2. INTERACTIONS OCCURRING DURING CUTTING 17

Observations from Cutting Experiments
Equilibrium Deflection of a Bandsaw Blade
Sawmill Conditions
Other Practical Considerations
Concepts and Assumptions

3. MODEL GENERATION AND ANALYSIS PROCEDURES 29

The Model of the Bandsaw Blade
The Contact between the Blade and the Sawn Surfaces
Representation of the Lateral Cutting Forces
Simulation of the Sawing System

4. NUMERICAL RESULTS 49

The Effect of Blade Parameters on Tooth-tip Stiffness
Cutting through a Simulated Knot
Response to Fractal Lateral Cutting Forces
The Contact Graph
The Effect of the Depth of Cut

5. DISCUSSION AND APPLICATIONS 90

Minimization of Fibre Loss
The Practice of Sawing
Complete Data Set

6. CONCLUSIONS 97

Future Work

LIST OF REFERENCES 102

APPENDICES

A Inertial and Gyroscopic Effects on Blade Behavior 105

B Verification of Blade Stiffness and Natural Frequency Calculations 107

C Contact Algorithm 111

D Derivation of the Statistical Representation of the Cutting Forces 120

LIST OF FIGURES

1-1 General Arrangement of a Bandsaw 5

1-2 The Geometry of the Tooth and the Tooth Marks 13

2-1 A Schematic of the Sawing System 18

2-2 Experimental Arrangement for Cutting Tests 21

2-3 Blade Deflection during Cutting 22
a) Displacement at the Front and Back Probes
b) Interpolated Position of the Blade

2-4 Spectrum of the Blade Deflection 24

3-1 Idealized Model of the Blade 30

3-2 In-plane Stresses in a Bandsaw Blade 33

3-3 Free Body Diagram of the Blade and a Tooth 36

3-4 Blade Deflection During Cutting: Example 1 41
a) Displacement at the Front Probe
b) Spectrum of the Displacement at the Front Probe

3-5 Blade Deflection During Cutting: Example 2 42
a) Displacement at the Front Probe
b) Spectrum of the Displacement at the Front Probe

3-6 Locations of the Contact Nodes on the Blade 46

3-7 Locations of Nodes on the Sawn Surfaces 47

4-1 Effect of Blade Parameters on Mid-span Tooth-tip Stiffness 51

4-2 Deflected Shape of the Blade for a Load on the Front Edge of the Blade 54

4-3 Simulated Cutting Forces near a Knot.. 57

4-4 Simulated Cut Path around a 'Knot' 58

4-5 Blade Deflections and Contact Locations for a Simulated Cut 59

4-6 The Deflected Shape of the Blade during a Simulated Cut 61

4-7 Effect of Blade Thickness on the Cut Path 62

4-8 Effect of Bandmill Strain on the Cut Path 63

4-9 Effect of Tensioning on the Cut Path 64

4-10 Effect of Clearance Gap on the Cut Path 66

4-11 Effect of Blade Parameters on Cutting Deviation 67

4-12 Blade Deflections and Contact Locations for a Simulated Cut
a) Example 1 69
b) Example 2 70
c) Example 3 71

4-13 Effect of Clearance Gap on Cutting Deviation 72

4-14 Probability Curve for Contact 76

4-15 Contact Graph.. 78

4-16 Normalized Cross-Section of Blade Deflection 80
a) Effect of Tensioning
b) Effect of Thickness
c) Effect of Bandmill Strain
d) Effect of Blade Width

4-17 The Deflected Shape of the Blade during a Simulated Cut 82

4-18 Progression of Contact 83

4-19 Effect of Load Variation Through the Depth of Cut 85

4-20 Effect of Depth of Cut on the Equivalent Stiffnesses 87

4-21 Effect of Depth of Cut on the Contact Graph.. 89

5-1 Effect of Side Clearance on Total Fibre Loss 92

B-1 Analytical and Experimental Blade Stiffness 109

B-2 Analytical and Experimental Normalized Blade Deflection 110

C-1 Geometry of the Constraining Surfaces 115

C-2 Geometry of the Interpolation for the Contact Algorithm 117

LIST OF TABLES

1-I Typical Cutting Forces 11

2-I Conditions for Experimental Cutting Tests 20

4-I Parameters for the Blade Model 52

A-I Inertial, Gyroscopic and Stiffness Terms 106

NOMENCLATURE

a	height of the tooth marks
A	flexibility (inverse of stiffness)
$[A]$	flexibility matrix
b	blade width; bite per tooth
c	blade speed
d	tooth depth; difference between s and g
D	plate bending stiffness = $Eh^3/12(1-\nu^2)$
D_c	depth of the cut
e	component of the cutting force about the mean force; width of tensile stress zone
E	Young's modulus
$E_{mn}(y)$	shape functions of blade deflection
f	frequency in cycles per second; force acting on a tooth
$\bar{f}$	mean lateral cutting force
f_c	filter cutoff frequency
F	lateral force on the blade
F_c	net forces acting on fixed degrees of freedom
F_e	force on a free degree of freedom
F_i	lateral cutting force at the i-th location along the length of the cut
F_L	lateral cutting force
F_n	external forces acting on the n-th degree of freedom
g	clearance gap
GFI	gullet feed index
$[G]$	gyroscopic matrix
h	plate thickness
k	stiffness

[K]	stiffness matrix
K_{eq}	equivalent tooth-tip stiffness
K_o, Q_o	effective tooth-tip stiffnesses
K_t	bending stiffness of a tooth
K_{tt}	tooth-tip stiffness of a single tooth
L	span between the guides
L_c	length of the cut
m	average cutting force at an instant in time
[M]	mass matrix
N_c	number of increments along the cut
N_t	number of teeth in the cut
N_y	number of contact nodes across the width of the blade
p	planer allowance
P	tooth pitch
{P}	Load vector for Galerkin formulation
q(x,y,t)	lateral loading per unit area
r	distance from the center of a knot
s	side clearance
{S}	Generalized coordinates for Galerkin formulation
S_{it}	cut path at the i-th increment into the cut for the t-th tooth
S_o	standard deviation of blade deflection when no contact occurs
S_e	standard deviation of e
S_f	standard deviation of the cutting forces
S_m	standard deviation of m
S_T	standard deviation of blade deflection when contact occurs
T	bandmill strain (axial preload)
U_n,V_n	constraint locations

$w(x,y,t)$	lateral blade deflection
(x,y,z)	coordinates on the blade
$\bar{x}$	mean tooth deflection for a cut
x_c	deflection of a free degree of freedom
x_f	deflection of a fixed degree of freedom
x_T	tooth-tip deflection
z	a Gaussian random number; probability variable
Z_o	nondimensional clearance gap
α	factor relating S_T to σ_T
β	outward shift of the constraints
δ	imbedment of a node
δ^v, δ^u	imbedments
γ	side clearance angle
ε	a small lever arm
κ	strain system parameter
λ	wave length; eigenvalue
μ	mass per unit area
ν	Poisson's ratio
ρ	density
σ_B	standard deviation of the between-board thickness; stress due to in-plane bending
σ_c	stress in center of the blade due to tensioning
σ_G	gullet stress
σ_R	roll tensioning stress at the edges of the blade
σ_W	standard deviation of the within-board thickness
σ_T	standard deviation of the total board thickness; stress due to bandmill strain
σ_x	axial stresses a stationary blade
τ, $\Delta\tau$	distance along the cut, and its increment

ϕ	hardness function
φ_{ni}	contact force at a node
ω	frequency in radians per second
$\Psi_{mn}(x)$	Galerkin shape function

ACKNOWLEDGMENTS

I would like to acknowledge the support provided by the Science Council of British Columbia through its G.R.E.A.T Award program, in which MacMillan Bloedel Ltd and CAE Machinery Ltd acted as industrial cooperators and sponsors.

I would also like to thank the following people for their support, advice and friendship: Dr Stanley Hutton, my supervisor, Dr Gary Schajer, John Taylor, Leonard Valadez of California Saw and Knife, and Mr Pat Crammond of CAE Machinery.

> ...the most lasting contribution to the growth of scientific knowledge that a theory can make is the new problems which it raises, so that we are led back to the view of science and the growth of knowledge as always starting from, and always ending with, problems - problems of ever increasing depth, and ever increasing fertility in suggesting new problems.
>
> Sir Karl Popper
> The Growth of Scientific Knowledge

CHAPTER 1

INTRODUCTION

Bandsaws have been used to cut wood since the middle of the nineteenth century. Bandsaws are more useful than circular saws for deeper cuts because thinner blades can be used, and hence, less wood is lost to sawdust. Until 1970 there was little interest in North America in improving sawing accuracy or in increasing the amount of solid wood recovered from a log because timber was relatively cheap. At present, in 1993, that situation does not exist; the cost of raw material, delivered to the sawmill, now accounts for fifty to eighty percent of the total production costs. Low lumber recovery factors are no longer acceptable. In addition, many purchasers are demanding that sawn lumber (i.e., unplaned) has a smooth finish and be manufactured to specified dimensional tolerances. Lastly, as ecological concerns becomes more important to society, the costs of timber and harvesting are likely to increase.

There are two categories of fibre loss. The first is the kerf loss, which is the volume of wood removed by the teeth. The second is called the planer loss, which is the extra thickness allowance added to the sawn board thickness so that the board, when planed, will be completely surfaced on all sides. The total loss is the sum of the kerf and planer losses.

One method for reducing the fibre loss is to use thin saws to reduce the kerf loss. However, thickness reduction can be carried only so far before the blade is weakened to the point where accurate sawing is no longer possible. The resultant inaccurate sawing causes larger planer losses. Clearly, there is an optimum thickness where the total loss is minimized. However, the effect of blade thickness on sawing deviation needs to be known for such an analysis to be conducted.

Blade stiffness is expected to be one indicator of the ability of the saw to cut in a straight line, but there are other factors such as side clearance (the amount by which the teeth protrude from the sides of the blade) which are known to affect sawing accuracy. Sawing is a very complex process with many interacting phenomena. The trial and error development of bandsaw technology that continues to this day is in part due to the lack of understanding of the mechanics involved.

A primary issue that confounds sawing research is the variability of the wood. Since no two pieces of wood are the same it is impossible to repeat a cutting experiment. Statistical methods such as an analysis of variance of board thickness are available for evaluating experimental results. These statistical measures do quantify known trends in saw behavior and can be used as indicators of certain sawing problems, but they do not help to explain the mechanics of sawing or lead to predictions of how changes in blade design will affect cutting accuracy.

The problems in sawing research at this time are:

1) to determine the essential variables that encapsulate the characteristics of the wood, the blade, and the performance of the cutting system as a whole.
2) to learn how the wood and the blade interact during sawing and to express these interactions with the above variables.
3) to determine how cutting performance is affected by the characteristics of the wood and the blade.

To solve these problems, the mechanics of sawing need to be described, understood and, where

possible, quantified.

OBJECTIVE

The objective of this thesis is to investigate the mechanics of sawing wood with a bandsaw with a view to predicting how blade and operating parameters affect cutting accuracy. Specifically, the effects of blade stiffness, the character of the cutting forces, and the side clearance on blade behavior and cutting accuracy will be investigated.

METHOD AND SCOPE

Because of the problems inherent in doing repeatable cutting experiments, this study is based upon a simulation of the sawing system. Simulation makes possible a systematic exploration of the mechanics of sawing. The danger of using simulation, especially on a system that has not been thoroughly studied before, is that important effects that cannot yet be expressed mathematically are ignored. To mitigate this shortcoming, a broad approach is taken in the literature review, in the initial investigations, and in the interpretation of the results.

The approach taken in this thesis consists of the following steps:

a) to identify, via a literature review and empirical observation, the interactions that occur between the components of the sawing system,
b) to construct a numerical model of the sawing process that includes the dominant interactions,
c) to investigate the mechanics of blade behavior by simulating cutting through prescribed

disturbances,

d) to discuss the mechanisms, and their relative importance, that explain why changes in blade or operating parameters affect cutting accuracy, and

e) to compare trends predicted by the model to known or experimental results and to suggest future work that could improve the predictive ability of the model.

The investigation and discussion concentrate on the effects of blade stiffness and side clearance because they are found to dominate sawing behavior.

BACKGROUND AND PREVIOUS RESEARCH

Few aspects of the process and practice of sawing are precisely quantified. The information in the literature on bandsaws is not yet comprehensive enough to be applied in practice. Much anecdotal information on mill practice is available, but one must keep in mind that the effect of certain commonly recommended procedures is to compensate for, but not to correct an underlying problem. The result is that cause and effect are confused. This is probably one reason why a change in blade or operating parameters improves sawing behavior on one bandmill, but has no effect or is detrimental on another. All of these factors must be considered when reviewing sawing literature.

For the purpose of presenting the literature on bandsaws and bandsawing, the information is partitioned into six areas of interest.

1. BANDSAW OPERATION AND PREPARATION

A bandsaw blade is a strip of steel with teeth along one or both edges that is welded to form a

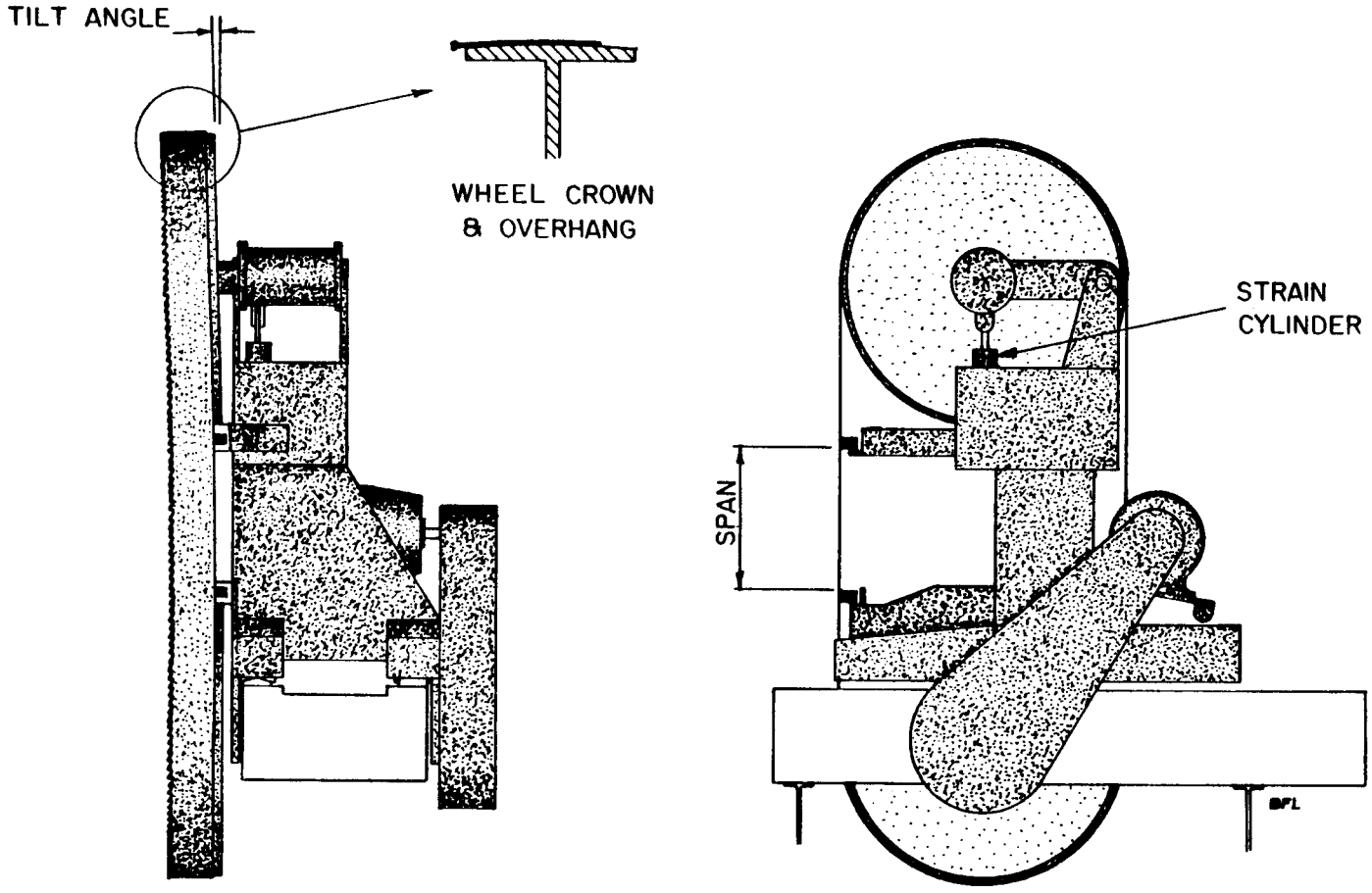

Figure 1-1. General Arrangement of a Bandmill.

continuous loop. This band runs on two wheels, one of which can translate to apply an axial preload to the blade. See Figure 1-1. The force pushing the wheels apart is termed the "bandmill strain". Adjustments are also available for changing the relative tilt angles and axial alignment of the wheels. The wheels are generally crowned to ensure the tracking stability of the band. The tilt adjustment is used to set the amount the teeth overhang the edge of the wheels. Guides are located just above and below the cutting region to provide support for the blade in the cutting area.

To improve the blade stiffness and tracking stability, residual stresses are put in the blade by plastically deforming the blade between two narrow pressure rollers. This process is called "tensioning" and a blade with residual stresses is said to be "tensioned". The result is that before straining, the edges of the blade have a tensile residual stress while the center is in compression. Additionally, the residual stresses are purposely made to be asymmetric so that the back of the blade is longer that the front edge. The blade is then said to have "backcrown"; the purposes of which are to increase the stiffness of the front edge and to compensate for thermal expansion of the front edge resulting from the heat generated during cutting.

2. EVALUATION OF SAWING PERFORMANCE

The quality control method developed to monitor the sawing process is important to sawing research for two reasons. Firstly, the method forms a basis, but not a complete method, for evaluating experimental data. Secondly, the method separately evaluates, to some extent, how well the saw is performing and the condition of the feed system.

The evaluation is an analysis of thickness variation of typically fifty boards [Brown, ed., 1982]. The thickness of the boards is measured at six places on each board. These data are used to find the mean thickness, the within-board variation, σ_W^2, and the between-board variation, σ_B^2 (the variation of the mean board thicknesses). The total variation, σ_T^2, is the sum of the within and

between-board variations. Generally, the within-board variation is considered to be a measure of the alignment and condition of the blade, the condition of the wood (knots, pitch, frozen, etc.) or the looseness of the feed system. The between-board variation is considered to be a measure of the positioning accuracy and repeatability of the setworks (the mechanism that positions the saw).

3. STATICS, DYNAMICS AND BUCKLING OF BANDSAW BLADES

Previous researchers have based their analyses of the bandsaw blade on a beam or a plate model that is simply supported at both guides and free on the other two edges [Mote, 1965, 1968; Foschi and Porter, 1970; Ulsoy and Mote, 1980, 1982; Taylor, 1985; Wang and Mote, 1985]. These models include the effects of bandmill strain (axial preload), the speed of the blade, and roll tensioning. The blade parameters are the blade width, the plate thickness and the span length between the guides. A further factor that affects the bandsaw is the mechanical method used to support the top wheel and apply the strain. Mote [1965] developed a non-dimensional stiffness parameter, κ, which varies between 0 and 1. For a deadweight strain system there is no stiffness in the top wheel, so it is free to move. In this case $\kappa = 0$. For a fixed top wheel, the stiffness of the strain system is infinite, and $\kappa = 1$.

The governing equation of an axially moving band is [Mote, 1965]

$$D\nabla^4 w + 2\mu c \frac{\partial^2 w}{\partial x \partial t} + \mu \frac{\partial^2 w}{\partial^2 t} + (\kappa\mu c^2 - h\sigma_x) \frac{\partial^2 w}{\partial^2 x} = q(x, y, t)$$

where

$D = \dfrac{Eh^3}{12(1 - \nu^2)}$

μ = mass per unit area

c = blade axial velocity

h = blade thickness

$\sigma_x(y)$ = axial stress distribution at zero velocity

κ = strain system parameter

q = lateral loading

$w(x,y,t)$ = lateral deflection

The terms on the left-hand side represent, respectively: the flexural stiffness, the gyroscopic coupling of the axial and lateral velocities, the inertial force, the centripetal forces and the effect of the in-plane axial stresses. The Ritz [Ulsoy, 1979], Galerkin [Mote, 1965; Ulsoy, 1979], and the finite element [Ulsoy, 1979; Taylor and Hutton, 1991] methods have been used to solve this equation. The types of analysis performed are the determination of natural frequencies and mode shapes, the lateral stiffness and the critical buckling loads caused by the cutting forces.

The natural vibration of bandsaws has been extensively investigated, mostly because resonance was thought to be a major cause of sawing inaccuracy [Ulsoy *et al*, 1978]. This is true for circular saws, but no experimental data have been presented to justify this assumption for bandsaws. This is not to say that bands do not resonate, especially during idling, but no one has shown that board thickness variation corresponds to the resonant vibration of the bandsaw.

The buckling of bandsaws caused by the feed and tangential cutting forces has been studied by Pahlitzsch and Puttkammer [1974, 1976], Foschi and Porter [1970], and by Ulsoy [1979]. Ulsoy *et al* [1978] concluded that for wide bandsaws used in sawmills, the cutting forces are too small to cause buckling.

The lateral stiffness of bandsaws has not been extensively studied. Pahlitzsch and Puttkammer [1974, 1976] and Porter[1971] used a beam model with axial loading for the bandsaw, for which the cross-section of the blade remains rectangular after the blade has deflected. For this model to be valid the span must be much greater than the width of the blade. This model is appropriate for the narrow resaw bands used by Pahlitzsch and Puttkammer for their verification tests, but may

not be appropriate for the wide bandsaws used for primary log breakdown. Taylor and Hutton [1991] used finite element analysis of a plate model of a wide blade to calculate the stiffness at the tooth-tip, the bottom of the gullet and the back edge of the blade. There was good agreement between the numerical and experimental results. The parameters that affected tooth-tip stiffness, in order of decreasing importance, were thickness, span length, strain and blade width.

4. FATIGUE ENDURANCE OF BANDSAWS

Fatigue is mentioned here because the parameters that govern fatigue life, blade thickness, strain and roll tensioning, also affect the stiffness, natural frequencies and critical buckling loads. A change in any parameter that increases stiffness, will, in general, result in a reduction in blade fatigue life.

Bandsaw blades frequently develop cracks in the gullet region that sometimes cause catastrophic failure of the blade. These cracks are known to result from metal fatigue [Jones, 1965, 1968]. The stresses that produce cracking are of two types: the constant stresses produced by bandmill strain and roll tensioning and the oscillating stress resulting from the blade being bent over the wheels. [Allen, 1973 a, b; Hutton and Taylor, 1991]

5. ACTION AT THE TEETH AND CUTTING FORCES

The cutting force acting upon the teeth may be considered as the sum of three orthogonal components: the feed, tangential and lateral forces. The feed and tangential forces act in the plane of the blade and have been studied extensively because they determine power requirements [Franz, 1957; McKenzie, 1964]. The lateral force has not received as much attention.

The primary problem encountered when investigating the cutting of wood is the variation in the

properties of wood. Szymani [1985] listed specific gravity, moisture content, and temperature as the determinants of the cutting forces. These properties have large variations, both between and within species, that are apparent in growth related characteristics such as spiral and interlocked grain, knots (irregular density and grain direction), and reaction wood. Also, sawing can release residual growth stresses that could cause the wood to pinch the blade.

Pahlitzsch and Puttkammer [1976] and Fujii *et al* [1984, 1986] measured blade deflection and the three components of the net force acting on short blocks as they were cut by a bandsaw. The shapes of the sawn surfaces were also measured. Both groups of researchers produced similar experimental results. The graphs of the cutting forces and the blade deflection show that the feed and tangential forces are fairly constant during the cut and then return to zero when the cut is finished. The lateral force, and the blade deflection graphs have similar shapes. From Pahlitzsch and Puttkammer's data Ulsoy *et al* [1978] produced typical and range values of the cutting forces, which are reproduced in Table 1-I. Fujii *et al* [1984] concluded that the blade deflection increased with increasing lateral force and assumed that the deflection was a result of the lateral force. Pahlitzsch and Puttkammer, however, noted that at the end of the cut the lateral force and the blade deflection did not always return to zero when the teeth left the wood. The deflection and lateral force became zero only after the back edge of the blade had cleared the end of the wood. They concluded that, in this instance, the wood was restraining the blade from returning to its equilibrium position. In other words, the lateral force measured by the dynamometer supporting the wood block was a result of the blade deflection and that the lateral forces do not always act solely on the teeth.

St. Laurent [1970, 1971] examined the effect of sawtooth edge defects and knots on the cutting forces. In his experiments, a single tooth was mounted on a three component force dynamometer. The three forces were recorded while a block of wood was pushed onto the tooth. The results showed that small defects on the corner of a tooth can cause the lateral force to be as large as

Table 1-I. Typical Cutting Forces [Ulsoy, *et al*, 1978]

Direction	Range	Typical
tangential	100-1000 N (23-225 Lbs)	500 N (112 Lbs)
feed	0-600 N (0-135 Lbs)	250 N (56 Lbs)
lateral	0-25 N (0-5.6 Lbs)	15 N (3.4 Lbs)

27% of the tangential force (i.e., F_L = 12 lbs.). For a perfect tooth the range of values of the lateral force was only 1 or 2 lbs. In the study on the effect of knots St. Laurent measured the tangential cutting force as well as the average and maximum lateral force near or in a knot. For softwoods the average lateral force was about 20-30% of the tangential force in the surrounding clear wood (i.e., 4 lbs. < F_L < 10 lbs.). However, the peak lateral force was between 30-100% of the tangential force in the clear wood (i.e., 40 lbs. < F_L < 60 lbs.).

Preliminary data showing the effect of density variations and fibre direction on the cutting forces has been presented by Axelsson *et al* [1991]. They used computer tomography to provide an image of the wood density and compared these images to the three components of the cutting force when the wood was later machined with a single tooth cutter. The in-plane forces were noticeably affected by wood density, especially around knots, but the lateral force only showed the effect of density when one of the tooth corners was purposely damaged. The effect of tooth damage was similar to that reported by St. Laurent [1970].

The action of the teeth produces the two sawn surfaces and the sawdust. Most of the sawdust is carried away in the gullet of the tooth but some escapes and falls into the space between the sawn surface and the side of the blade. Sawdust spillage could result in blade heating, and, hence, in poor cutting accuracy because the thermal stresses could reduce the stiffness of the blade.

The flow and spillage of sawdust has been studied by Chardin [1957], who used high speed photography to photograph the tooth and gullet as the tooth emerged from the bottom of a cut. Reineke [1956] described in detail how sawdust compacted in the gullet, the conditions for the onset of spillage and the characteristics of the sawdust chips. See Figure 1-2. The following observations and conclusions were made:

a) The density of compacted sawdust is about 70 percent that of solid wood. Therefore, the volume of solid wood to be removed by one tooth can be only 70 percent of the volume of the tooth gullet, otherwise sawdust will be forced out of the gullet. The Gullet Feed Index (GFI) is the ratio of the area of the wood removed by a tooth (equal to the advance or bite per tooth multiplied by the depth of cut) to the area of the gullet. Hence, if the GFI is greater that 0.7, spillage should be expected.

b) There is a wide range of particle sizes for any given bite per tooth. Some of these fine particles could escape the gullet. Also, some particles could lodge in irregularities of the sawn surfaces.

c) The spilled sawdust shows a large percentage of fine particles. Of the larger spilled particles, there were thin flakes produced by the flanks of the teeth. These flakes could easily fall between the blade and the sawn surfaces.

The flanks of the teeth sever the chips from the kerf walls. Because of the clearance angle of the teeth, each tooth leaves a mark on the sawn surfaces. See Figure 1-2. The height of this mark has two components: Firstly, a geometric effect due to tooth shape equal to $a=b\mathrm{Tan}(\gamma)$, where b is the bite per tooth and γ the side clearance angle. Secondly, an effect due to the deformation of the wood fibres during the cut and their subsequent "springback". Johnston and St. Laurent [1975] measured the springback with a single tooth apparatus and found, for example, that when cutting

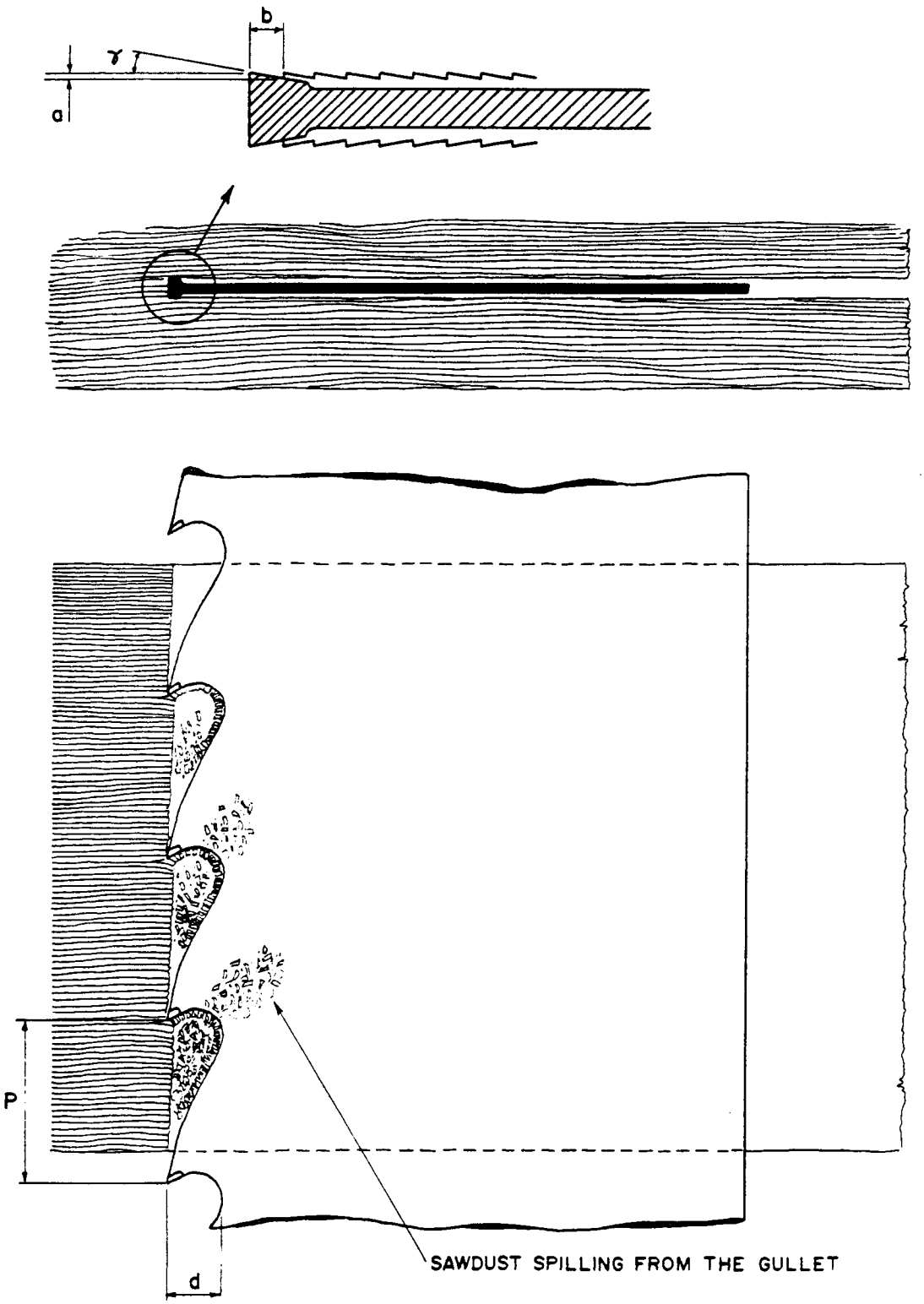

Figure 1-2. Geometry of the Tooth and the Tooth Marks.

wet spruce at a bite per tooth of 0.050 inches and a side clearance angle of 3 degrees, the springback was 0.0053 inches. The geometric effect, 'a', was 0.0026 inches for this case, so the clearance gap between the blade and the sawn surfaces is reduced by a total of 0.0079 inches.

Breznjak and Moen [1972] calculated the kerf width by measuring the width of the wood block before cutting and then subtracting the total width of the remainder of the block and the board. They also calculated the kerf width based upon the difference in weight between the original block and the sum of the remaining block and board. Their result was that the width of the tooth was greater than the kerf width based on weight difference, which was in turn greater than that based on thickness difference. The kerf based on weight difference was about 0.007 inches smaller than the tooth width, and for the thickness difference method, 0.014 inches (at a bite per tooth of 0.047 inches). The reduction in kerf width decreased as the bite was decreased. The authors concluded that surface roughness, tooth marks and fiber springback caused the reduction in kerf width.

6. RESULTS FROM CUTTING TESTS

There have been few systematic full scale cutting tests carried out. Statistical analysis requires a large number of cuts to be made (20-100) [Brown, ed., 1982, Allen, 1973b] under controlled conditions for each condition being tested. It is a time consuming and expensive task to conduct extensive experiments. On the other hand, many boards can be cut in the sawmill, but the conditions are not under the control of the researcher.

As a part of a larger study on bandsaw vibration during cutting, Breznjak and Moen [1972] showed that there is a relationship between log quality, expressed by the number of knots per unit surface area of the log, and the maximum blade deflection. Taylor and Hutton [1991] used the sum of the knot diameters on the sawn surface to account for variation in experimental results.

Basically, if more knots are present then the sawing accuracy is worse.

Pahlitzsch and Puttkammer [1976] measured the deflection of a bandsaw blade during the cutting of short blocks of wood. In the traces of blade motion that were presented, the frequency of the oscillation was not greater than 2 Hz. They made the following general observation concerning recorded blade motion:

> "The blade, in general, oscillated about the ideal cutting line with a relatively large period in the feed direction and a more or less large amplitude in the direction perpendicular to the cutting plane."

The wave lengths of the oscillations were 200 mm and larger, while the lateral deflections were 0-2 mm (0-0.050 inches). Feed speeds up to 0.4 m/s (79 in/s) were used. The blade width was 100 mm (3.4 inches).

Allen [1973 a, b] presented data showing the effect of blade thickness, strain, and feed speed on the within-board sawing deviation. The sawing deviation was approximately inversely proportional to the square root of strain. As the feed speed was increased, such that the Gullet Feed Index increased from 0.65 to 0.90, the sawing deviation increased. In a set of the cutting performance tests, a 0.058 inch thick by 8 inch wide blade run at 15000 lbs. strain had the same sawing accuracy as a 0.042 inch by 7.5 inches blade running at 24000 lbs. strain, but the thinner saw saved 0.030 in kerf.

Kirbach and Stacey [1986] showed that there is a minimum critical side clearance, below which the sawing deviation increases rapidly. They ascribed the reduced sawing accuracy to the increased likelihood of contact between the blade and the sawn surfaces that would cause heat, and hence, thermal stresses in the blade that would reduce the blade stiffness. The example given was of a

0.058 inch thick by 8 inches wide blade at 18000 lbs strain, cutting a 7.3 inches thick block of western red cedar: the critical side clearance was 0.028 inches. They also noted that there is a maximum allowable side clearance. If the side clearance is larger than the bite per tooth then excessive amounts of sawdust will spill in to the space between the blade and the sawn surfaces, so, they postulated, that blade heating and increased sawing deviation will occur.

Grönland and Karlsson [1980] conducted extensive cutting tests with a small resaw at the Swedish National Sawmilling School, where six boards were cut from each of 850 cants. These results clearly showed the undesirable effects of having a Gullet Feed Index greater than 0.7. The effect of small spring-setting on the teeth was found to be undesirable, as Kirbach and Stacey showed for swaged teeth. Kirbach [1985] presented experimental results that showed the within-board deviation beginning to increase when the GFI is between 0.5 and 0.6, and increasing very rapidly when the GFI reaches 0.7.

A set of tests conducted in the University of British Columbia Sawing Laboratory confirmed the trend that reduced side clearance increases sawing deviation. For the smallest side clearance tested, the blade cut fairly straight for the first 18 inches then suddenly deflected more than 1 inch over a distance of 6 inches, after which the blade left the wood. It seems unlikely that the temperature of a blade that is cooled by the guide lubricant water and by the convection cooling generated by a blade moving at 9400 fpm could increase so much in the half second the blade was in the cut. Also, the power required to heat the blade to temperatures that would cause a significant loss in blade stiffness is greater than the power of the saw motor. This observation does not disprove that heat is a factor in causing the wild cutting, but it does indicate the possibility of other mechanisms.

Research is to see what everybody else has seen, and to think what nobody else has thought.

Albert Szent-Gyorgyi
Nobel Laureate

Imagination is a good servant, and a bad master.

Agatha Christie
The Mysterious Affair at Styles

Imagination is more important than knowledge.

Albert Einstein

CHAPTER 2

INTERACTIONS AND PROCESSES OCCURRING DURING CUTTING

The purpose of this chapter is to generate the concepts and assumptions that will form the basis of the mathematical model of the sawing process developed in this thesis. Also included is a discussion of the conditions under which a bandsaw must operate and the consequences of the assumptions used. This is accomplished by presenting a systematic view of sawing based on information in the literature, and, where necessary, by conducting experiments to fill any gaps in the information.

The sawing system is composed of a number of entities that interact with one another. See Figure 2-1. The entities are:

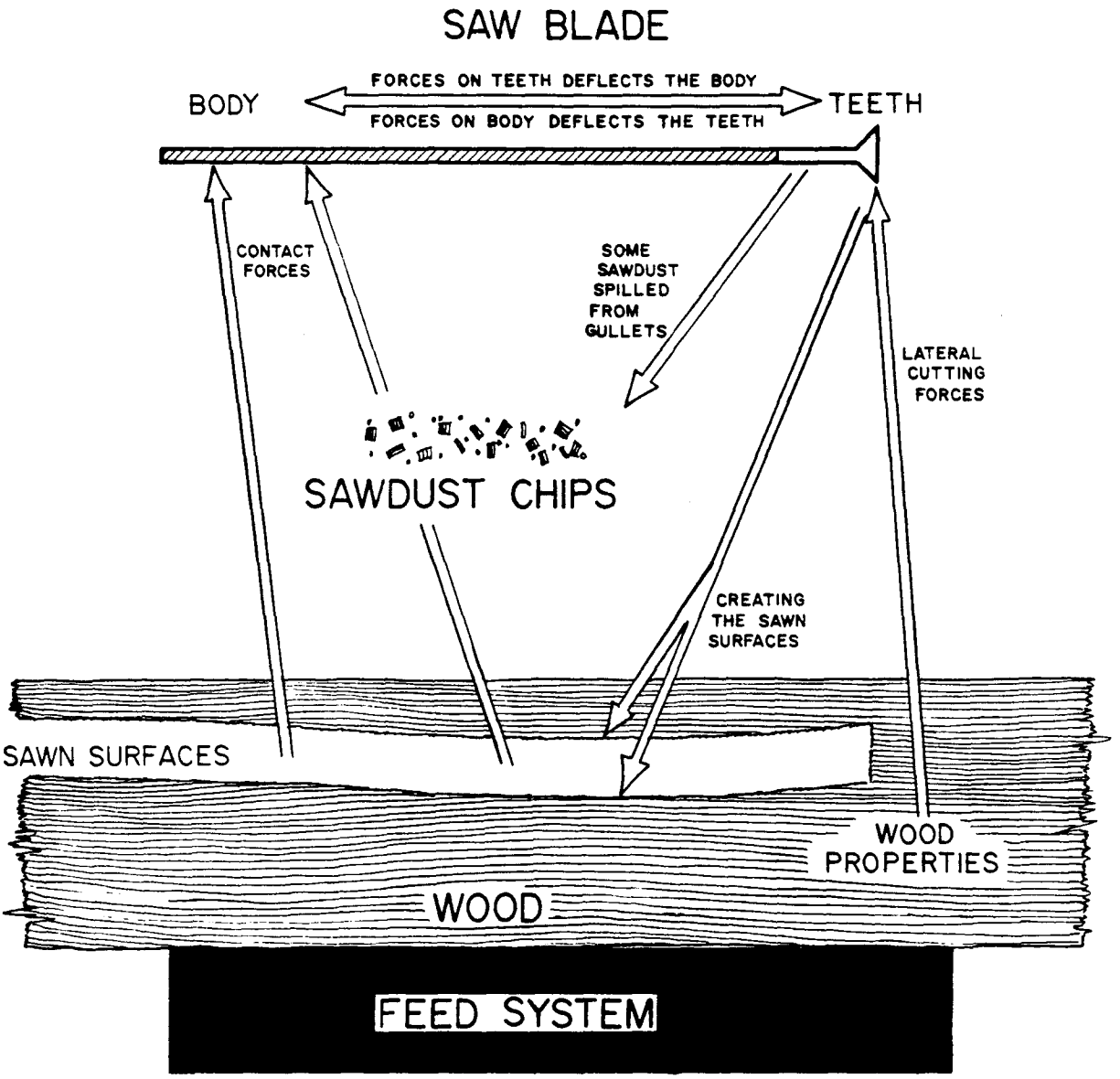

Figure 2-1. A Schematic of the Sawing System.

1) the wood, which includes the sawn surfaces,
2) the feed system that carries the wood through the saw,
3) the saw blade, which includes the body of the saw as well as the teeth, and
4) the sawdust.

The interactions and processes in which the entities participate are:

1) the lateral cutting forces that act between the wood and the tooth,
2) the creation of the sawn surfaces by the teeth,
3) the spillage of the sawdust from the gullets,
4) the contact forces caused by the body of the blade touching the sawn surfaces
5) the contact forces caused by the sawdust coming between the blade and the sawn surfaces,
6) the support of the wood provided by the feed system, and
7) the structural connection between the body of the blade and the teeth

Of the entities, processes and interactions listed, only the saw blade has been previously modelled accurately. The definition of the sawn surfaces can be understood as the instantaneous location of the teeth, although some allowances must be made for surface roughness and springback. The approximate range of the magnitude of the lateral cutting force is known, but not the details of how it varies along the length and through the depth of the cut.

Although some information is available on sawdust spillage, there are so many variables involved that few general statements can be made about the amount and eventual location of the spilled chips. Spillage is known to increase when the Gullet Feed Index becomes greater than 0.6. More spilled sawdust ends up near the bottom of the cut because this is where the gullet becomes full and because the saw drags chips downward. There is no literature that quantitatively describes the

rigidity or the accuracy of travel for the various feed systems used in sawmills.

The effect of the contact between the sawn surfaces and the blade on blade equilibrium is only briefly commented on by Ulsoy *et al* [1978]. All other articles and books consider this interaction only as a source of blade heating.

OBSERVATIONS FROM CUTTING EXPERIMENTS

One of the gaps in the knowledge of sawing is the effect of the contact between the sawn surfaces and the blade. To investigate this and other effects, the motion of the blade during cutting was examined. A bandsaw was instrumented with non-contacting displacement probes, the arrangement of which is shown in Figure 2-2. Figure 2-3(a) is a typical set of traces of the motion of the blade measured simultaneously near the front and back edges of the blade. The total time of the cut was 1.20 seconds. Note that the measurements were made above the cut: the deflection of the blade in the wood could be as much as 50% greater than that measured at the probes. The blade dimensions and the operating conditions are given in Table 3-I.

Table 2-I. Conditions for Experimental Cutting Tests

Strain	15000 lbs
Blade thickness	0.065 inches
Blade width	9.375 inches
Tooth width	0.140 inches
Feed speed	200 fpm
Bite per tooth	0.037 inches

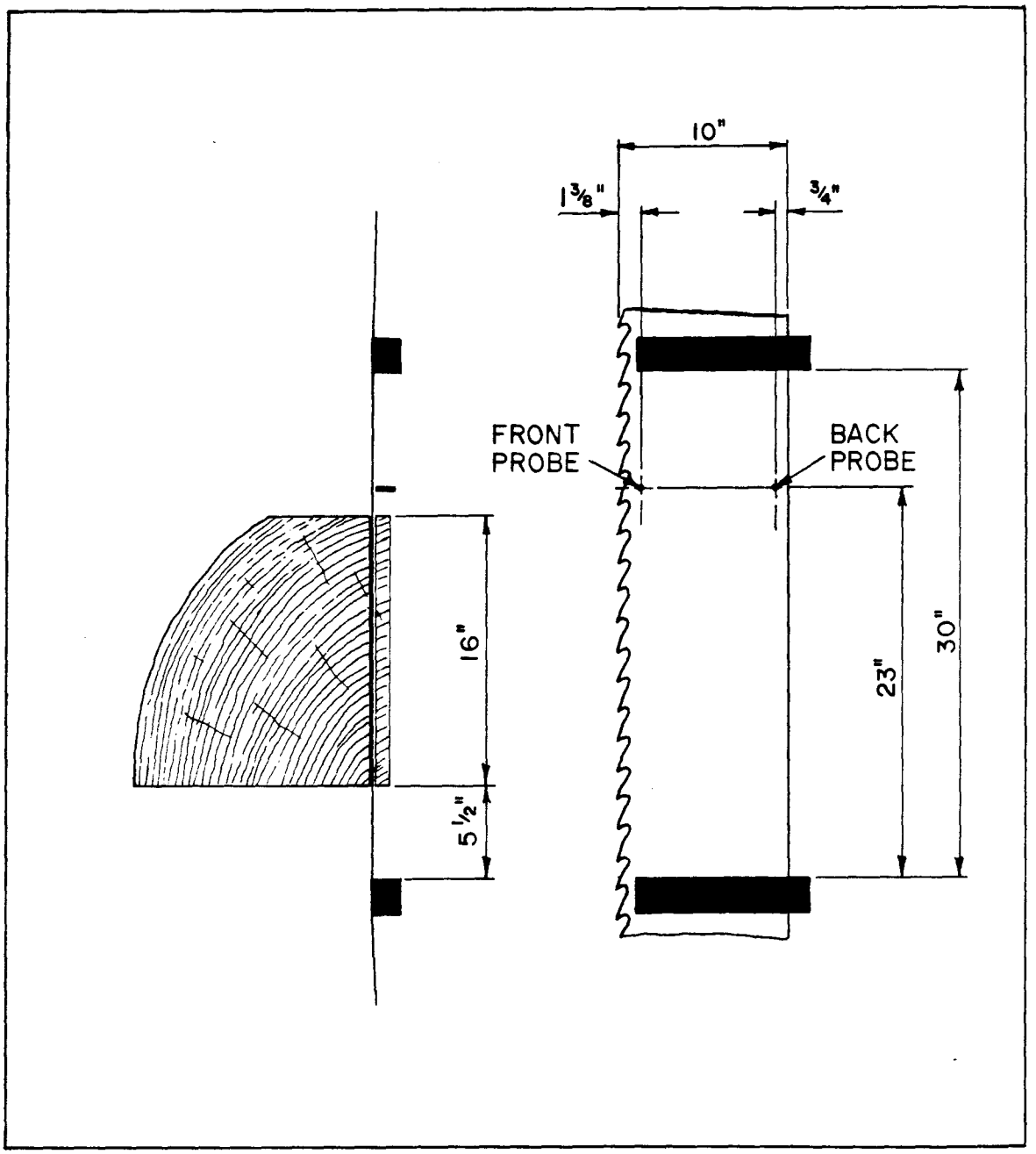

Figure 2-2. Experimental Arrangement for Cutting Tests.

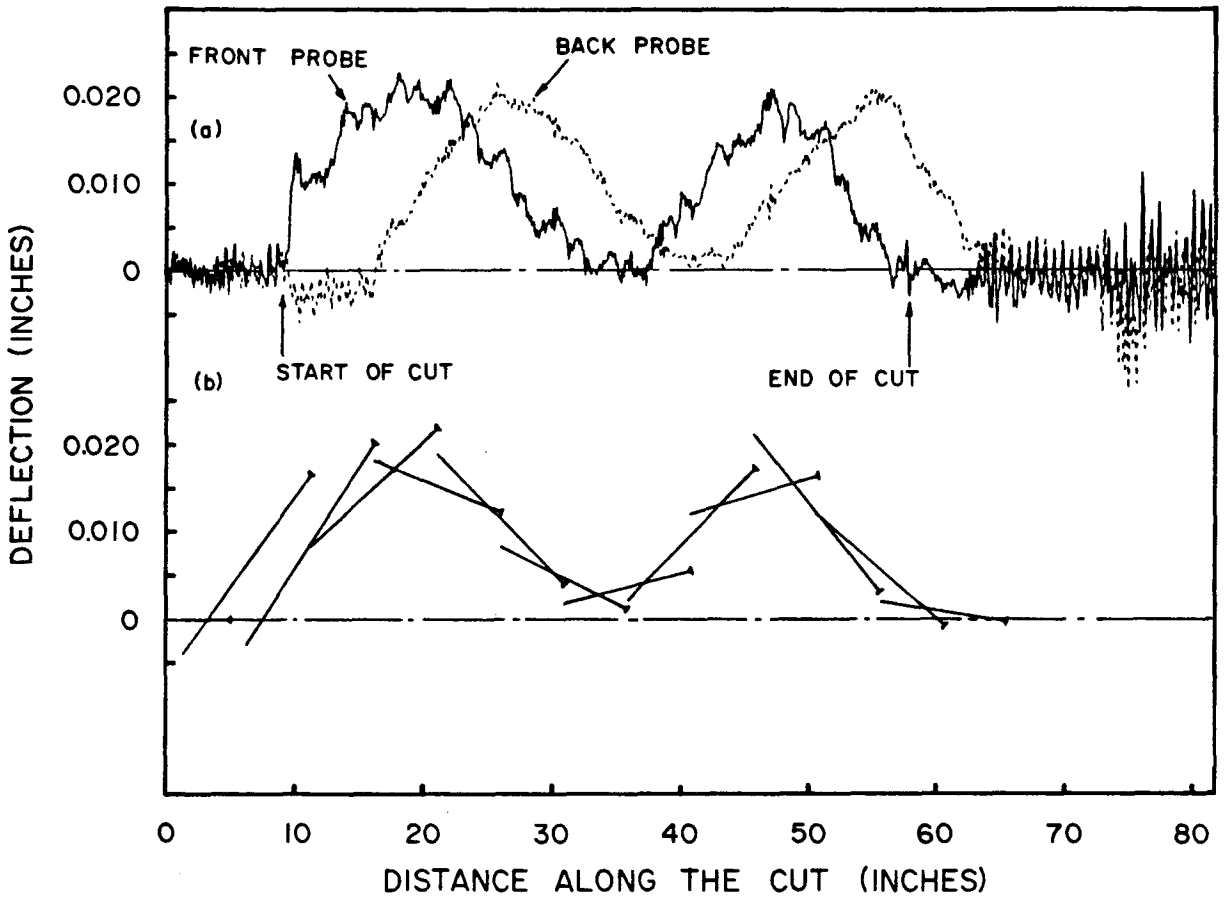

Figure 2-3. Blade Deflection During Cutting
a) Displacement at the Front and Back Probes
b) Interpolated Position of the Blade

The spectrum of the trace of the front probe is given in Figure 2-4. The lowest natural frequencies of the blade correspond to the peaks at 60 Hz. Although the blade is vibrating before and after the cut (see Figure 2-3), the natural vibration is damped out during cutting. The peaks at 10 and 20 Hz. correspond to the wheel rotation frequency and its first harmonic. The dominant blade deflection occurs at frequencies less than 5 Hz.

The first observation is that the low frequency content dominates the character of the signal. The cutting deviation is occurring at frequencies less than 5 Hz, as compared to the lowest natural frequency of 60 Hz. One can, therefore, conclude that blade stiffness, not blade dynamics, is the most significant factor in determining cutting deviation. A comparison of the relative effects of the inertial, gyroscopic and stiffness forces is given in Appendix A. It is shown that for excitation frequencies below 30 Hz. the stiffness effect dominates. Resonant behavior of the blade does not affect the cutting deviation.

A second observation is that just after the front of the blade deflects the back of the blade will also deflect. In fact, the signal from the back of the blade is a delayed version of the signal from the front. The delay approximately equals the distance between the probes. To aid visualization of how the blade deflected in the cut, the blade position at several points during the cut was extrapolated from the deflection traces. This is shown in Figure 2-3(b). (It will be seen in Chapter 4 that the cross-section of the blade does not stay straight when the blade deflects, so the straight-line extrapolation is not exact.)

In two regions of the cut, the deflection of the back of the blade is greater than that of the front. It is not possible that the cutting forces acting upon the teeth could, by themselves, produce this deflection. There must be lateral forces acting on the back half of the blade. The only entity that could provide such a force is the sawn surface, which acts as a geometric constraint on the motion of the blade.

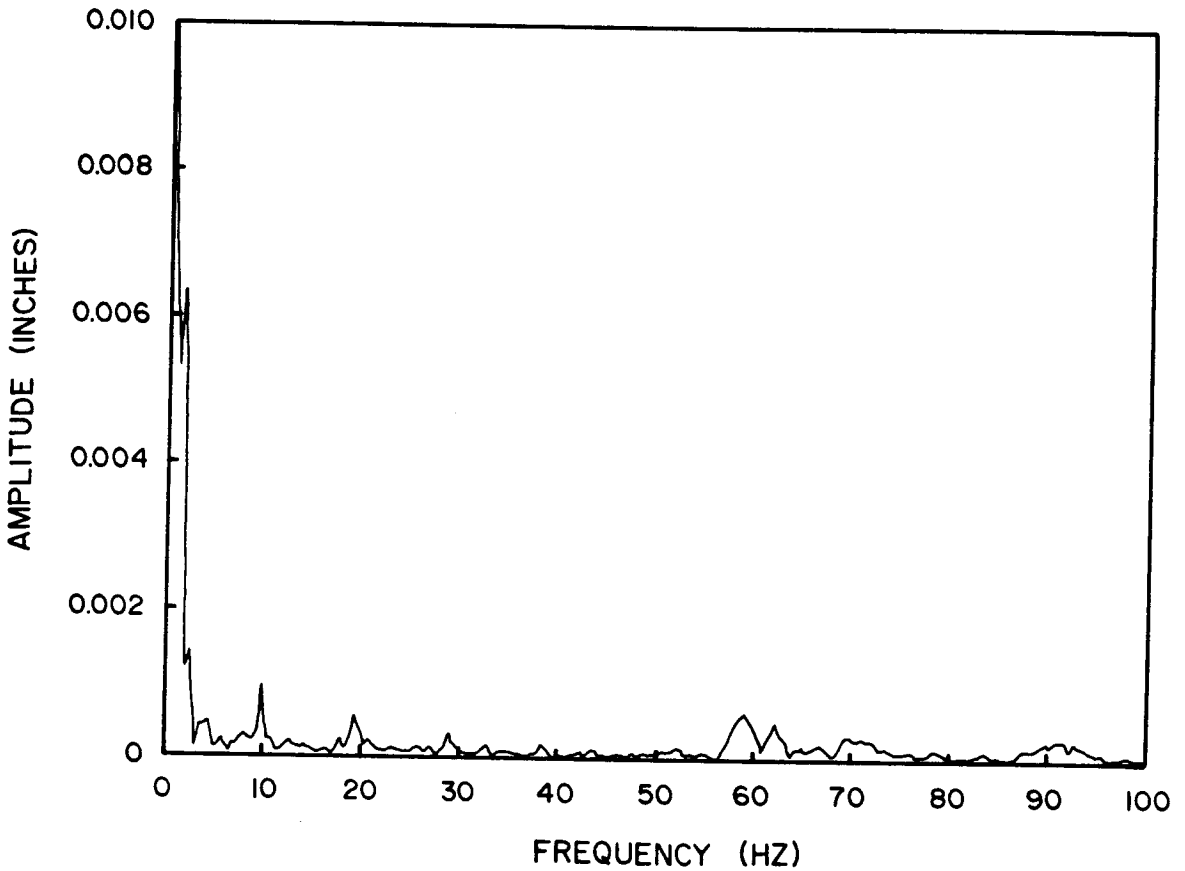

Figure 2-4. Spectrum of the Blade Deflection.

The body of the blade must follow in the path made by the teeth. If the teeth deflect by an amount greater than the side clearance, it is certain that the blade will contact the sawn surfaces at some point during a cut.

EQUILIBRIUM DEFLECTION OF A BANDSAW BLADE

Since contact is occurring between the blade and the sawn surfaces, the deflection of the blade is not solely the result of cutting forces acting upon the teeth. It has also been shown that the blade dynamics are not involved in the sawing accuracy of a bandsaw, although blade vibration could affect surface roughness. These observations lead to the conclusion that at every instant in time, or at every point along the cut, it may be assumed that the cutting force, the contact forces and the resistance of the blade to deflection are in quasi-static equilibrium. This assumption applies even though the lateral cutting forces will vary as the blade advances into the cut. The resulting deflection of the tooth-tips defines the newest addition to the cut path.

SAWMILL CONDITIONS

The operating conditions imposed on a bandsaw in a sawmill are much more adverse than those seen in a laboratory setting, primarily because the condition and alignment of the machinery cannot be maintained so precisely. As mentioned above, the rigidity and alignment of the feed system are important. There are four basic types of feed systems, each having their own characteristic problems.

1) The carriage system is the most rigid because the log is held at several points, but it is not economical for small diameter logs.

2) For the sharp chain system, the log is carried on a chain running in a guide way and held on the chain by press rolls. The alignment of this system is difficult because the chain is generally loose in its guide way. In addition, the press rolls do not stop the log from rolling laterally as it is fed into the saw, which results in the log leaning against the blade.

3) In the line-bar system a sawn edge is pressed against a flat plate and/or a bank of rollers. Problems arise if the infeed and outfeed are not aligned to each other, if the rollers are misaligned, worn or loose, or if the press rolls are applied after the cut has started or released before the wood has cleared the saw. In any event the wood will jump and not have a straight motion through the saw. In practice, the saw often mitigates these jumps.

4) In the end-dogging system the log is held at its ends, and then travels on a carriage arrangement. The middle of the log is unsupported and will flex as residual stresses in the log are released by the sawing. This problem also applies to the sharp chain feeds.

Whichever system is used, there is the likelihood that the wood will move independently relative to the blade and even press against the blade.

The blade can be damaged by rocks and pieces of metal that are occasionally found in a log. Damage can also occur if the bandmill is still being set when the cut starts. The blade must be rugged enough to survive these incidents. Allowances must also be made in designing a blade for variations in the skill of the sawfilers and of the sawyers.

The preceding discussion on the effects of sawmill conditions give rise to two conclusions. Firstly, saw blades may have to be oversize to limit damage or to make the blade insensitive to variations in

their preparation and operating conditions. Secondly, the predictive ability of a model of the sawing process may depend upon how well these non-ideal conditions are represented. This is specially true concerning the rigidity and alignment of the feed system.

FURTHER PRACTICAL CONSIDERATIONS

1) The blades are never perfectly flat. Peak to peak lateral runout is typically between 0.002 to 0.005 inches.

2) Because of the bending moments generated when the blade bends over the guides and the wheels, the span between the guides does not form a plane; instead, the blade bows outward. Also, because of the backcrown and wheel tilt, the front edge of the blade bows out less than the back edge. Hence, at mid-span, the blade is not parallel to the carriage tracks. The cross-section of the blade is curved, presumably because of the combined effects of tensioning, anti-clastic bending and the stretching of the band over the wheel crown. These distortions from the plane are small: typically 0.002 inches maximum.

3) The teeth are frequently not aligned in the lateral direction. Either the teeth have more clearance on one side on the blade than the other, or the clearance is not uniform from tooth to tooth.

The above non-ideal aspects of the blade may have measurable effects on the contact between the blade and the sawn surfaces, either because the clearance gap is reduced or is less on one side of the blade than the other.

4) The teeth not only overhang the wheels, they also overhang the guides, so that the blade is not always fully supported out to the gullet line. Too much overhang (more than 0.5 inches) has a

noticeable effect on tooth-tip stiffness and cutting accuracy.

CONCEPTS AND ASSUMPTIONS

The representations of the lateral cutting forces and the contact between the blade and the wood will be developed in the next chapter. With these representations it is possible to construct a numerical model of all the important entities, processes and interactions present in sawing.

The following assumptions were made when constructing the model of the sawing system:

1) the feed system and the wood are perfectly rigid,
2) the blade is simply supported at the guides and it lies in a plane between the guides,
3) the process of cutting is quasi-static, so that inertial and gyroscopic effects on the blade can be ignored,
4) the effects of heat generated when the blade rubs against the sawn surfaces or from the cutting process will not be included,
5) the clearance gap in the model will not be equal to the side clearance of the teeth because of tooth marks, springback and spilled sawdust, but it will be the same on both sides of the blade and constant through the depth of the cut, and,
6) the behavior of the blade between the guides is isolated from other parts of the bandmill and the rest of the blade.

> The sciences do not try to explain, they hardly even try to interpret, they mainly make models. By a model is meant a mathematical construct which, with the addition of certain verbal interpretations, describes observed phenomena. The justification of such a mathematical construct is solely and precisely that it is expected to work.
>
> John Von Neumann

CHAPTER 3

MODEL GENERATION AND ANALYSIS PROCEDURES

In this chapter the numerical models representing the bandsaw blade, the contact between the blade and the sawn surfaces and the lateral cutting forces are developed. These representations are then combined to form the model of the cutting process.

THE MODEL OF THE BANDSAW BLADE

The blade is assumed to be a flat plate, simply supported at the guides and free on the other two edges. The governing equation (repeated from Chapter 1) is

$$D\nabla^4 w + 2\mu c\frac{\partial^2 w}{\partial x \partial t} + \mu\frac{\partial^2 w}{\partial^2 t} + (\kappa\mu c^2 - h\sigma_x)\frac{\partial^2 w}{\partial^2 x} = q(x,y,t) \tag{3.1}$$

The coordinate system, which is fixed space, and the blade geometry are shown in Figure 3-1. The boundary conditions are no moments or shears forces on the free edges; expressed as

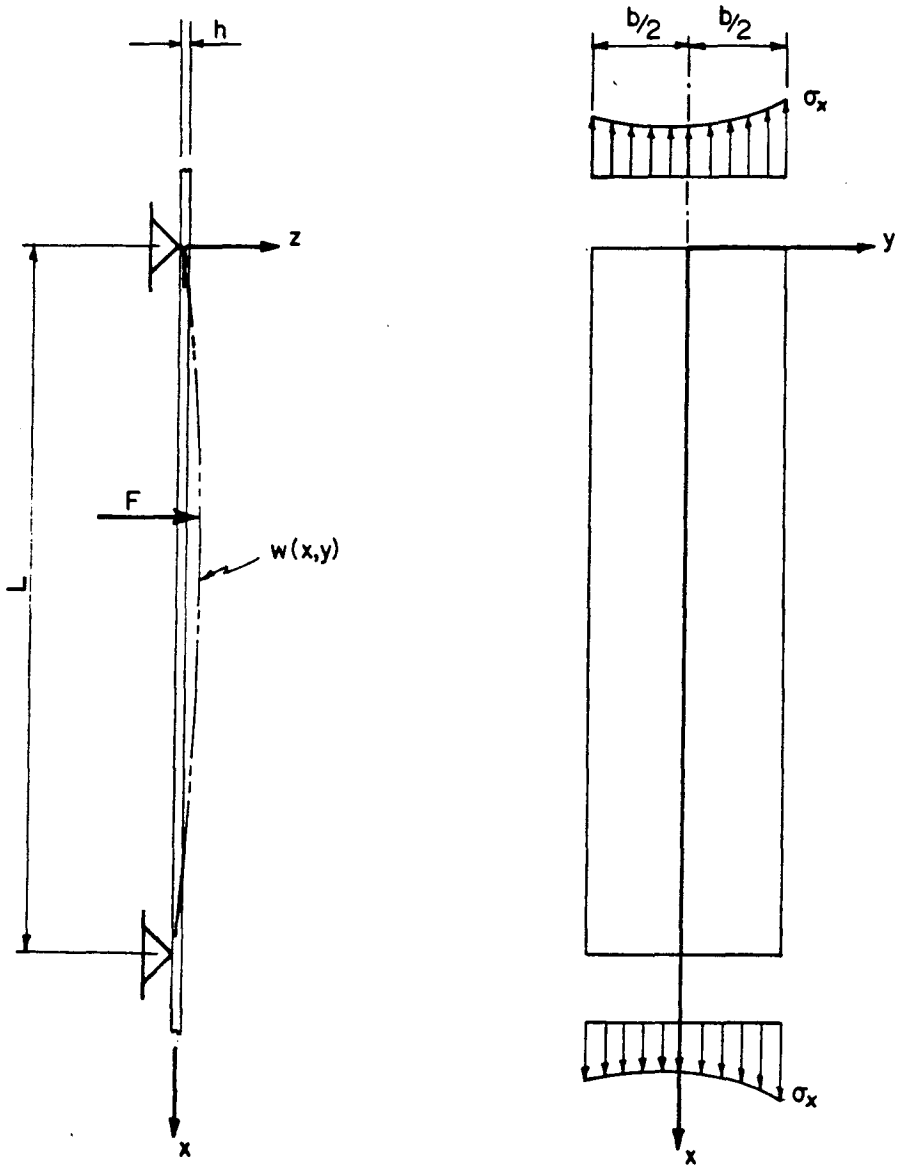

Figure 3-1. Idealized Model of the Blade.

$$\left.\begin{aligned} M_y &= 0 = D\left(\frac{\partial^2 w}{\partial^2 y} + \nu\frac{\partial^2 w}{\partial^2 x}\right) \\ V_y &= 0 = D\left(\frac{\partial^3 w}{\partial^3 y} + (2-\nu)\frac{\partial^3 w}{\partial^2 x \partial y}\right) \end{aligned}\right\} y = \pm b/2 \tag{3.2}$$

and no deflection or bending moment at the guides

$$\left.\begin{aligned} & w = 0 \\ M_x &= 0 = \frac{\partial^2 w}{\partial^2 x} + \nu\frac{\partial^2 w}{\partial^2 y} \end{aligned}\right\} \begin{matrix} x = 0 \\ \text{and} \\ x = L \end{matrix} \tag{3.3}$$

The Galerkin method was used to solve the governing equation. The displacement of the blade was assumed to be the summation of shape functions,

$$\Psi_{mn}(x,y) = E_{mn}(y)\mathrm{Sin}(n\pi x/L) \tag{3.4}$$

The total deflection was expressed as

$$\begin{aligned} w(x,y,t) &= \sum_{m=1}^{M}\sum_{n=1}^{N} S_{mn}(t)\Psi_{mn}(x,y) \\ &= \sum_{m=1}^{M}\sum_{n=1}^{N} S_{mn}(t)E_{mn}(y)\mathrm{Sin}\left(n\pi x/L\right) \end{aligned} \tag{3.5}$$

Each shape function, Ψ_{mn}, satisfies, implicitly, the boundary conditions at x=0 and x=L. The function $E_{mn}(y)$ must satisfy the boundary conditions at y=± b/2. Because of the symmetry of the boundary conditions about the centerline of the blade, there are only two independent boundary equations. A polynomial series was used for $E_{mn}(y)$, but it was necessary to separate $E_{mn}(y)$ into even and odd functions due to the character of the boundary equations. These functions were:

$$E_{mn}(y) = \begin{cases} G_{mn}^{(1)} + G_{mn}^{(2)}\left(y/b\right)^{m} + G_{mn}^{(3)}\left(y/b\right)^{m+2} & ;\text{m even} \\ G_{mn}^{(2)}\left(y/b\right)^{m} + G_{mn}^{(3)}\left(y/b\right)^{m+2} + G_{mn}^{(4)}\left(y/b\right)^{m+4} & ;\text{m odd} \end{cases} \tag{3.6}$$

The constants G_{mn} are choosen to satisfy the boudary condistions at $y=\pm b/2$. An arbitratry third condition $E_{mn}(b/2) = 1$ makes the solution for the constants G_{mn} deterministic.

The axial stress in a stationary blade, $\sigma_x(y)$, has three components: the stress from bandmill strain; the residual stress from roll tensioning; and the in-plane bending stress resulting from the interaction of the effects of backcrown, wheel tilt, wheel crown and blade overhang. These stresses are shown schematically in Figure 3-2. The change in axial stress that occurs because the blade is forced to accelerate around the wheels is accounted for in the term $\kappa\mu c^2\left(\partial^2 w/\partial^2 x\right)$ in the governing equation. Note that these are the stresses when the band is running on the wheels, and are assumed to be the net result of the above stresses. The following relationships exist:

$$\sigma_T = T/2bh \tag{3.7}$$

$$2e\sigma_R = (b-2e)\sigma_c \tag{3.8}$$

where

T	= bandmill strain
σ_T	= stress due to bandmill strain
e	= width of the tensile stress region
σ_R	= tensile stress on the edges of the blade (gullet stress)
σ_c	= compressive stress in the centre of the blade

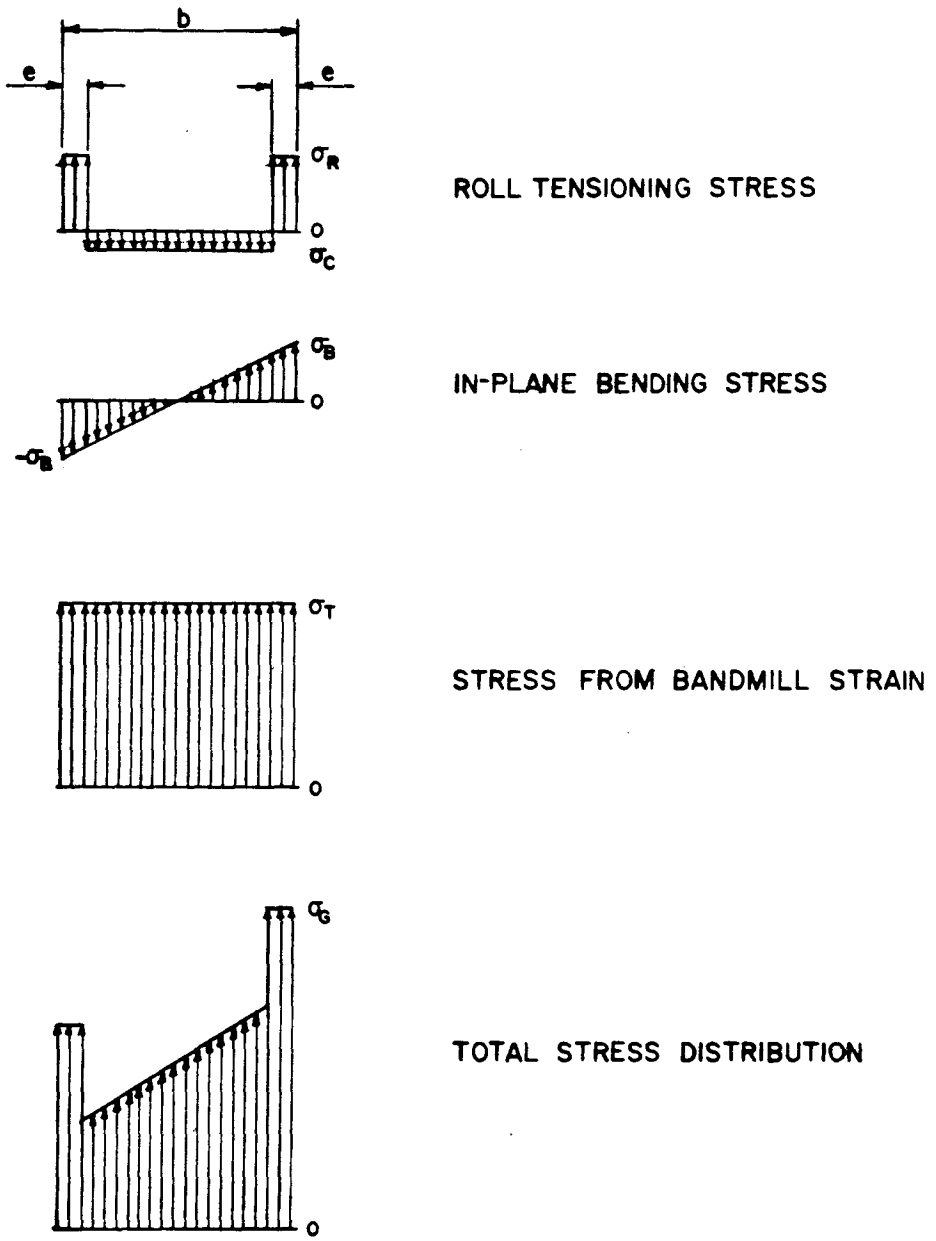

Figure 3-2. In-plane Stresses in a Bandsaw Blade.

The lateral loads acting upon the blade are assumed to be point loads of magnitude F_f acting at the coordinates (x_{of}, y_{of}). This is expressed mathematically as

$$q(x,y) = \sum_{f=1}^{Q} F_f \delta(x - x_{o_f}) \delta(y - y_{o_f}) \tag{3.9}$$

where $\delta()$ is the Dirac delta function.

The Galerkin procedure is carried out by multiplying both sides of the governing equation by each shape function,

$$\Psi_{kl} = E_{kl}(y) \mathrm{Sin}\left(\frac{l\pi x}{L}\right) \quad \begin{cases} k = 1,2,\ldots,M \\ l = 1,2,\ldots,N \end{cases} \tag{3.10}$$

and integrating over the area of the plate. This generates MN number of equations which can be expressed in matrix notation by

$$[M]\{\ddot{S}\} + [G]\{\dot{S}\} + [K]\{S\} = \{P\} \tag{3.11}$$

where $\{S\} = \{S_{11}, S_{12}, \ldots, S_{21}, \ldots, S_{MN}\}^T$

The deflection at any point on the blade caused by static loads is found by first solving

$$[K]\{S\} = \{P\} \tag{3.12}$$

and then substituting the S_{mn} into Equation 3.5.

The natural response is found by first defining

$$\{X\} = \begin{Bmatrix} \dot{S} \\ S \end{Bmatrix} = \{\overline{X}\} e^{\lambda t} \tag{3.13}$$

so that

$$\left\{\begin{bmatrix} M & G \\ 0 & M \end{bmatrix}\lambda - \begin{bmatrix} 0 & -K \\ M & 0 \end{bmatrix}\right\}\{\overline{X}\} = 0 \tag{3.14}$$

The eigenvalues, λ, and eigenvectors $\{\overline{X}\}$ of this equation are complex. The natural frequency ω_n is the imaginary part of the eigenvalue. Since the model has no damping (the G matrix contains only gyroscopic terms), the real part of the eigenvalue is generally zero. However, if the K matrix looses its positive definiteness, as when the axial stresses are arranged so that the blade buckles, the real parts will be non zero.

The mode shape is taken to be the real part of

$$V(t) = [\Re(\tilde{S}) + i\Im(\tilde{S})][\mathrm{Cos}(\omega_n t) + i\mathrm{Sin}(\omega_n t)] \tag{3.15}$$

which is equal to

$$\Re(V(t)) = \Re(\tilde{S})\mathrm{Cos}(\omega_n t) - \Im(\tilde{S})\mathrm{Sin}(\omega_n t) \tag{3.16}$$

where $\{\tilde{S}\}$ is the eigenvector in the coordinates of $\{S\}$.

This model of the bandsaw as a moving rectangular plate has been well developed by previous researchers. A comparison of the results of the computer program written for this work to the results in the literature is given in Appendix B. Also included in Appendix B is a comparison of experimental and calculated blade stiffnesses.

Modelling Tooth Deflection

The Galerkin method is not convenient when irregularly shaped boundaries, such as the toothed edge of a bandsaw, must be represented. For this reason, the following approximation is used for calculating the tooth-tip stiffness. A free body diagram showing the cross-section of the blade and the tooth is shown in Figure 3-3. The tooth is cantilevered from the edge of the blade and has a lateral force, F, acting on the tooth-tip. The equilibrium equations are:

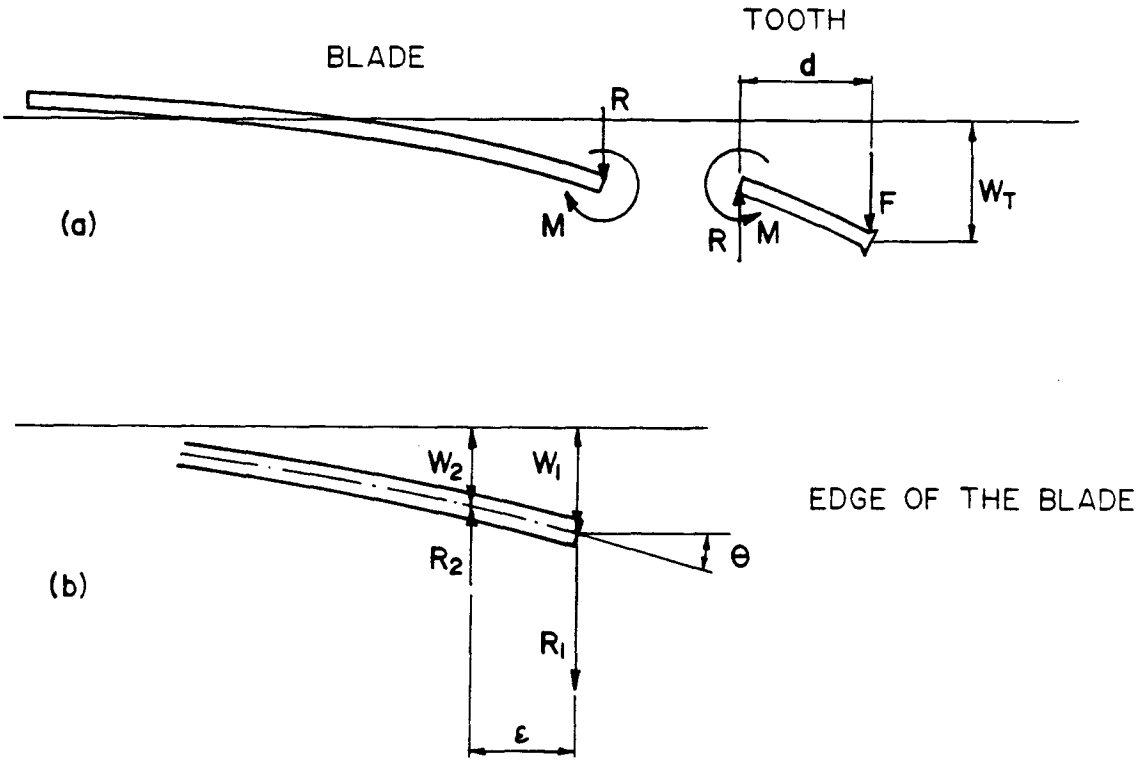

Figure 3-3. Free Body Diagram of the Blade and a Tooth

$$M = Fd \tag{3.17}$$

$$R = F \tag{3.18}$$

where d is the depth of the tooth. The moment, M, and force, F, acting on the edge of the blade and the rotation of the edge, θ, can be approximated by a wrench made up of two loads, R_1 and R_2, separated by a small distance, ε.

$$R = R_1 - R_2 \tag{3.19}$$

$$M = (R_1 - R_2)\varepsilon/2 \tag{3.20}$$

$$\theta = (w_1 - w_2)/\varepsilon \tag{3.21}$$

where

$$R_1 = F(1/2 + d/\varepsilon) \tag{3.22}$$

$$R_2 = F(1/2 - d/\varepsilon) \tag{3.23}$$

The deflections w_1 and w_2 can be calculated by applying the loads R_1 and R_2 to the plate model. The tooth itself has a cantilevered bending stiffness K_t which is proportional to the cube of the plate thickness. The deflection of the tooth-tip is

$$\begin{aligned} w_t &= w_1 + \theta * d + F/K_t \\ &= w_1 + (w_1 - w_2)d/\varepsilon + F/K_t \end{aligned} \tag{3.24}$$

The tooth-tip stiffness is equal to F/w_t.

Flexibility Matrix

In the development that follows a flexibility matrix [A] for the part of the blade that is in possible contact with the sawn surfaces is needed. The degrees of freedom in this case are the lateral deflections rather than the generalized Galerkin coordinates. The flexibility matrix is generated by first specifying the locations of the degrees of freedom, say a grid pattern. A column of [A] is the

vector of the deflections for a unit load at one node. These deflections are calculated with the Galerkin development given above. The flexibility matrix includes the degrees of freedom of the teeth.

THE CONTACT BETWEEN THE BLADE AND THE SAWN SURFACES

The problem of determining the amount of contact between a bandsaw blade and the saw surfaces will be described in terms of constraining an elastic body between two arbitrary parallel surfaces. (For the analysis developed here the surfaces are assumed to be perfectly rigid and frictionless.) The difficulty in solving contact problems is that the zone of contact is not known. Since the contact area changes, the relationship between force and deflection is nonlinear.

A number of methods, including variational methods with penalty functions and load increment techniques, have been developed for solving contact problems. The method chosen for this thesis follows, with some modifications, the method developed by Okamoto and Nakazawa [1979] and expanded upon by Tseng [1980], for solving contact problems in conjunction with a finite element procedure (or any method that produces a stiffness matrix for a discretized body). In this study the method is slightly altered in that the flexibility matrix instead of the stiffness matrix is used. This flexibility matrix for the bandsaw is generated from the Galerkin solution of the continuous plate model by the method descibed in the previous section.

The details of the contact algorithm are given in Appendix C.

REPRESENTATION OF THE LATERAL CUTTING FORCE

There are, as yet, no experimental results showing how the lateral cutting forces vary along the length of the cut. The only available indicator of the lateral cutting force is the motion of the front edge of the bandsaw during cutting, as shown in Figure 2-3. If there were no contact between the blade and the sawn surfaces then the deflection of the blade would be directly proportional to the lateral cutting force. However, contact does occur, so the indicator is imperfect, but is the best available.

In the absence of any direct information on how the lateral cutting forces vary along the length of the cut, two artificial methods of generating a disturbing force are used.

Simulation of the Cutting Force Around a Knot

The first disturbing force to be considered is one similar to that existing when cutting around a knot. This disturbance furnction will be used in much the same way that a unit step input is used to evalulate the response of control systems To approximate the variations in grain direction and wood density around a knot that would cause a saw to deviate, a potential or hardness function is used and defined as

$$\varphi = \begin{cases} C/r_i & ; r < r_i \\ C/r & ; r_i \le r \le r_o \\ 0 & ; r > r_o \end{cases} \tag{3.25}$$

where

$$r = \sqrt{y^2 + z^2}$$

is the radial distance from the center of the 'knot'. The axis of the knot is parallel to the x-axis of the blade. Outside the radius r_o the knot has no effect and within the inside radius, r_i, the knot has

a high uniform hardness. To convert hardness to a lateral cutting force the gradient of the hardness function in the lateral, z, direction is taken:

$$F(y,z) = -\frac{\partial\phi}{\partial z} = \begin{cases} \dfrac{Cz}{\left(y^2+z^2\right)^{3/2}} & ; r_i \le r \le r_o \\ 0 & ; \text{otherwise} \end{cases} \tag{3.26}$$

The basis for this approach is that the change in density results in different forces acting on the two sides of the tooth. The net lateral force is then proportional to the gradient of the density.

For values of $z \neq 0$ the function F(y,z) first increases from zero to a maximum when y=0 then decreases to zero as y is increased. This corresponds to the expected lateral forces around a knot where in the clear wood on either side of the knot the lateral forces are near zero but reach a maximum near the center of the knot.

General Cutting Forces

The 'knot' function presented above provides a reasonable representation of a general feature seen in much of the blade deflection data. However, the experimental data shows that blades are subjected to multiple disturbances of varying lengths and amplitudes. To investigate the character of the actual cutting forces the specta of the blade deflection data were taken. Typical cutting deflection data and their spectra are shown in Figures 3-4 and 3-5. The spectra show a 1/f behavior, where f is the frequency (measured in units of cycles/sec. or cycles/unit length). This result is typical and applies for straight as well as cuts with high deviations.

The spatially dependent characteristics of wood that affect the cutting forces, such as density and the direction dependent strength properties appear to be well suited to being represented by slowly varying functions. An examination of the surface of a piece of wood shows the general direction of growth, but there are variations and irregularities. On a smaller scale these variations have smaller variations superimposed on them.

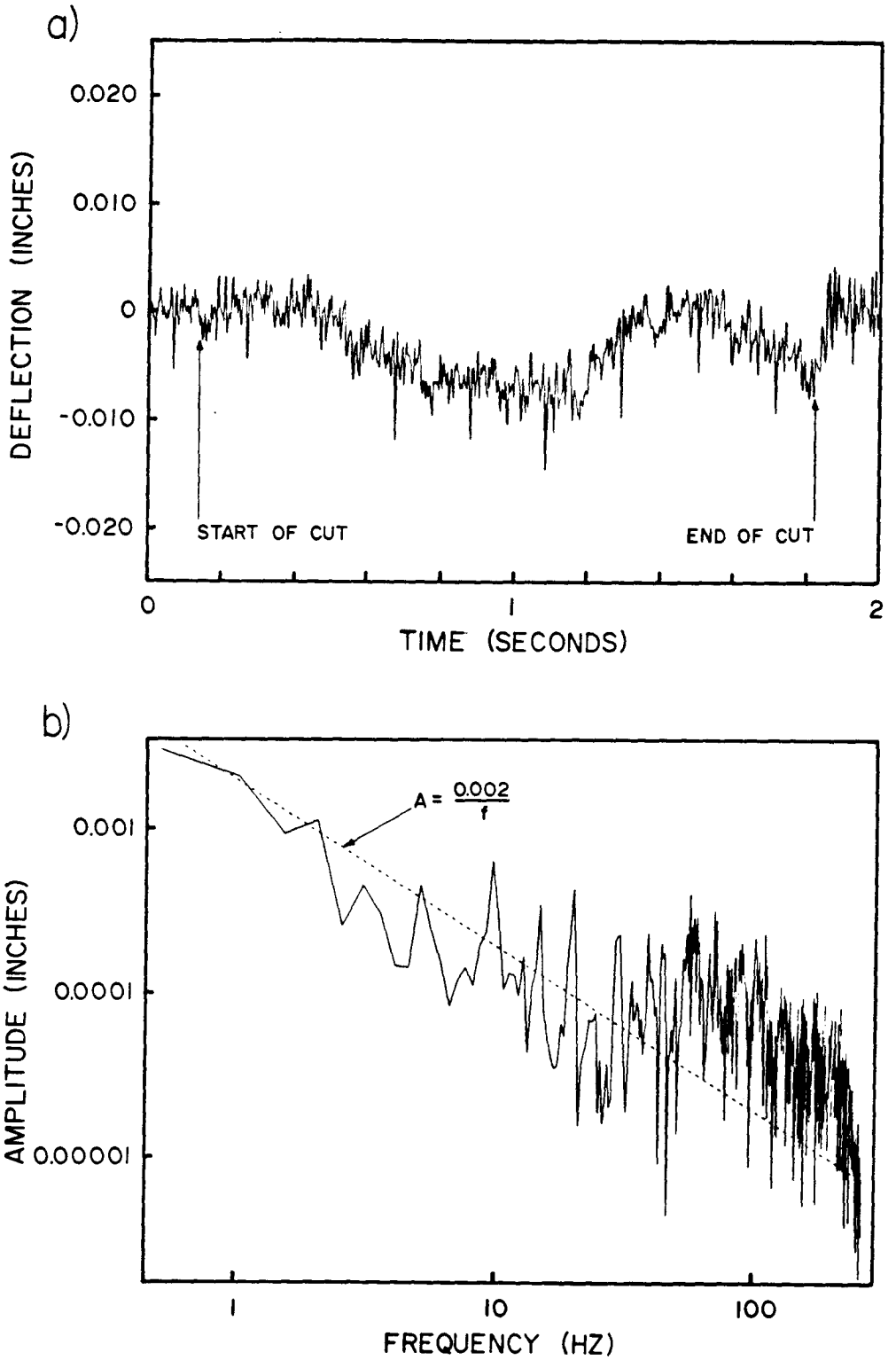

Figure 3-4. Blade Deflection During Cutting: Example 1.
a) Displacement of the Front Probe
b) Spectrum of the Displacement at the Front Probe

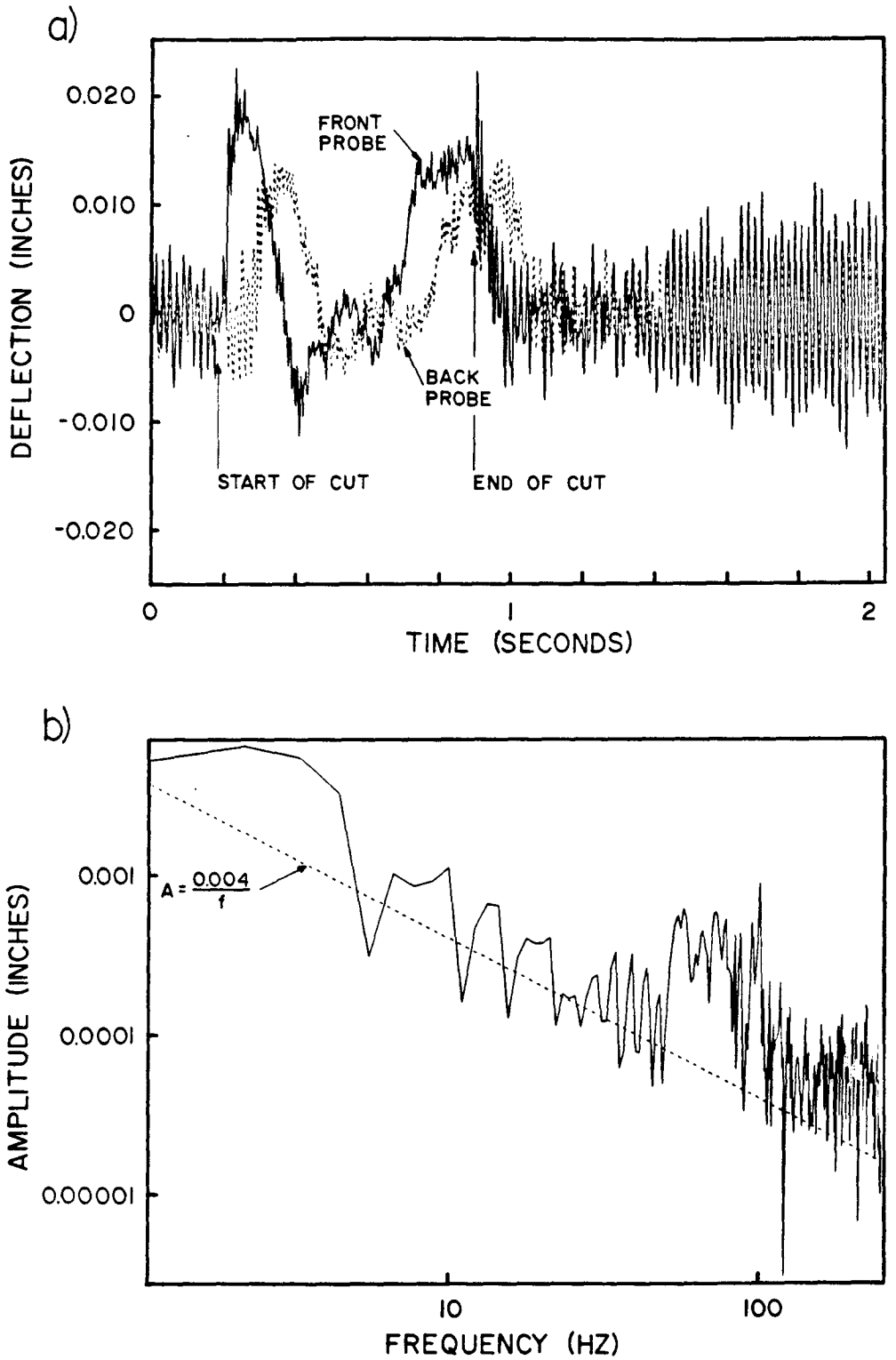

Figure 3-5. Blade Deflection During Cutting: Example 2.
a) Displacement at Front and Back Probes
b) Spectrum of the Displacement at the Front Probe

It is proposed that the lateral cutting force along the length of the cut be simulated with by function having a 1/f characteristic. If the deflected paths of the blade produced by the simulation are comparable to measured blade deflections, then it is possible to estimate the effect of changes in blade design on sawing variation. These concepts are discussed in the next chapter.

The algorithm used to generate a function with a 1/f frequency characteristic follows the one given by Peitgen and Saupe [eds., 1988]. First a series of Gaussian random numbers, z_i, is generated that has a mean of zero and a variance of σ^2. If y_{ij} are random numbers uniformly distributed on the interval [0,A], then z_i will be approximately Gaussian if it is calculated as

$$z_i = \sigma\left[\frac{1}{A}\sqrt{\frac{12}{n}}\sum_{j=1}^{n} y_{ij} - \sqrt{3n}\right] \tag{3.27}$$

The values A = 1 and n = 12 were used.

To produce the series representing the force along the length of the cut, F_i, the series of z_i is then passed through a low pass filter with a 1/f roll-off and a very low cutoff frequency (measured in cycles per unit distance), f_c. A recursive filter was used:

$$\begin{aligned} F_1 &= z_1 \\ F_i &= \frac{2\pi f_c \Delta\tau \cdot z_i + F_{i-1}}{(1 + 2\pi f_c \Delta\tau)} \quad ; i = 2,3,4,\ldots,N_c \end{aligned} \tag{3.28}$$

where

$\Delta\tau$ = the incremental distance along the cut

N_c = the total numbere of increments along the cut.

The magnitude of the fractal force is controlled by the standard deviation, σ, and different functions can be generated by changing the seed value supplied to the random number generator. The lateral force on each tooth is assumed to be equal, which is a reasonable assumption for

shallow depths of cut, but is probably not a good assumption for deep cuts. An assessment of this assumption is given in Chapter 4.

SIMULATION OF THE COMPLETE SAWING SYSTEM

Mathematical descriptions of the elements of the sawing process have been developed in this chapter, but they have not yet been assembled into a system that simulates the whole process. The construction of the simulation model is presented by describing the main steps of the computer program.

In practice, the sawn surfaces are parallel and separated by an amount equal to the width of the tooth less springback and the tooth marks. However, in the geometry of the contact problem, it is only the distance that the blade can move laterally before it contacts the sawn surface that is essential. This distance is, by definition, the clearance gap, g. From the point of view of the geometry of the contact problem the thickness of the blade is not important. In this model, therefore, the sawn surfaces are assumed to be separated by an amount equal to twice the clearance gap.

The sawn surfaces are created by the teeth. If the variable S represents the deflection of the teeth from the ideal cutting plane at all points through the cut, then the sawn surfaces are defined as

$$V = S + g \tag{3.29}$$

and

$$U = S - g. \tag{3.30}$$

Because the solution algorithm works with discrete points along the length of the cut and with discrete locations on the blade and the sawn surfaces, one task of the computer program is to

generate grid systems that define these points.

Step 1) The user sets all the blade parameters, the clearance gap, the variables that define the cutting forces, and the dimensions of the "wood".

Step 2) The user sets the forward increment that the blade moves between each time step, $\Delta\tau$. The total number of increments along the cut is equal to N_C.

Step 3) Determine the maximum number of teeth, N_T=Int(D_C/P)+1, that could be in the cut. (D_C is the depth of cut and P is the tooth pitch.) The teeth are positioned symmetrically through the depth of the cut at the instant that the blade deflection is calculated.

Step 4) A grid of nodes on the blade that could come into contact with the sawn surfaces is formed consisting of N_y nodes across the width of the blade and N_T nodes through the depth of cut. See Figure 3-6. Also, a grid of nodes on the sawn surface is formed of N_T nodes located symmetrically through the depth of cut and N_C nodes along the length of the cut. The nodes are the locations of the teeth at each increment along the cut. See Figure 3-7. The deflection of the teeth at these nodes defines the sawn surface. These deflections are given the variable S_{it}, where i = 1,2,3,...,N_C and t = 1,2,3,...,N_T.

Step 5) Generate the flexibility matrix, [A],of the blade for the nodes, including the teeth and any arbitrarily located "probe" positions.

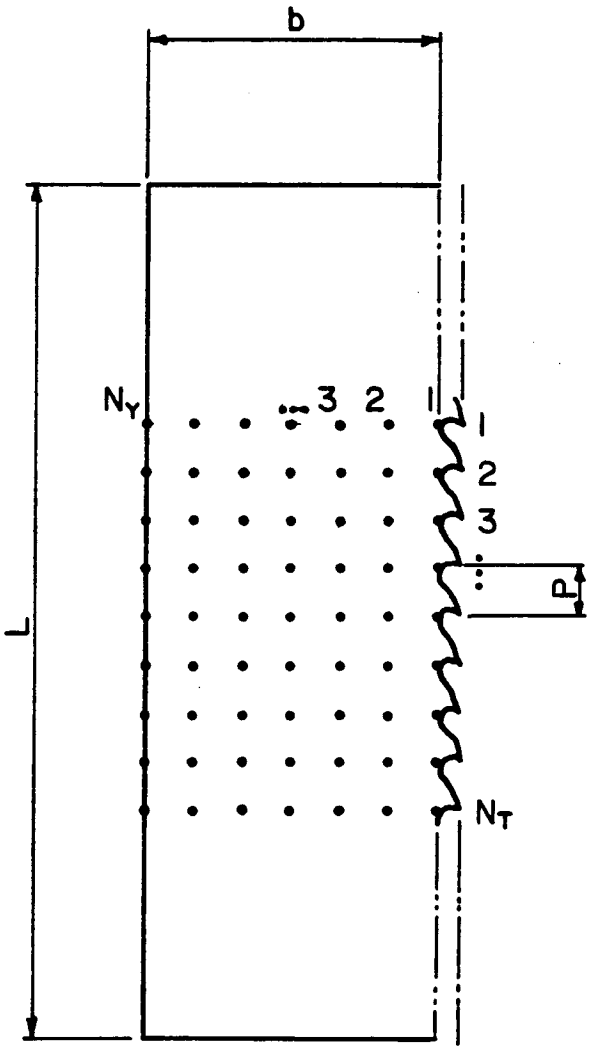

Figure 3-6. Locations of the Contact Nodes on the Blade.

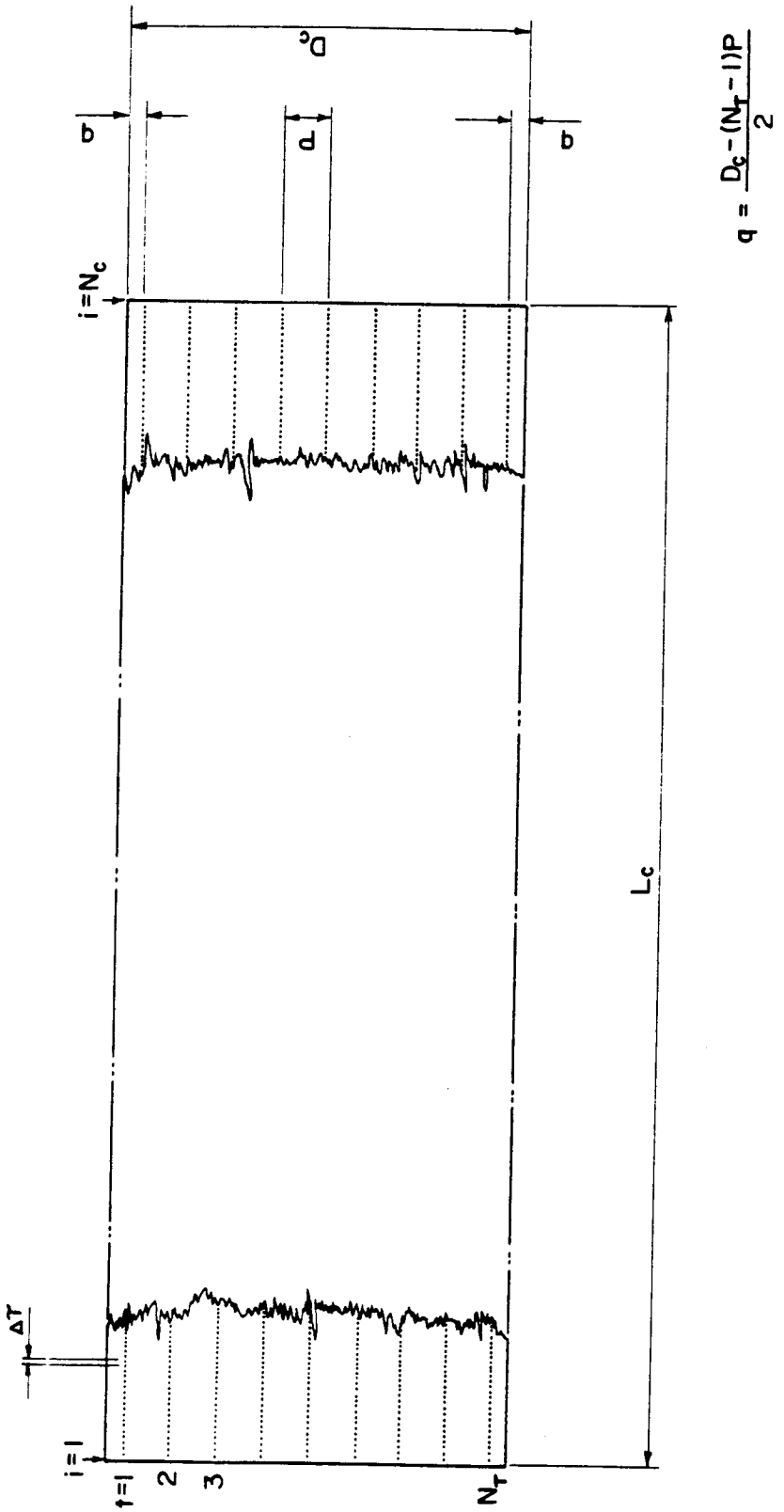

Figure 3-7. Location of Nodes on the Sawn Surfaces.

Step 6) Generate the lateral force, F_i, for each tooth for the whole length of the cut ($i = 1,2,3,...,N_c$). Either the 'knot' function or a fractal function is used. The same lateral force is applied to each tooth for each increment.

Step 7) Start to incrementally advance the "wood" onto the blade. For the first increment only the teeth are in contact with the "wood": the body of the blade is unconstrained.

Step 8) Determine the constraints for each node on the blade. These constraints are $U_{nt} = S_{jt} - g$ and $V_{nt} = S_{jt} + g$, where j is the number of the position along the sawn surface physically closest to the node n on the blade.

Step 9) Calculate the deflection at each node of the blade with the contact algorithm. See Appendix C for details.

Step 10) The deflections of the teeth, x_T, are stored as the newest addition to the cut path, S_{it}.

Step 11) Advance the "wood" one increment, $\Delta\tau$.

Step 12) Determine the position of the sawn surfaces that constrain the nodes. The teeth are never constrained as they have the assumed ability to cut laterally.

Step 13) Repeat steps 8 though 12 until the whole length of the "wood" has advanced past the blade.

The output of the program is the cut path S_{it}. The time histories of the blade deflections at arbitrary "probe" locations are also available. The mean and standard deviation of the surface S_{it} and the effective stiffnesses K_o, Q_o, and K_{eq} (as discussed in Chapter 4) are also calculated.

> Science is built with facts, as a house is built with stones. But a collection of facts is no more a science than a heap of stones is a house.
>
> Jules Henri Poincare

CHAPTER 4

NUMERICAL RESULTS AND DISCUSSION

This chapter has five objectives:

1) To show and discuss how bandsaw blade design parameters affect the tooth-tip stiffness and the cross-stiffness between the tooth-tip and points on the body of the blade.

2) To use the cutting simulation model to investigate the mechanics of blade deflection and recovery caused by the knot-like cutting force.

3) To explore the use of a fractal cutting force representation to estimate the effect of changes in blade design on cutting accuracy.

4) To present the results in nondimensional form.

5) To examine how the depth of cut affects sawing behavior.

EFFECT OF BLADE PARAMETERS ON TOOTH-TIP STIFFNESS

Of the many blade parameters involved in bandsawing, most are controlled by the saw filer and others are dictated by the process requirements. The filer chooses the thickness of the blade, the bandmill strain, the tooth design, and the amount of roll tensioning. The selection of blade width is somewhat arbitrary because band steel is produced in standard widths and because the blade becomes narrower at each sharpening. The decision then is to specify the initial blade width and how narrow the blade becomes before it is discarded. The filer also controls the in-plane bending stresses resulting from the interacting effects of backcrown, wheel tilt, wheel crown and blade overhang. These effects are not fully understood, but the result is that the front edge of the blade is stiffer than the back, and stiffer than a blade without these in-plane bending stresses.

The filer does not control the span length, which must be greater than the depth of cut. There are, however, devices that automatically adjust the position of the top guide as the depth of cut changes. The blade speed is generally set by the bandmill manufacturer and is usually between 8000 and 10000 fpm.

For the conditions specified in Table 4-I (based on a common five foot bandmill) the blade model developed in Chapter 3 predicts a tooth-tip stiffness of 182.4 lbs/inch. This stiffness was calculated for a tooth located at mid-span. The predicted effect of a change in any of the above parameters is shown in Figure 4-1. These results are similar to those obtained by Taylor and Hutton [1991]. The parameters can be grouped by their relative significance, starting with the most significant, as:

1) Plate thickness, span and strain parameter
2) Strain, in-plane bending and tensioning
3) Blade width and tooth depth
4) Tooth bending stiffness and speed

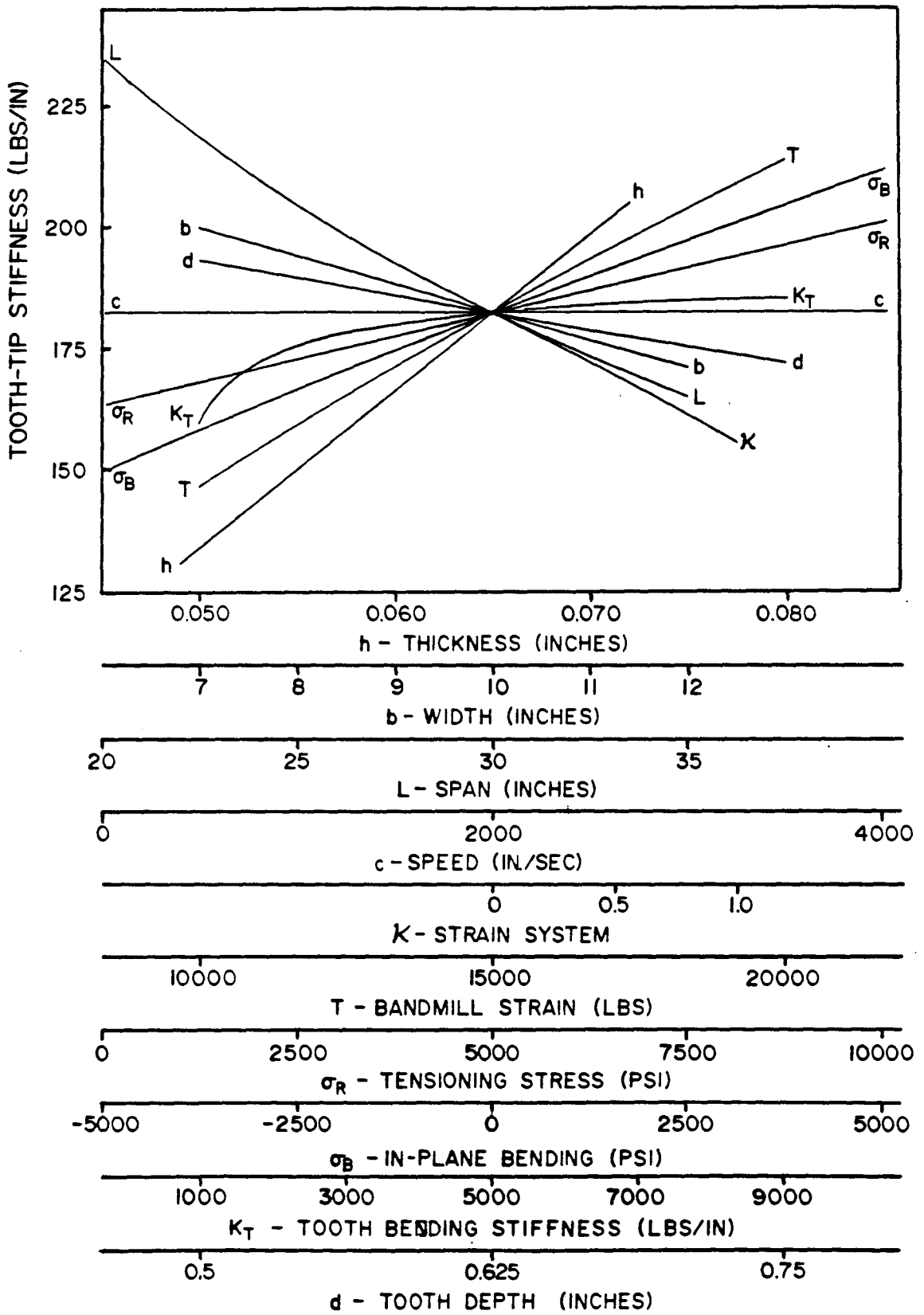

Figure 4-1. Effect of Blade Parameters on Mid-span Tooth-tip Stiffness.

Table 4-I. Parameters for the Blade Model

Strain	T = 15,000 lbs
Blade width	b = 10 inches
Blade thickness	h = 0.065 inches
Span	L = 30 inches
Tensioning	e = 1 inches
	σ_T = 5,000 psi
Bending stress	σ_B = 0 psi
Tooth bending stiffness	K_t = 5,000 lbs/inch
Tooth depth	d = 0.625 inches
Strain parameter	κ = 0.0
Speed	c = 2,000 inches/sec

There are three components to the tooth-tip stiffness of a stationary (c=0) bandsaw blade. These are, 1) the string or tie-rod stiffness due to the tensile axial load on the blade; 2) the torsional or twisting stiffness of a rectangular plate; and 3) the local bending stiffness of the plate or the teeth (i.e., the cross section of the blade does not stay rectangular). The span and the axial stress in the band determine the size of the string stiffness effect. The roll tensioning stresses, other axial stresses and the blade dimensions determine the size of the torsional stiffness effect. The blade thickness determines the size of the local bending effect.

When the blade is running there are some additional effects that affect the tooth-tip stiffness and the lateral stiffness of the blade in general. Firstly, there are extra tensile axial stresses in the blade due to the centrifugal action of the blade running around the wheels. Secondly, there is an inertial effect that affects the blade stiffness [Mote, 1965]. This inertial term is proportional to $\mu c^2(\partial^2 w / \partial^2 x)$. Lastly, the straining mechanism may not be able to keep the pressure between the wheels and the band constant if the speed is increased.

In the following paragraphs the effects of changes in a blade parameter on tooth-tip stiffness are described in more detail. The large loss of stiffness due to reduced blade thickness accounts for the difficulty in using thin blades. The reduction in stiffness has three causes; all related to the fact that the bending stiffness of a plate is proportional to the cube of the thickness:

1) The deflection of the edge of the blade that supports the tooth increases as the blade becomes thinner. For thinner blades, the deflection of the blade becomes more localized in the region near the point of application of the load. In other words, a thick blade does not bend much when viewed in cross-section, whereas a thin blade shows much bending. See Figure 4-2.

2) The bending stiffness of the tooth itself, K_t, decreases as the blade thickness decreases. As a result, the tooth-tip deflects relative to the edge of the blade. For the blade parameters examined, it is acceptable to model the tooth as a rigid cantilevered beam that rotates about the edge of the blade as long as the tooth bending stiffness is greater than 2000 lbs/inch .

3) The moment stiffness of the edge of the blade that supports the tooth also decreases as the blade thickness decreases. This allows the whole tooth to rotate, which increases tooth-tip deflection. The moment on the edge of the blade increases as the depth of the tooth, d, increases, so increasing the depth of the tooth increases tooth-tip deflection.

Since increasing tooth bending stiffness does not have much effect unless the tooth is very weak, it would be better to reduce the tooth depth, d, as this reduces the moment on the edge of the blade, and, hence, the rotation of the tooth and the deflection of the tooth-tip. Using shallower teeth would also increase the bending stiffness of the teeth.

The effect of the in-plane stresses, whether caused by tensioning, strain or in-plane bending, is significant. If the axial stress at the front edge of the blade is increased then the tooth-tip stiffness also increases.

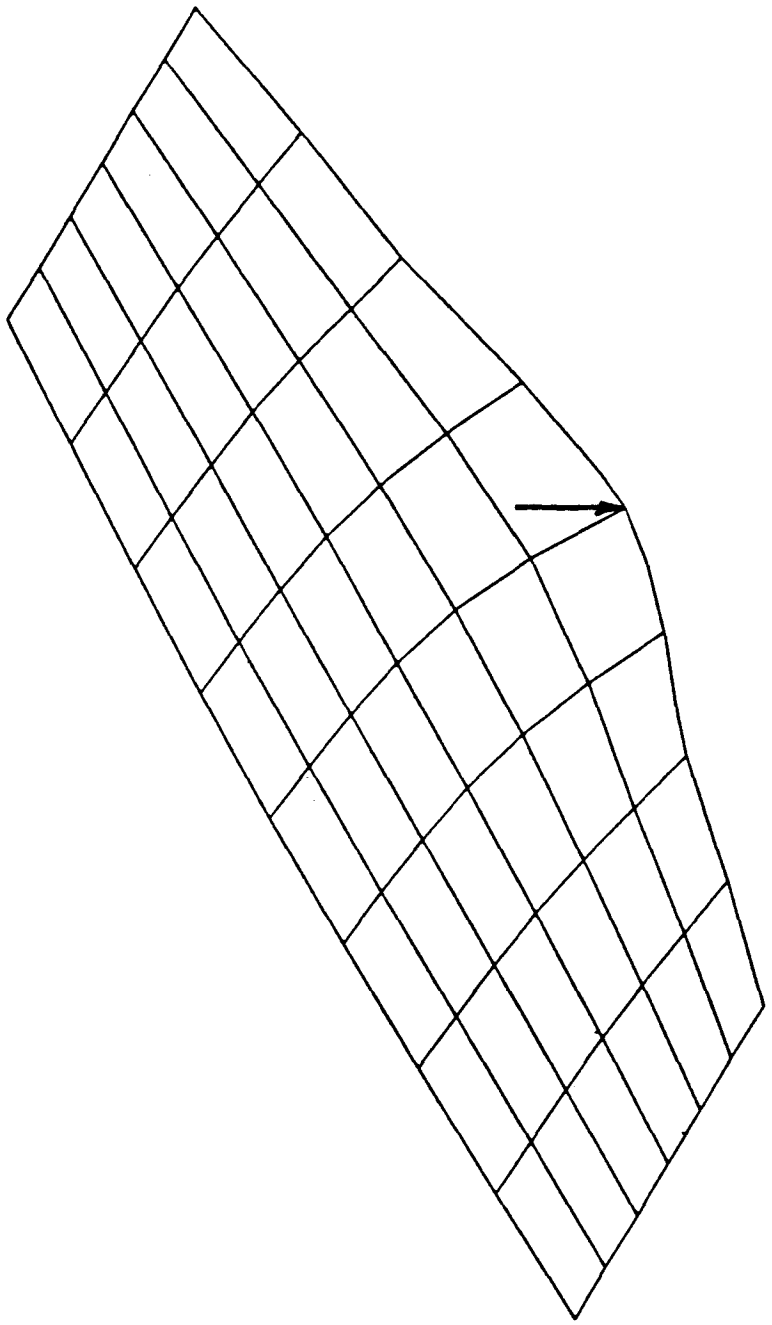

Figure 4-2. Deflected Shape of a Blade for a Load on the Front Edge of the Blade.

The effect of blade width, which shows that narrower blades are stiffer than wider blades, is somewhat non-intuitive. Firstly, the strain was not changed, so the axial stress is increasing, which causes the lateral and torsional stiffness of the blade to increase. Secondly, the deflection of wide blades caused by a load on the edge is more localized. In other words, the load is not transmitted to the center or back of the blade.

The effect of blade speed, c, on tooth-tip stiffness is dependent on the strain system parameter, κ. When $\kappa=0$, which is the case for a well maintained bandmill, the top wheel of the bandmill can translate to keep the pressure on the band constant. As the speed increases the component of band axial stress due to centrifugal effects increases, which increases the overall stiffness of the bandsaw. At the same time the inertial component of the blade stiffness due to the axial translation of the blade is decreasing. The effect of the additional axial stress due to the centrifugal effects exactly compensates for the loss in inertial component of the stiffness. Hence, when $\kappa=0$, the blade stiffness is independent of speed. If κ is not zero then, as the speed is increased, the top wheel does not move enough to maintain a constant pressure between the wheels and the band. Consequently, the sum of the axial stresses due to wheel pressure and the centrifugal effects does not increase enough to counter the loss in inertial component of the stiffness. The net result is a reduction in lateral blade stiffness as the band speed is increased.

CUTTING THROUGH A SIMULATED KNOT

In this section, the response of the blade to a simple disturbance that could represent the forces encountered when cutting near a knot is investigated. With such a disturbance it is possible to observe the mechanisms that govern blade deflection. In the results that follow, the disturbance force function will not be changed. The parameters of the 'knot' function (Equation 3.25) are C = 40 lb-in^2, r_i = 1 inch, r_o = 10 inches. The centre of the knot is located at a point 20 inches along

the cut. Figure 4-3 shows how the lateral force varies along the cut for paths that are 2, 3, and 4 inches away from the center of the knot. Only the results from the path 2 inches from the center of the knot will be used because for this case the maximum force is 10 lbs., which is in the range of the peak lateral force near a knot found by St. Laurent [1971]. The maximum force is reached at a point 20 inches into the cut.

A plot of the resulting cut path for the base bandsaw specified in Table 4-I is shown in Figure 4-4. The force acts on a tooth at mid-span and the contact nodes are on a line across the mid-span of the blade, (i.e., the geometry of cutting a 1 inch thick board at mid-span). As would be expected, the blade begins to deflect as the 'knot' is approached and reaches a maximum just as the force reaches a maximum. In the deflection stage the shape of the cut path is the same as that of the lateral force function: the proportionality constant being the tooth-tip stiffness.

The recovery stage is much different from the deflection stage. The blade deflection does not decrease as quickly as the force decreases. Also, the blade overshoots the ideal cutting line in the final part of the recovery stage. To understand what is happening, more information is needed than is provided by the cut path. Since contact between the blade and the sawn surfaces is occurring, it is necessary to know where the contact is occurring and how the blade has deflected.

This information is provided in Figure 4-5. The lower section shows the deflections of the tooth, the front and back edges of the blade, and the middle of the blade at each point during the cut. The upper section shows where the contact occurred relative to the front and back edges of the blade. The direction of the arrow indicates the direction of the contact force acting on the blade. For example, at about 33 inches into the cut, contact is occurring only at the back edge of the blade and is restraining the blade from deflecting toward the positive direction.

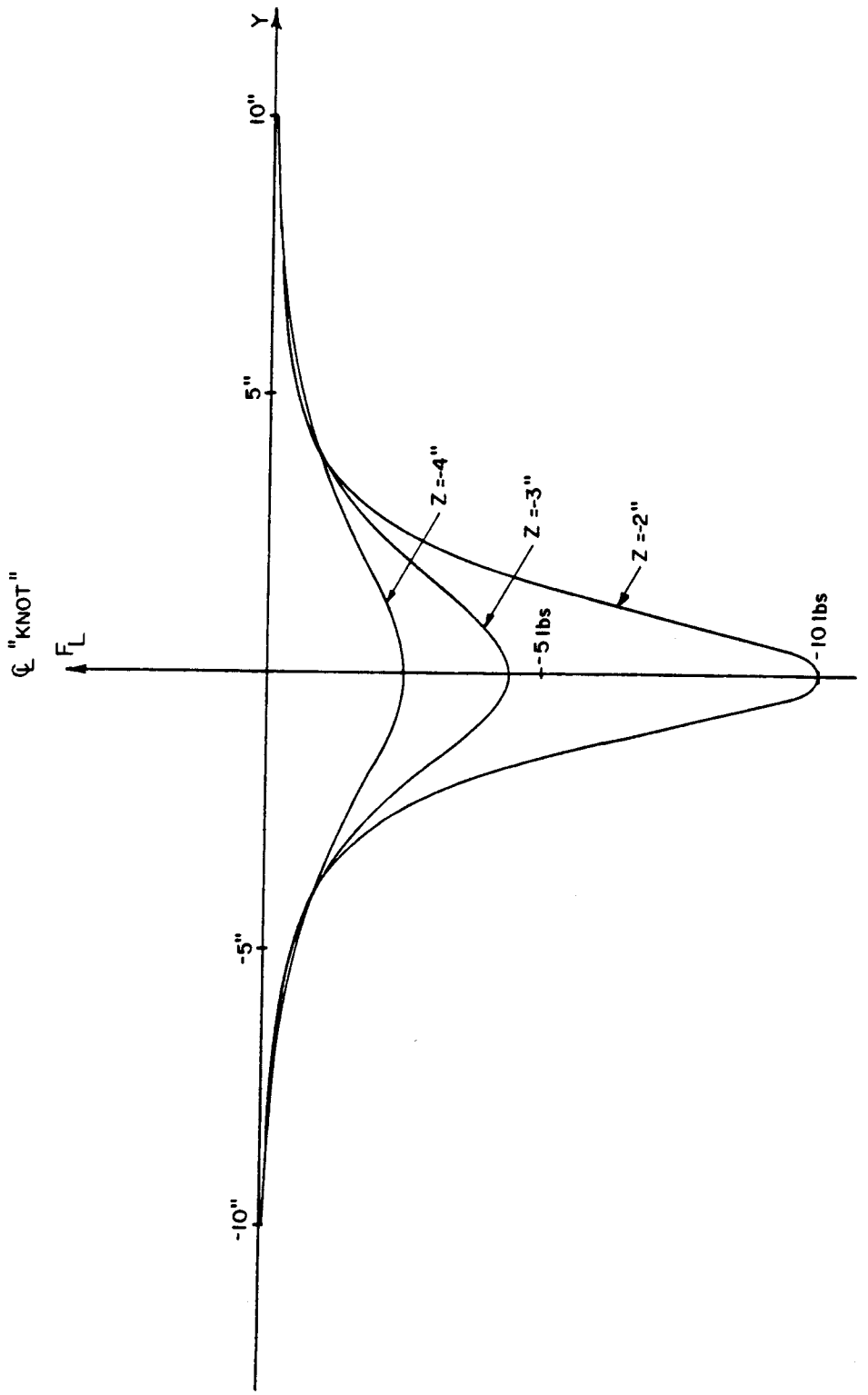

Figure 4-3. Simulated Cutting Forces near a Knot.

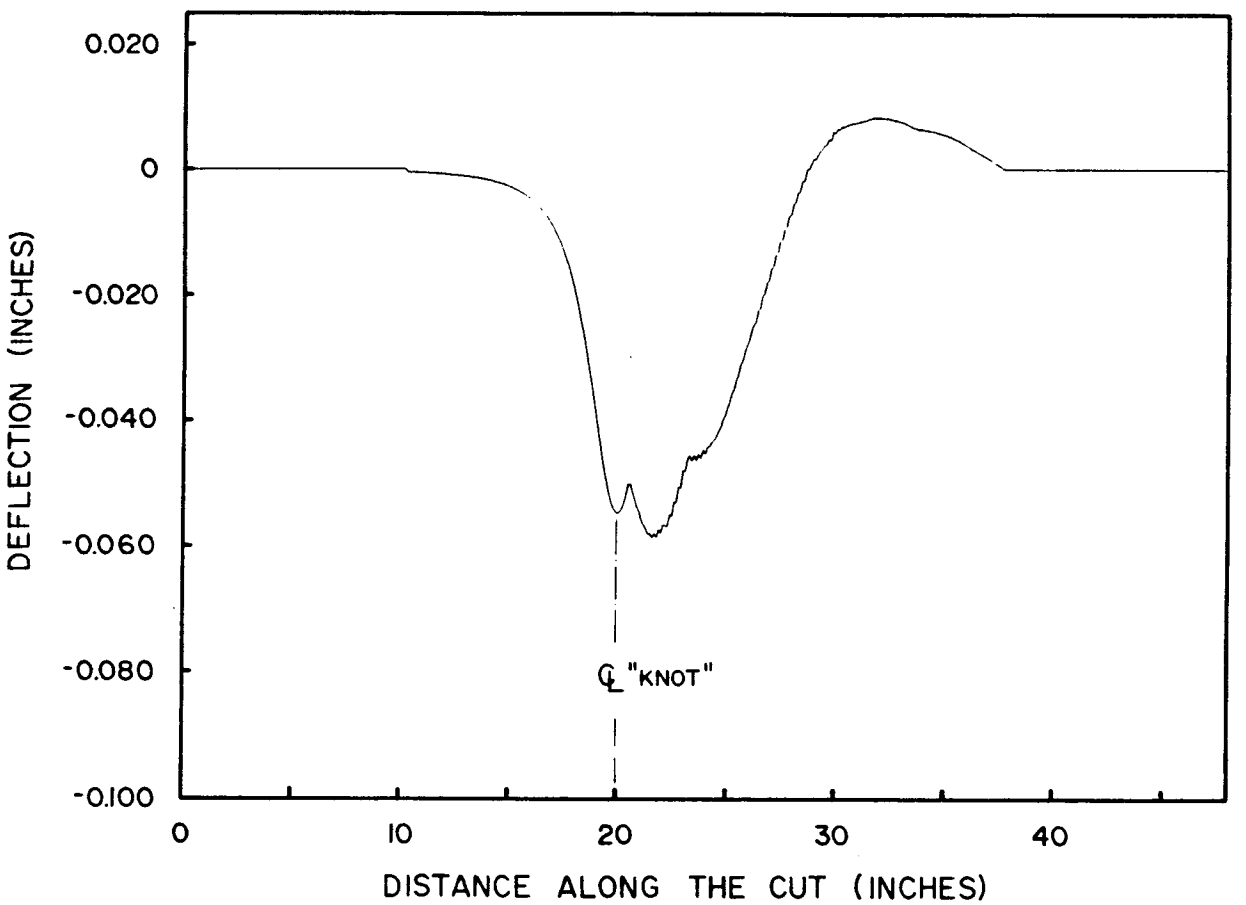

Figure 4-4. Simulated Cut Path Around a 'Knot'.

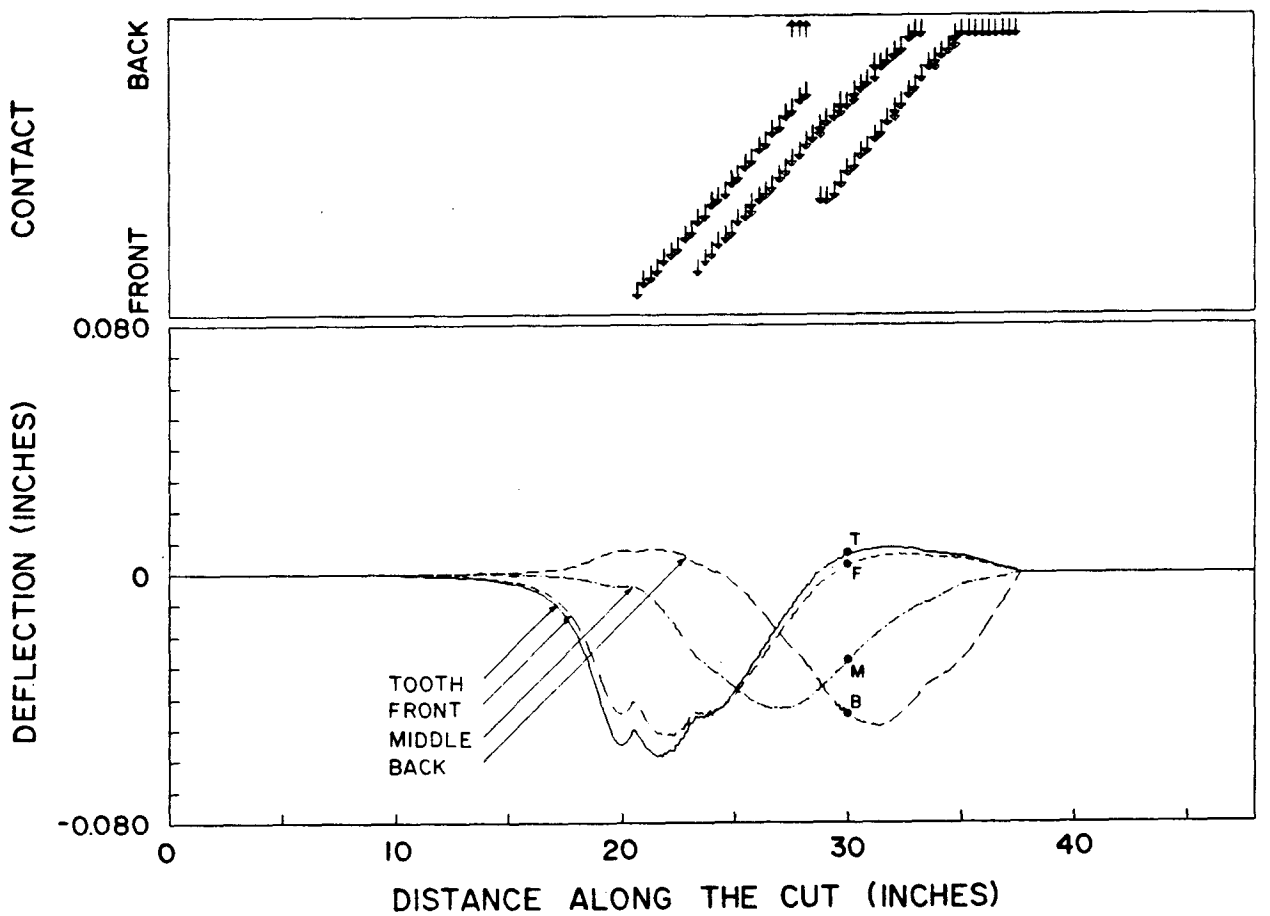

Figure 4-5. Blade Deflections and Contact for a Simulated Cut. Arrows show the Location and Direction of the Contact Forces. Lines in Lower Section show the Deflections of the Blade at Instants Along the Cut.

Figure 4-5 is a very compact representation of what happened in the cut, but some visual imagination is needed to place the blade between the two sawn surfaces because the figure contains no visual information about the clearance gap or the width of the blade. The position of the blade at various instants during the cut is shown in Figure 4-6 to aid the reader in interpreting Figure 4-5. The points labeled T, F, M, and B are for the instant when the tooth is 30 inches into the cut. Note how the blade is dragged over the bump in the sawn surface at 20 inches along the cut, and over the smaller bump at 22 inches. This progression of the contact from the front to the back of the blade is what produces the straight line groups of contact indicators. It is clearly shown that when the cut path is not proportional to the lateral force, then contacting is occurring.

Contact is guaranteed to occur at some point during the cut once the deflection is greater than the clearance gap. However, contact on the front 1/3 of the blade has the greatest effect on tooth deflection. For instance, as the tooth moves from 20 to 25 inches along the cut, the deflected shapes of the blade show that the contact at the back of the blade has a large effect on the deflection of the back of the blade, but has almost no effect on tooth deflection.

Contact does not affect the deflection stage significantly unless the gap is very small because there is very little contact, but contact does amplify and prolong the recovery stage. Contact does not affect the deflection stage as much because the blade must deflect an amount greater than the gap before contact can occur. On the other hand, the blade is almost certainly in contact when the recovery stage begins.

The effect of changes in bandsaw parameters on the behavior of the blade will now be investigated. Figure 4-7 shows how blade thickness affects the cut path. As would be expected, the thinnest blade deflects the farthest because its stiffness is the lowest. The effects of bandmill strain and tensioning are also as expected: more strain or tensioning results in more stiffness and smaller deflections. See Figures 4-8 and 4-9.

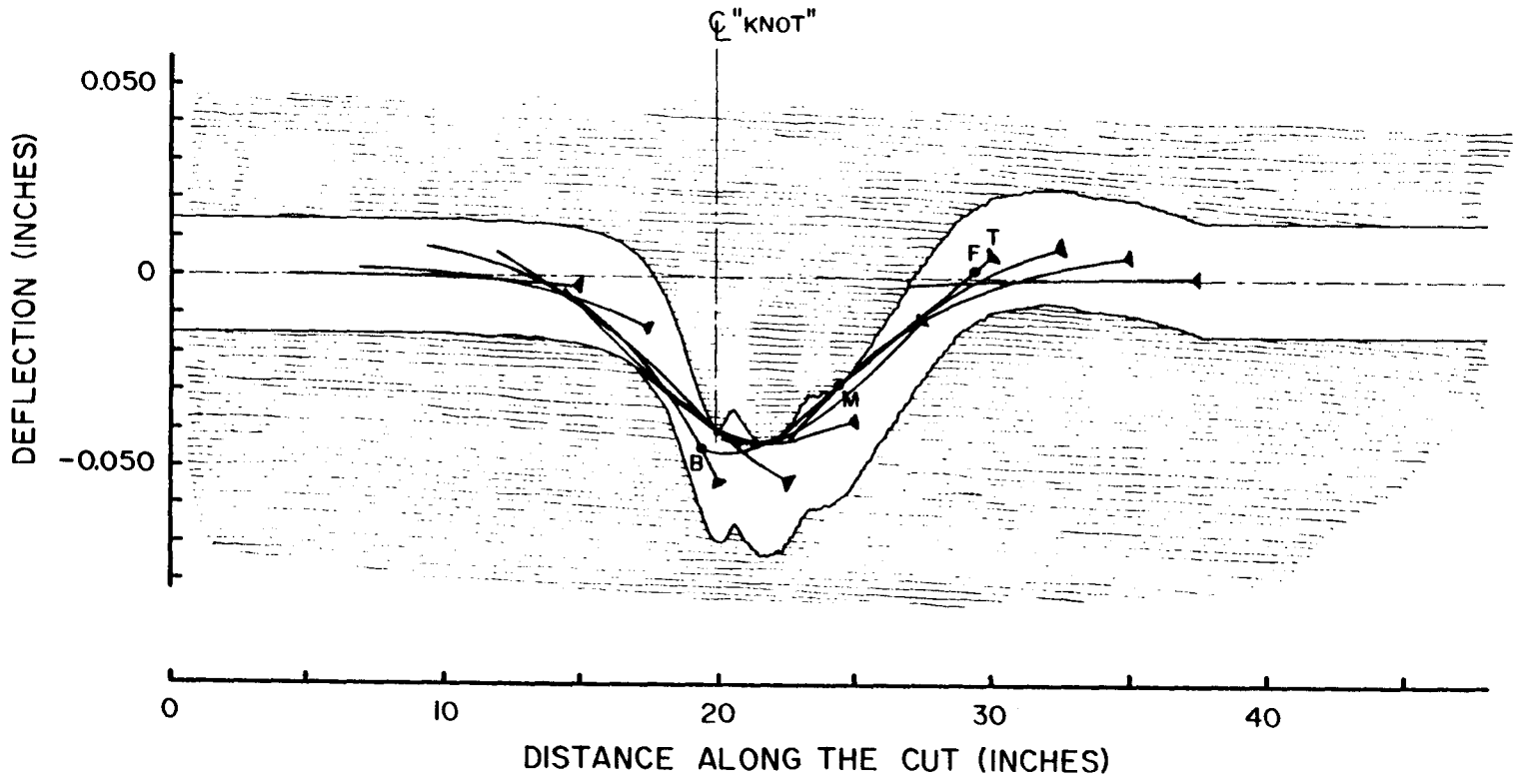

Figure 4-6. The Deflected Shape of the Blade during a Simulated Cut for the Cut Path Shown in Figures 4-4 and 4-5.

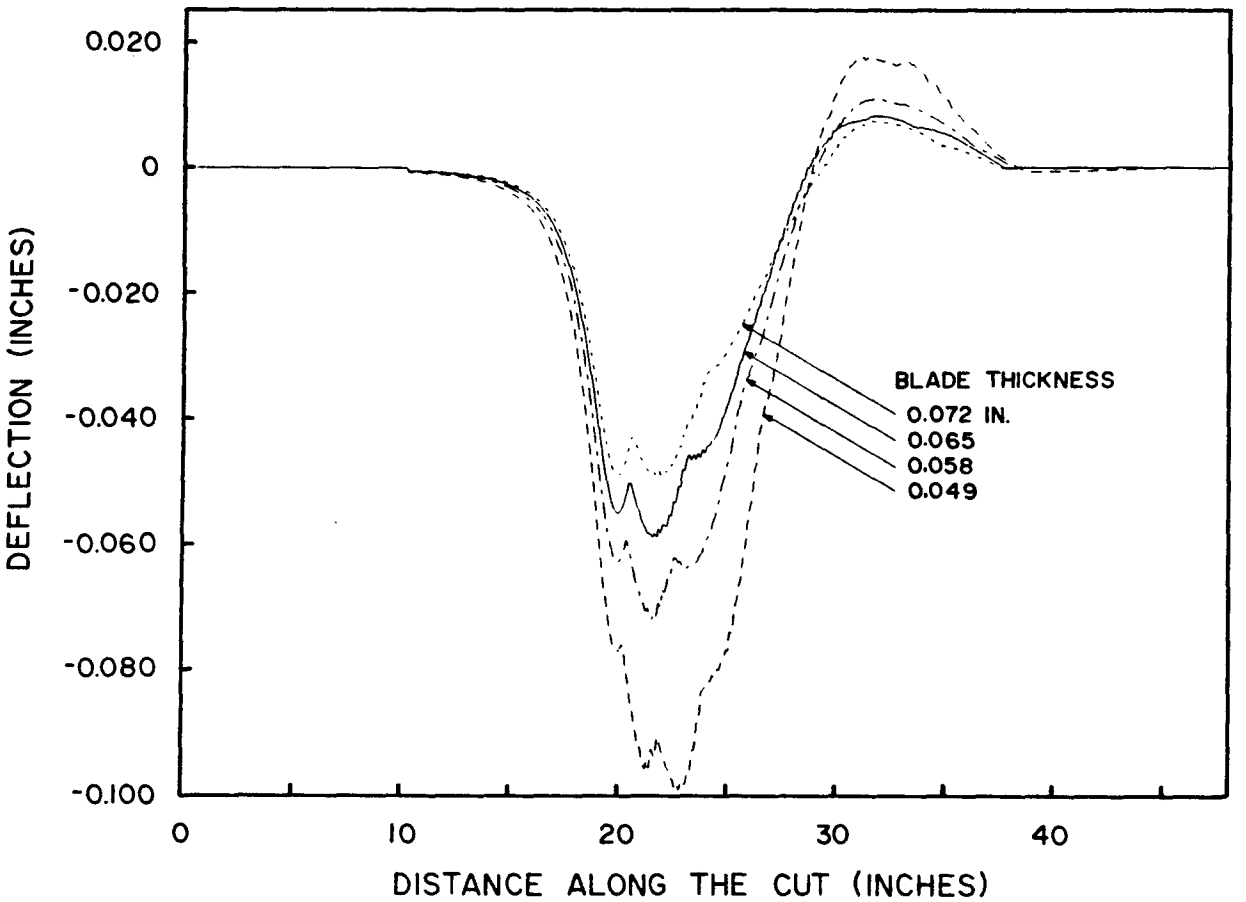

Figure 4-7. Effect of Blade Thickness on the Cut Path. All other Parameters are as in Table 4-I.

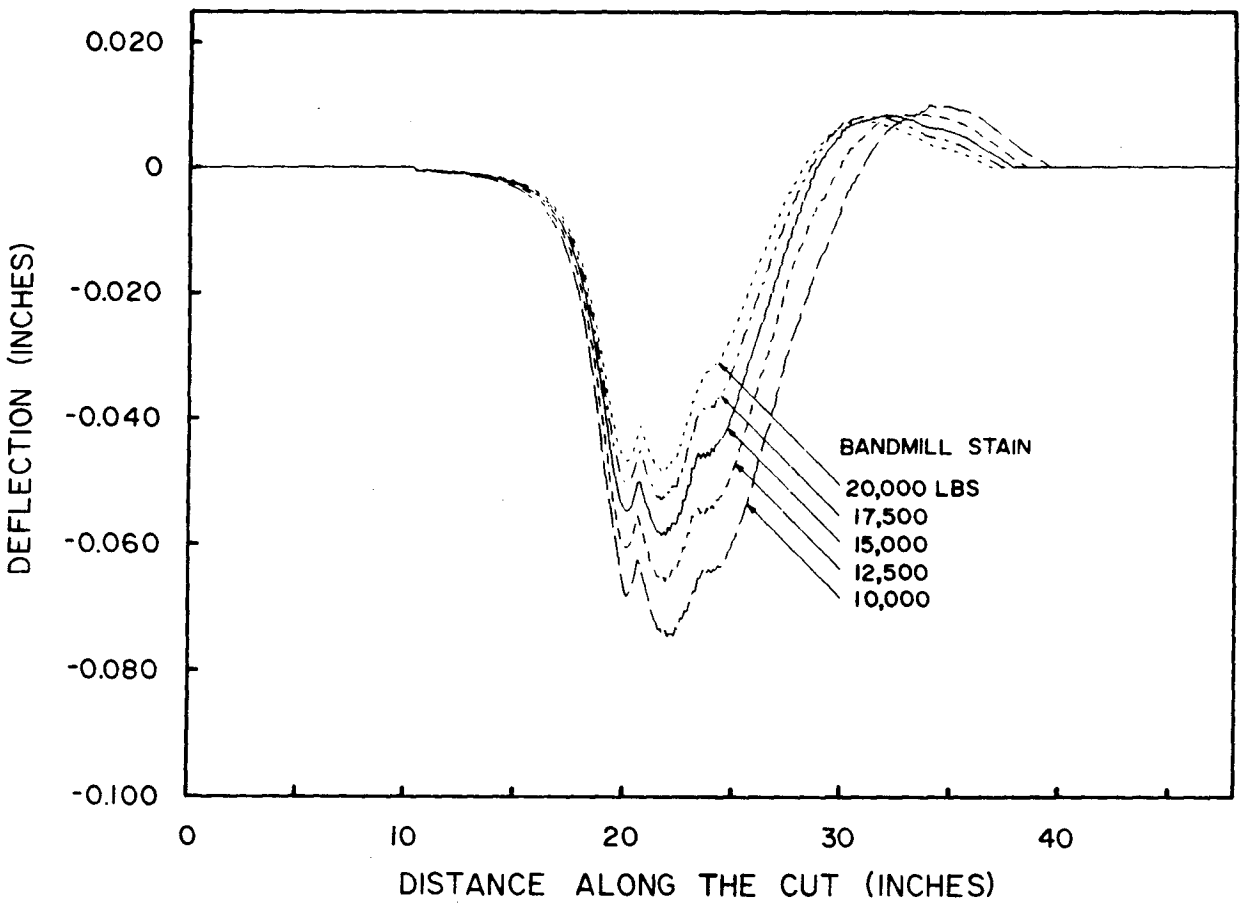

Figure 4-8. Effect of Bandmill Strain on the Cut Path. All other Paramters as in Table 4-I

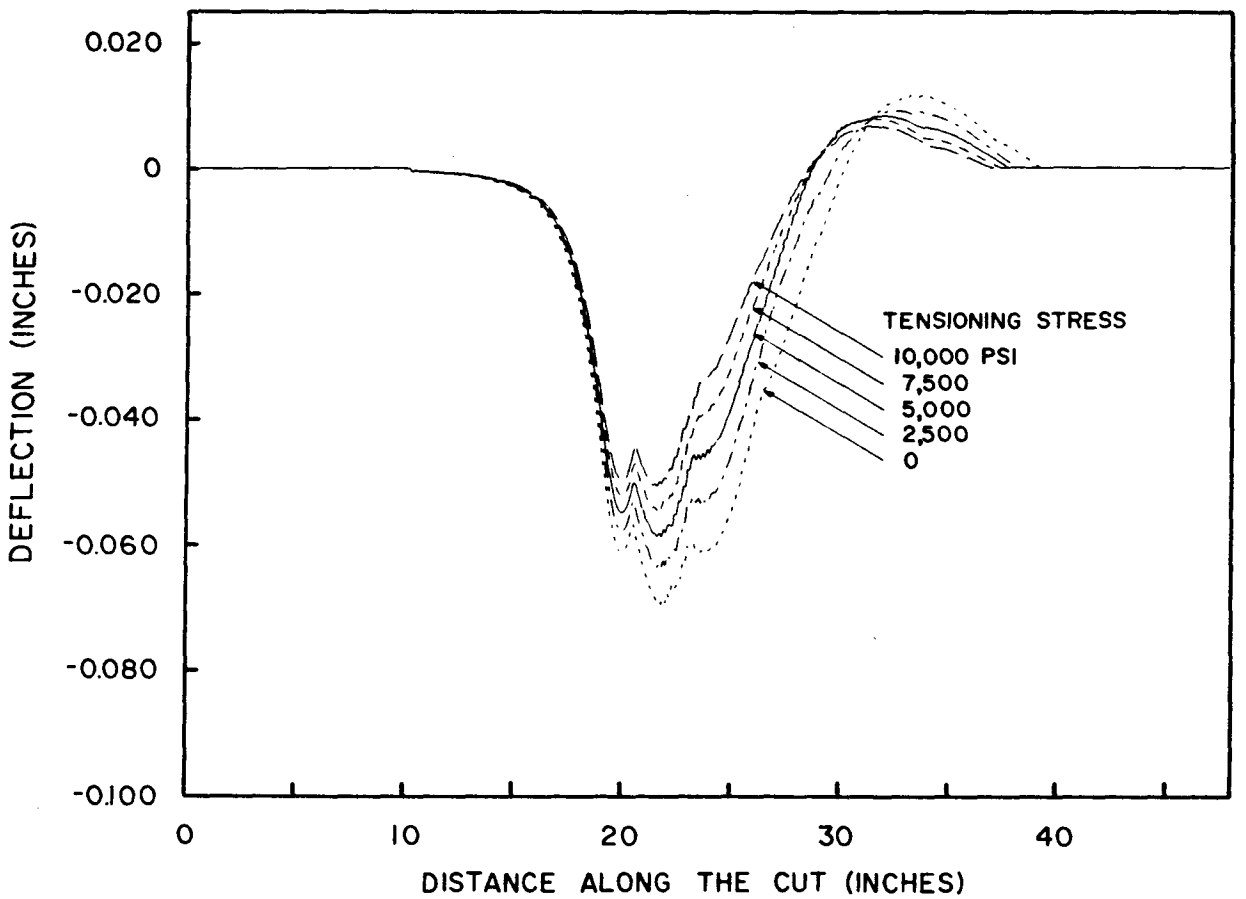

Figure 4-9. Effect of Tensioning on the Cut Path. All other Parameters are as in Table 4-I

Note that the maximum deflection often occurs after the center of the 'knot' has been passed and that the blade overshoots the ideal cutting line when returning. The contact between the blade and the sawn surfaces causes both of these phenomena.

The effect of the clearance gap is shown in Figure 4-10. The differences in blade behavior are entirely a result of the contact between the blade and the sawn surfaces. The smaller the gap the more the blade is inhibited from changing direction in the cut. This is shown most clearly for the gap of 0.005 inches, where the constraining effect of the sawn surfaces did not allow the blade to change direction even after the disturbing force had dropped away. The only reason the blade turns back is that the restoring forces of the blade pulled the front of the blade around. The same overshooting occurs when the blade returns to the ideal cutting line.

RESPONSE TO FRACTAL LATERAL CUTTING FORCES

In the previous section the response of the blade to a simple disturbance was investigated. Such a function is useful for investigating the mechanics underlying blade behavior. However, this simulation does not provide information that quantifies the cutting accuracy of the blade because the character of the lateral cutting forces is generally more complex than that of the 'knot' function. The purposes of this section are to present the simulated blade behavior with fractal force excitation and to ascertain if the results correspond to observed saw behavior.

The effects of changes in blade design on the cutting deviation, S_T (the standard deviation of the tooth deflection), are shown in Figure 4-11. These results were obtained from the simulated cutting of twenty sixteen foot long blocks of "wood". Each block had a different seed and standard deviation for the fractal force generator. The advance per time step was $\Delta\tau = 0.1$ inches;

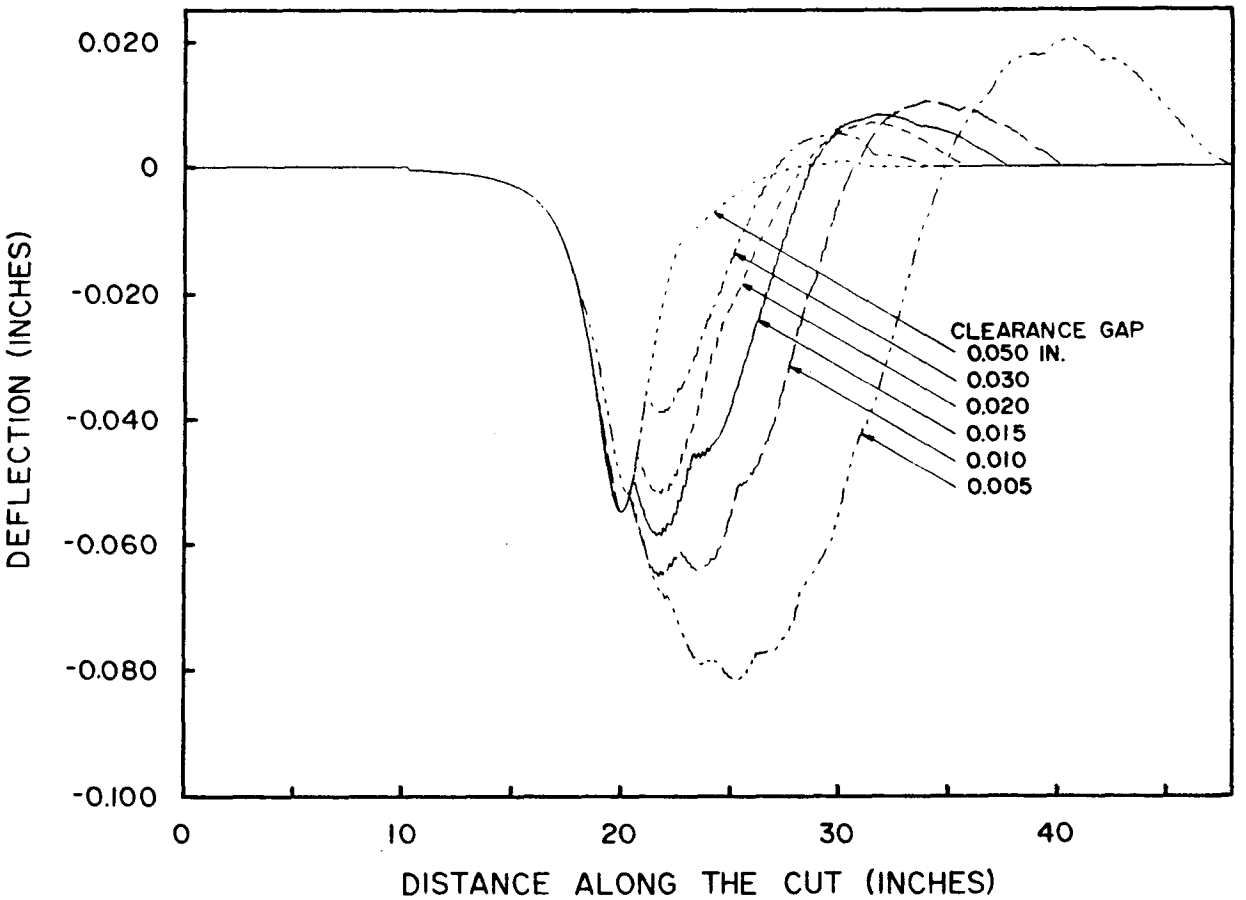

Figure 4-10. Effect of Clearance Gap on the Cut Path. All other Parameters are as in Table 4-I.

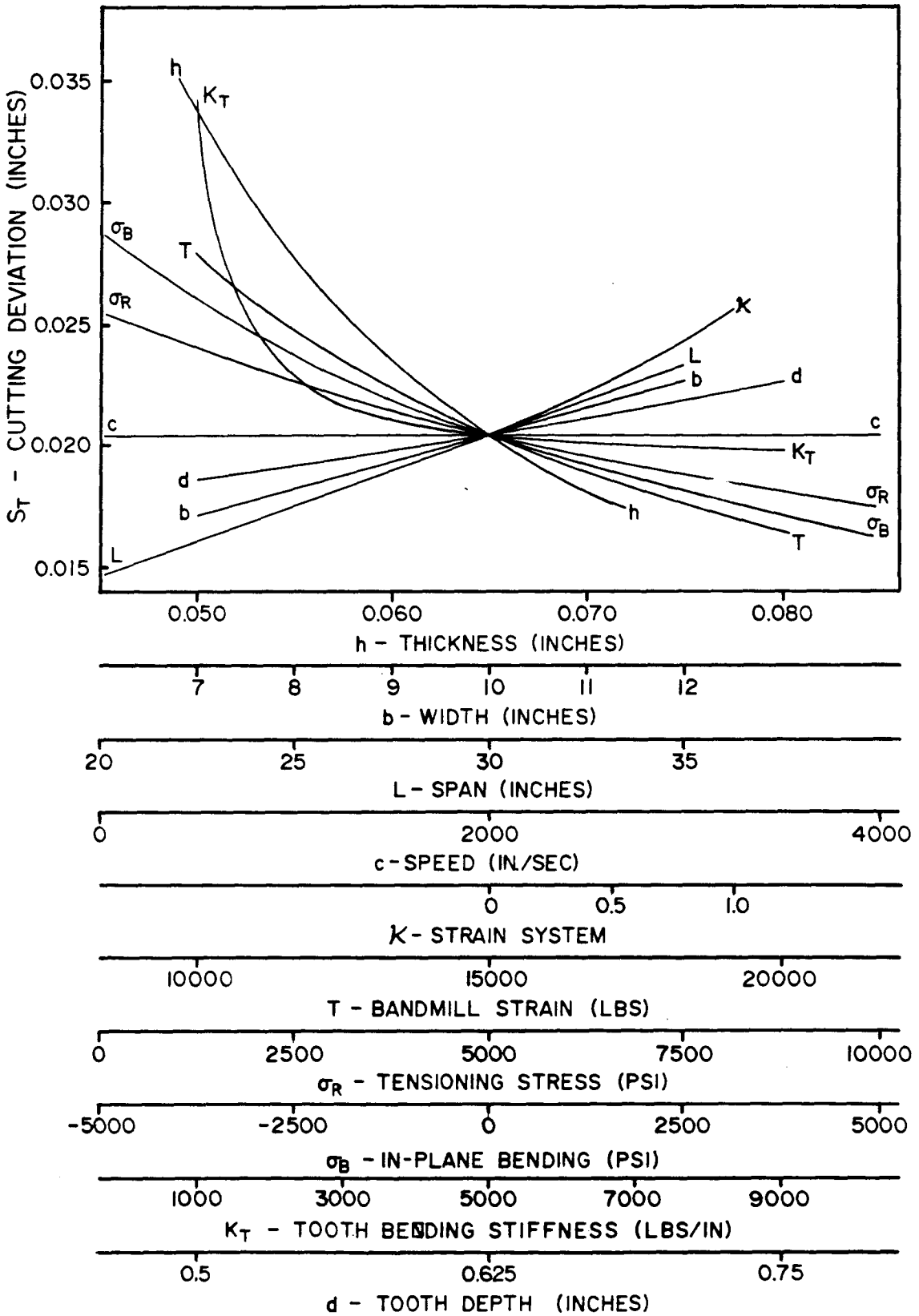

Figure 4-11. Effect of Blade Parameters on Cutting Deviation

the cutoff frequency was f_c = 1/192 cycles per inch; and the number of nodes across the blade was N_y=50. Only one tooth located at mid-span is assumed to be cutting: the effect of depth of cut is discussed later. The standard deviation of the cutting force is S_f=3.36 lbs. The clearance gap was 0.015 inches. The results are as expected: any change in blade design that improved the tooth-tip stiffness also decreased the sawing deviation.

Examples of some cut paths are shown in Figure 4-12. The similarity of these paths to the experimental traces (Figure 2-3) is quite good in that the deflections have a slow, meandering character and the back of the blade deflected some time after the front of the blade deflected.

The effect of clearance gap on sawing deviation is shown in Figure 4-13 for four different blade thicknesses. There are two significant behavior patterns shown in these results. Firstly, for large gaps a change in the gap has no effect on the cutting deviation. This occurs because for large gaps there is not much contact between the blade and the sawn surfaces. In this situation the effect of the contact forces is negligible compared to that of the cutting forces, so changing the gap will not have a measurable effect.

The second effect occurs for small gaps where the contact forces begin to have a significant effect on saw deflection. This is the region investigated by Kirbach and Stacey [1986] in their critical side clearance study. In this region (e.g., 0.010 inches < g < 0.015 inches for the 0.065 inches thick blade), there is a transition from contact having almost no effect (g > 0.015 inches) to the condition where the contact forces dominate (g < 0.010 inches). The results of the simulation agree with Kirbach and Stacey's experimental results in that once the side clearance (or clearance gap) becomes smaller than some critical value, the sawing deviation increases rapidly for small changes in the clearance.

Although there is agreement between the behavior predicted by the model and the results obtained

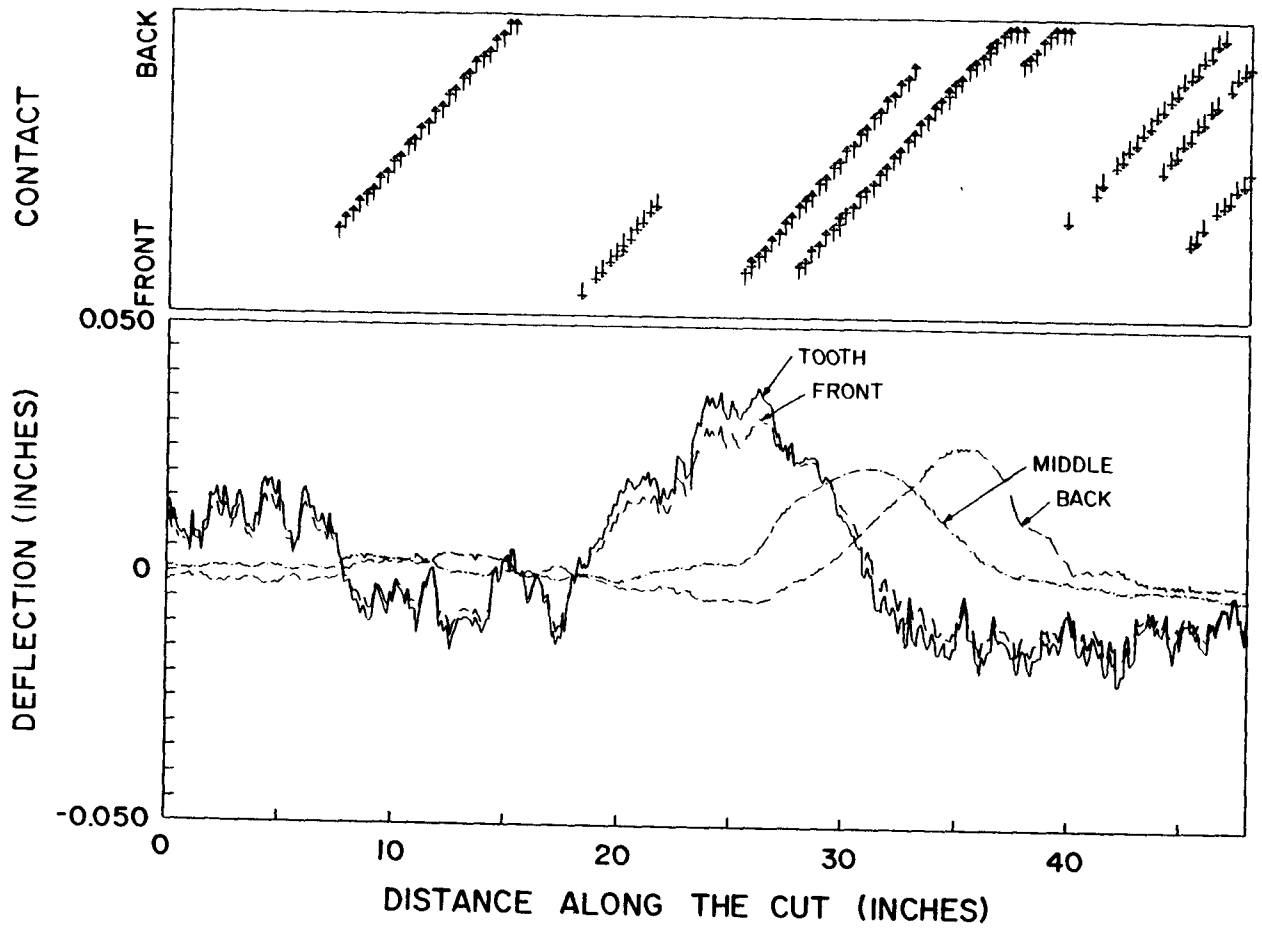

Figure 4-12a. Blade Deflections and Contact Locations for a Simulated Cut. Example 1.

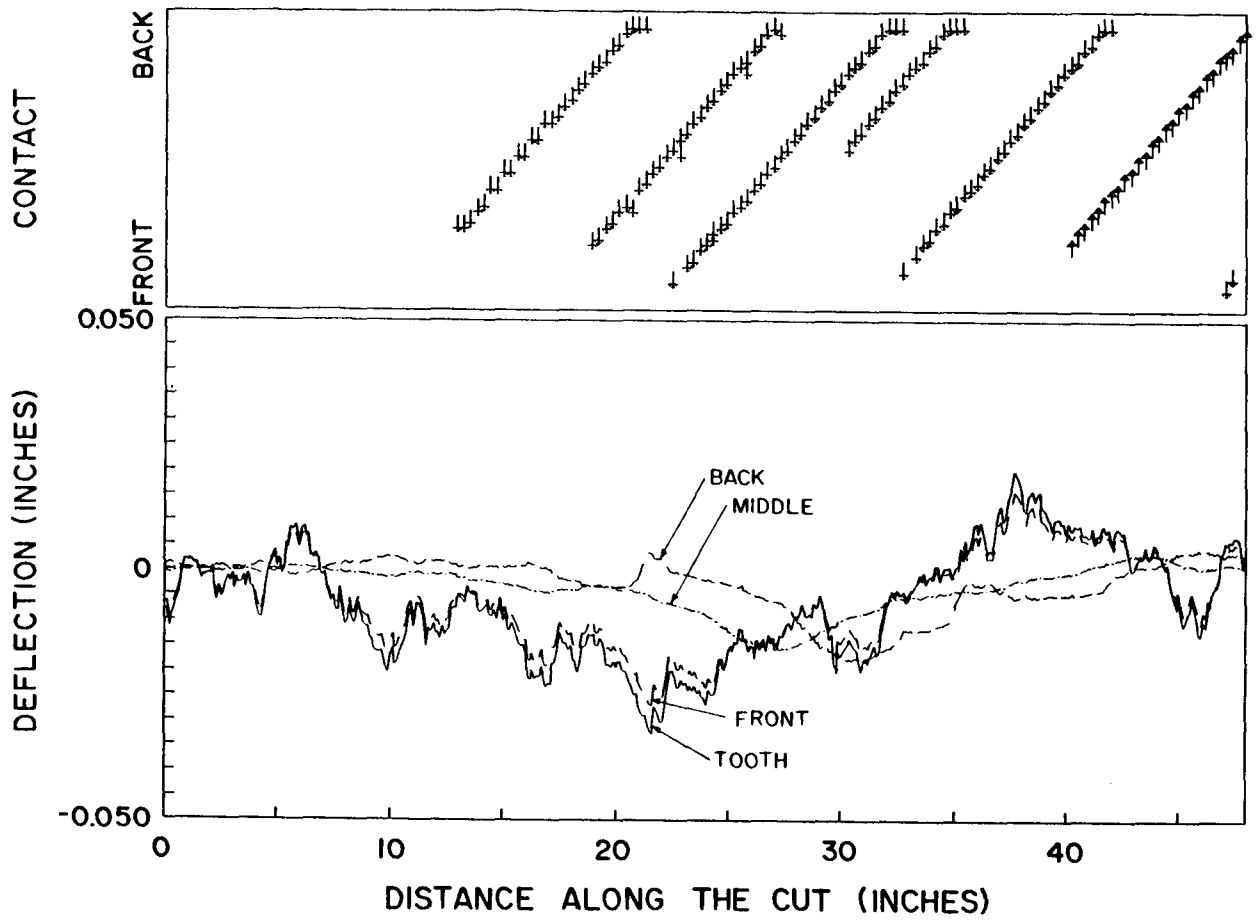

Figure 4-12b. Blade Deflections and Contact Locations for a Simulated Cut. Example 2.

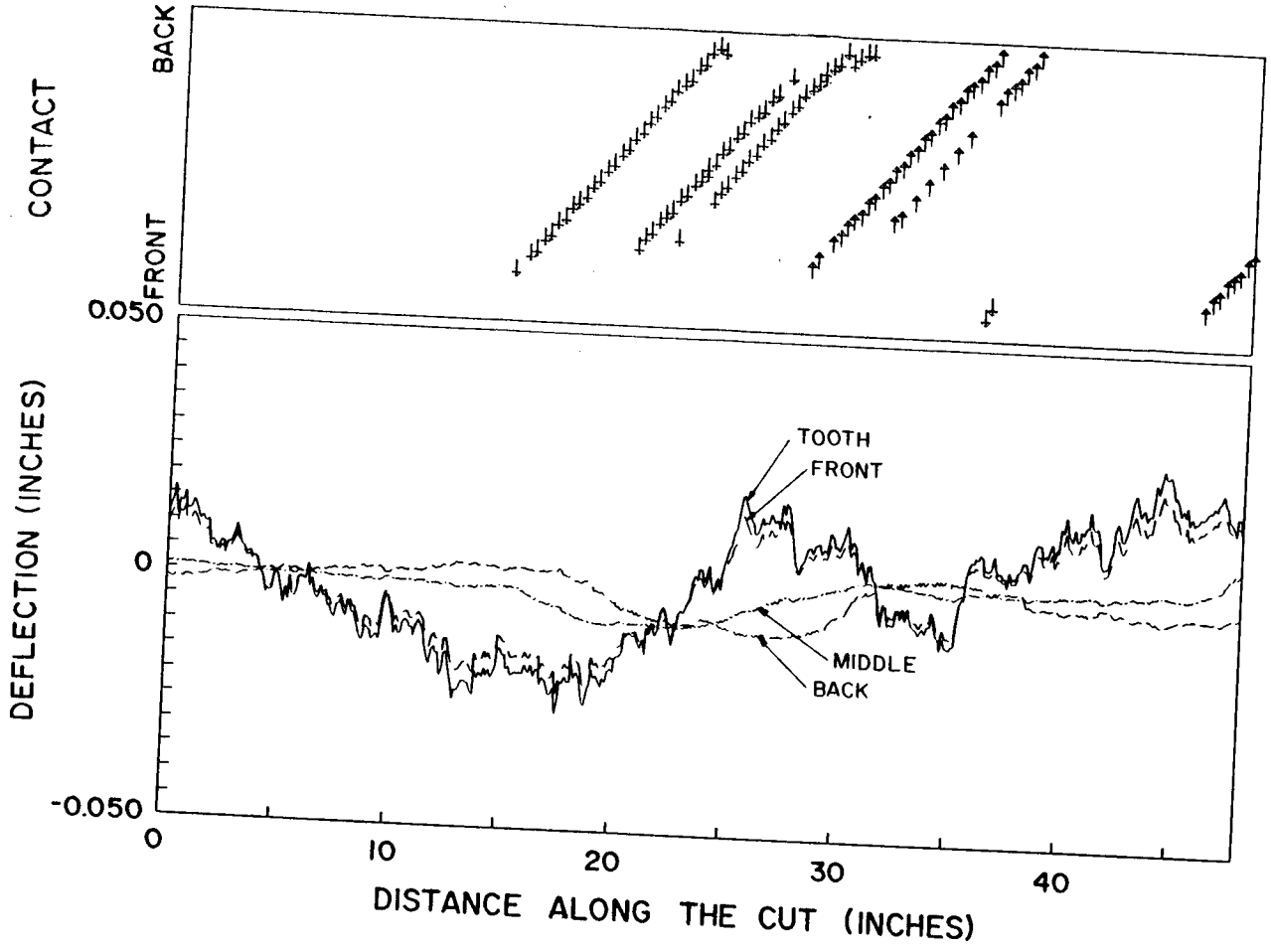

Figure 4-12c. Blade Deflections and Contact Locations for a Simulated Cut. Example 3.

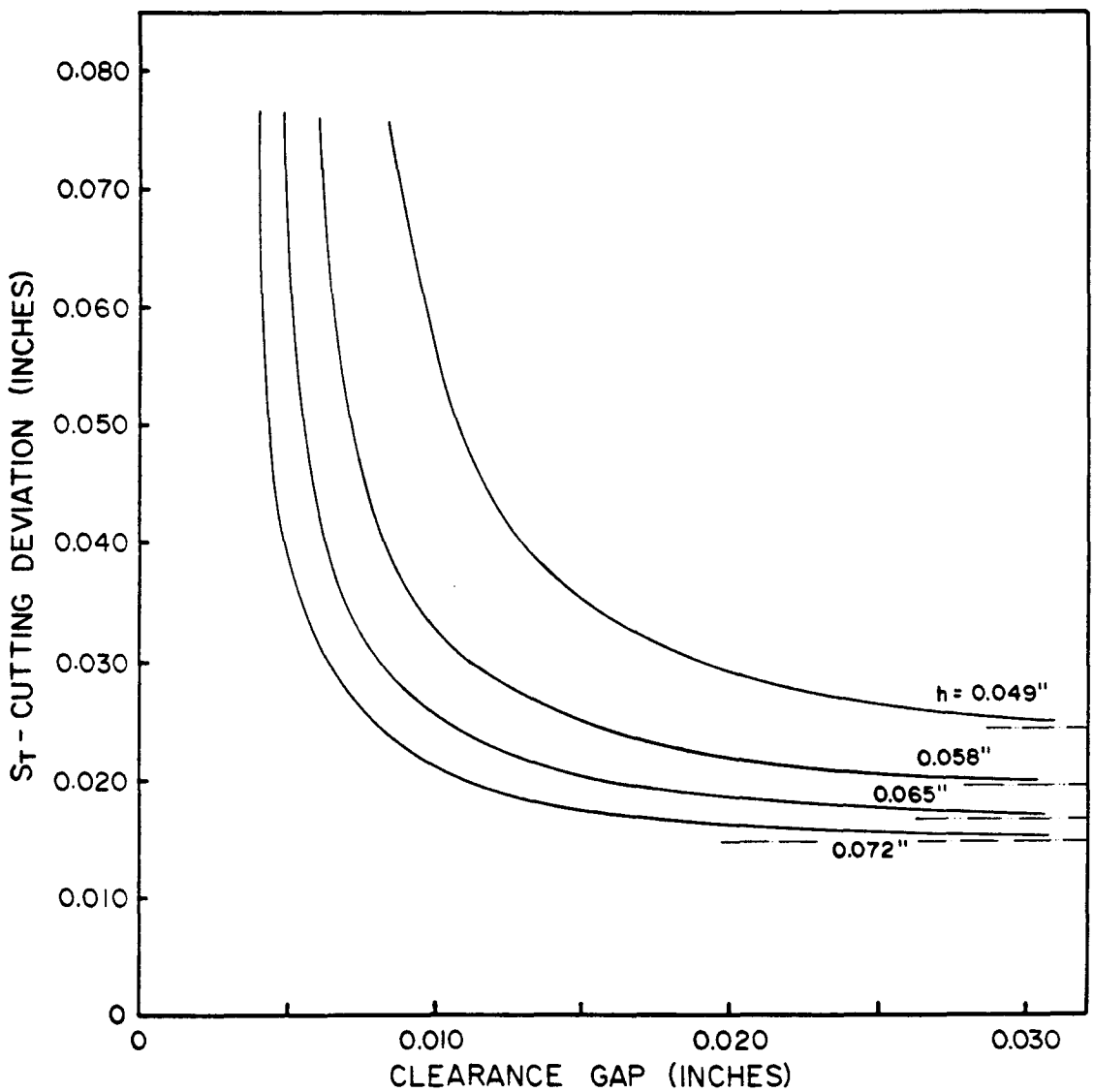

Figure 4-13. Effect of Clearance Gap on Cutting Deviation. Horizontal Lines Show Asymptotic Limits for $g \rightarrow \infty$.

by Kirbach and Stacey, the explanation of the behavior is different. Kirbach and Stacey state that less side clearance causes more contact, which is true, but they assumed that the sole cause of the poor cutting behavior was due to the heating of the blade. The present model does not include the effects of thermal stresses in the blade. Nevertheless, the model predicts the critical side clearance phenomenon. This would indicate that the longer recovery times that occur when the gap is small are the primary cause of the increase in sawing deviation and that the heating produced by the contact is a secondary effect that may further aggravate the deflection. There is also the possibility that spilled sawdust may pack very tightly, thus causing heating and, hence, increased sawing deviation. However, it seems more likely that this scenario would cause a relatively uniform change in the temperature and stress distributions across the blade, which would not affect the blade stiffness if the strain system is well maintained (i.e., $\kappa \approx 0$).

THE CONTACT GRAPH

In the previous sections the simulated behavior of specific bandsaws was investigated. In this section two dimensionless variables are presented that determine how a bandsaw behaves. The principal benefit of these variables is that they have a physical interpretation, a feature that significantly contributes to the understanding of blade behavior. It is important to know the concepts that led to their development.

Nondimensional Sawing Deviation

When the clearance gaps are so large that no contact occurs then the tooth deflection is proportional to the cutting force. It is then possible to say that the standard deviation of the tooth deflection, when no contact occurs, is

$$S_o = {S_f}/{K_{tt}} = \lim_{g \to \infty} S_T \tag{4.1}$$

where

S_f = standard deviation of the lateral cutting force

K_{tt} = tooth-tip stiffness

S_T = standard deviation of the tooth deflection.

S_o = S_T when no contact occurs

Since S_T converges to S_o (see Figure 4-13), it is convenient to nondimensionalize the sawing deviation as

$$\frac{S_T}{S_o} = \frac{S_T K_{tt}}{S_f} \tag{4.2}$$

Nondimensional Clearance Gap

Contact is guaranteed to occur at points during the cut whenever the deflection of the tooth, x_T, equals or exceeds the clearance gap, g. There is an infinite number of combinations of the lateral cutting force and the contact forces that could cause the tooth deflection to equal the clearance gap. The complicating factor is the variety of contact conditions that could occur. However, the effect of contact is generally to amplify and prolong the blade deflection. Contact is still guaranteed to occur as long as the lateral cutting force is, by itself, large enough to produce a tooth deflection equal to the clearance gap. This force is $f_g = gK_{tt}$.

The fraction of time that the lateral cutting force equals or exceeds f_g is therefore a crude indicator of how much contact occurs during a cut. Mathematically, this concept is expressed as the probability that the lateral cutting force, f_L, exceeds the range $\pm f_g$.

In the following development it is assumed that no contact occurs. Hence, the lateral cutting force is proportional to the tooth-tip deflection and the probability distribution curves for the lateral cutting force and the tooth deflection are identical. Hence, the variable

$$z = \frac{f_L}{S_f} = x_T \frac{K_{tt}}{S_f} = \frac{x_T}{S_o} \tag{4.3}$$

can be used for normalizing the lateral force and the blade deflection. See Figure 4-14. A normalized contact variable can therefore be defined as

$$Z_o = \frac{f_g}{S_f} = g \frac{K_{tt}}{S_f} = \frac{g}{S_o} \tag{4.4}$$

This variable is the nondimensional form of the clearance gap. The physical interpretation of Z_o is that it is an inverse indicator of the fraction of time that the lateral cutting force exceeds f_g, or the fraction of time that the tooth deflection exceeds the clearance gap.

As expected, the clearance gap, g, governs the amount of contact that occurs. However, gap, as a *measure* or *indicator* of the amount of contact, must be taken relative to how much the blade deflects. For instance, a stiffer blade will not deflect as much and hence will not allow as many deflections that would result in contact. Also, if the magnitude of the cutting force were to decrease, the blade will not deflect as much and, hence, there will be fewer deflections that would result in contact.

The area outside $z = \pm Z_o$, A, in Figure 4-14 would be an elegant measure of the amount of contact. This area, A, could be called the probability of contact, but there are too many assumptions separating A from the actual amount of contact for this variable to be considered reliable. These assumptions are 1) the probability distribution is for the no-contact case; and 2) the limits of the area at $z = \pm Z_o$ are somewhat arbitrary. The variable Z_o is considered a more reliable indicator of the amount of contact due to its directness and simplicity.

In this thesis the clearance gaps on each side of the blade are assumed to be equal and the average lateral cutting force is near-zero. A non-zero value of the mean clearance gap, $\bar{g}$, means that the blade deflection during cutting could be biased towards the side of the blade having the larger gap. A non zero value of the mean cutting force, $\bar{f}$, means that the wood properties, a grinding

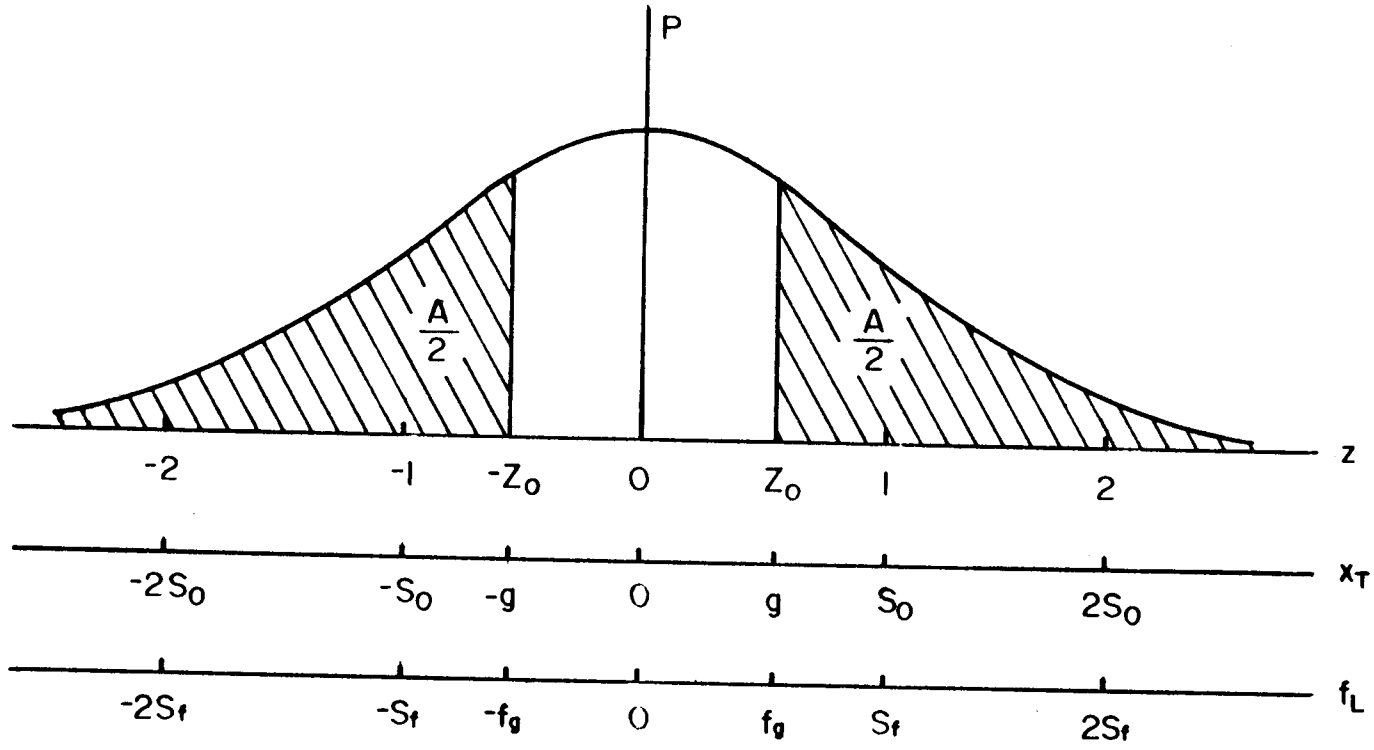

Figure 4-14. Probability Curve for Contact.

problem and/or a misalignment of the blade has caused a bias in the cutting force. Since these problems are generally correctable (although very common), their effects will not be examined in this work.

Generality of the Contact Graph

The dimensionless form, $S_T K_{tt}/S_f$ versus gK_{tt}/S_f, of the data in Figures 4-11 and 4-13 is shown in Figure 4-15. Essentially, all of the data lie on the best fit curve

$$S_T K_{tt}/S_f = 1 + 0.089\left(gK_{tt}/S_f\right)^{-2.755} \tag{4.5}$$

(The regression coefficient, r^2, was 0.983.) Although there is some scatter about this curve, Equation 4.5 predicts S_T within five percent.

It is important to realize that this curve applies for as wide a range of blade parameters as is used in practice, at least for a 5 foot bandmill. This means that the blade design, in the structural sense, is totally represented by the tooth-tip stiffness, K_{tt}. It does not matter how the value of K_{tt} was generated, whether it was from any combination of blade thickness, strain, tensioning, etc.: only the resulting value of K_{tt} matters.

Insensitivity to Blade Design

The dominant effect of K_{tt} infers that the effect of the contact forces on S_T is insensitive to changes in blade design. To see why this is so, consider writing the tooth deflection as

$$x_T = \frac{F_T}{K_{tt}} + \sum_{n=1}^{N_y}\left(\frac{F_n}{K_{nt}}\right) = \frac{1}{K_{tt}}\left\{F_T + \sum_{n=1}^{N_y} F_n\left(\frac{A_{nt}}{A_{tt}}\right)\right\} \tag{4.6}$$

where

F_T = the lateral force on the tooth

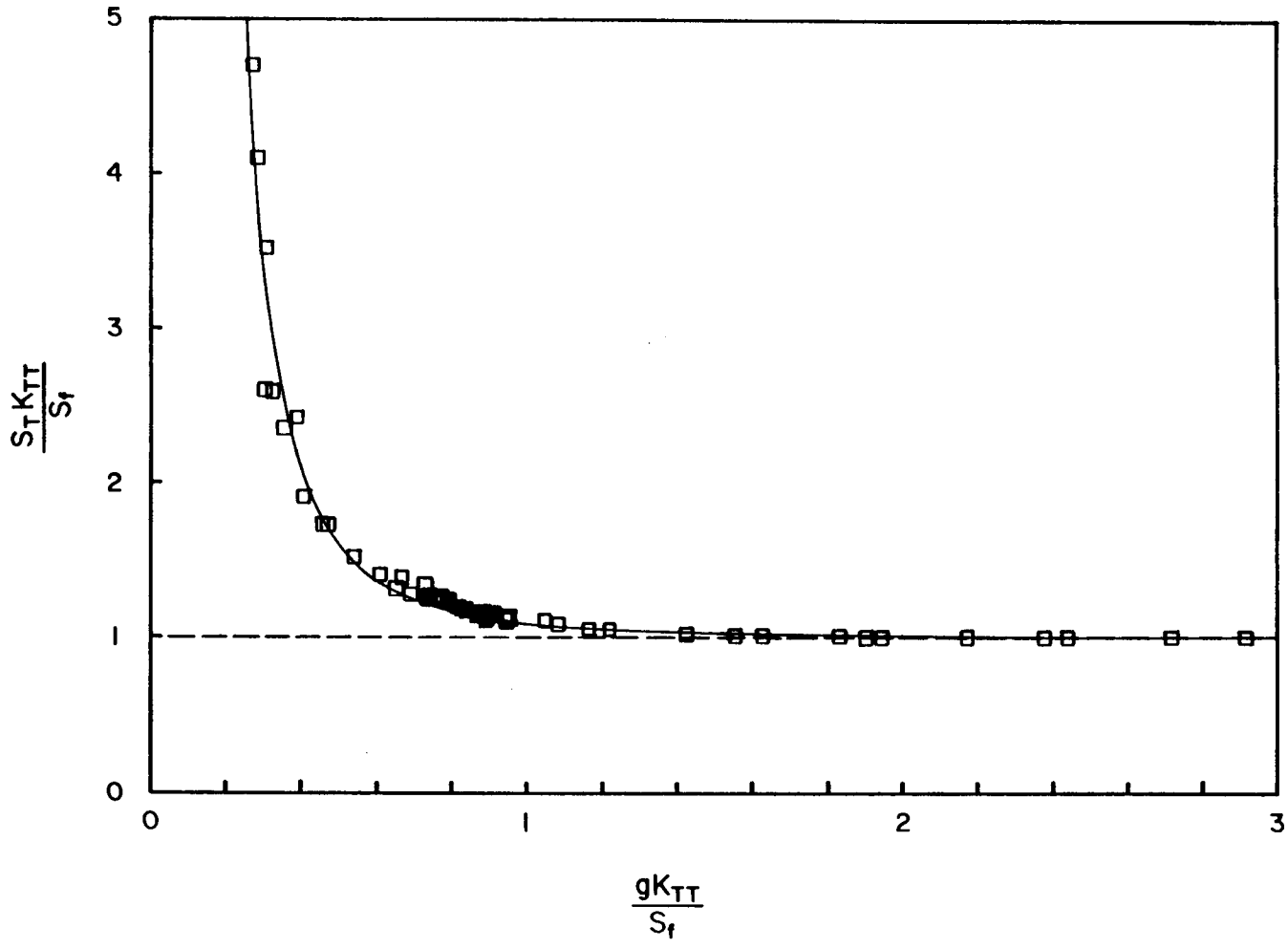

Figure 4-15. Contact Graph.

F_n = the contact force on node n

$K_{nt} = 1/A_{nt}$ = the cross stiffness between node n and the tooth tip.

$A_{tt} = 1/K_{tt}$ = tooth-tip flexibility

Although the contact force, F_n, is affected by present and past values of the cutting force acting on the tooth, F_T, the next most important factor of how contact affects X_T is the ratio A_{nt}/A_{tt}. Since this ratio is a function of the node location across the width of the blade, the influence of the contact forces will vary depending on the location of the contact force. By Maxwell's reciprocal theorem, A_{nt}/A_{tt} is equivalent to the normalized shape of the blade caused by a load on the tooth-tip. This shape is fairly insensitive to changes in blade design (see Figure 4-16) because the effects of lateral and torsional ('rigid body') bending effects remain fairly constant relative to each other. The local bending is more affected by changes in blade design, but the local bending has a smaller effect on the shape of the cross section of the blade.

The variation of the cross-stiffness across the width of the blade has many features that help explain the effect of contact on tooth deflection. Firstly, contact forces acting on the back half of the blade have little effect and may even reduce the tooth deflection because $A_{nt} < 0$. At a point about two thirds of the blade width from the front edge, the cross stiffness is zero and a contact force acting here will have no effect on tooth deflection. It is only when the contact forces act on the front third of the blade that they have much effect. Contact forces acting on the gullet line will have the greatest effect.

Progression of Contact

One can conclude that the closer the contact gets to the front of the blade the more effect it will have on tooth deflection. There is also the concept, discussed earlier, of the likelihood of contact. The effect of contact, therefore, has two components: 1) the probability that a certain contact mode will occur, and 2) the severity of the effect of the contact mode. By contact mode is meant anything

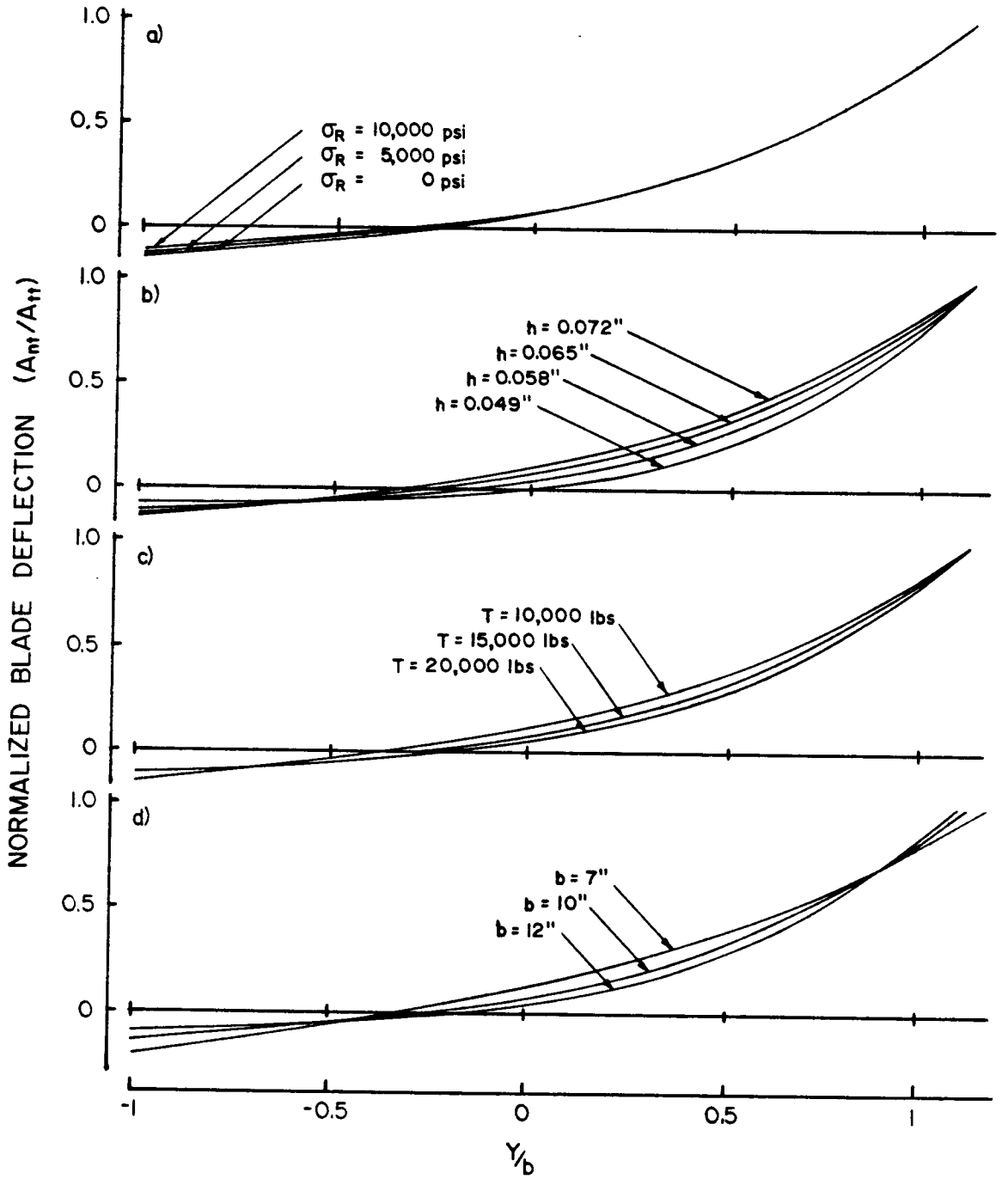

Figure 4-16. Normalized Cross-section of Blade Deflection.
a) Effect of Tensioning b) Effect of Thickness
c) Effect of Bandmill Strain d) Effect of Blade Width.

from no contact to binding. These modes were identified from examining the blade deflections produced by the simulation, an example of which is shown in Figures 4-6, 4-7 and 4-17. There is a progression of contact modes and these are shown in Figure 4-18. Generally, the severity of the contact increases as the deflection increases and/or the curvature of the cut path increases. In both cases the contact moves closer to the front of the blade.

In summary, reducing the value of gK_{tt}/S_f increases the likelihood that contact will occur and that more severe modes of contact will occur. The effect of the contact forces relative to that of the cutting forces is quantified by the value of S_T/S_o. The relationship between S_T/S_o and gK_{tt}/S_f is a quantification of the effect of contact. Hence, a graph of S_T/S_o versus gK_{tt}/S_f has been termed the contact graph.

From a practical point of view, this development, for the first time, provides an equation (Equation (4.5)) that relates the saw design to its cutting performance. The implications of this relationship will be investigated in the next chapter.

THE EFFECT OF THE DEPTH OF CUT

In the analysis and simulation presented it was assumed that only one tooth was cutting. A realistic simulation of the multi-tooth case can only be achieved if information on how the lateral cutting force varies through the depth of cut is available. The approach adopted here, instead, is to investigate the consequences of assuming that the forces on each tooth are equal.

A question that arises is how to define tooth-tip stiffness when each of the tooth-tips in the cut has a different stiffness, depending on its distance from the guides. This is an important question because the tooth-tip stiffness has been identified as the parameter that encapsulates the effects of

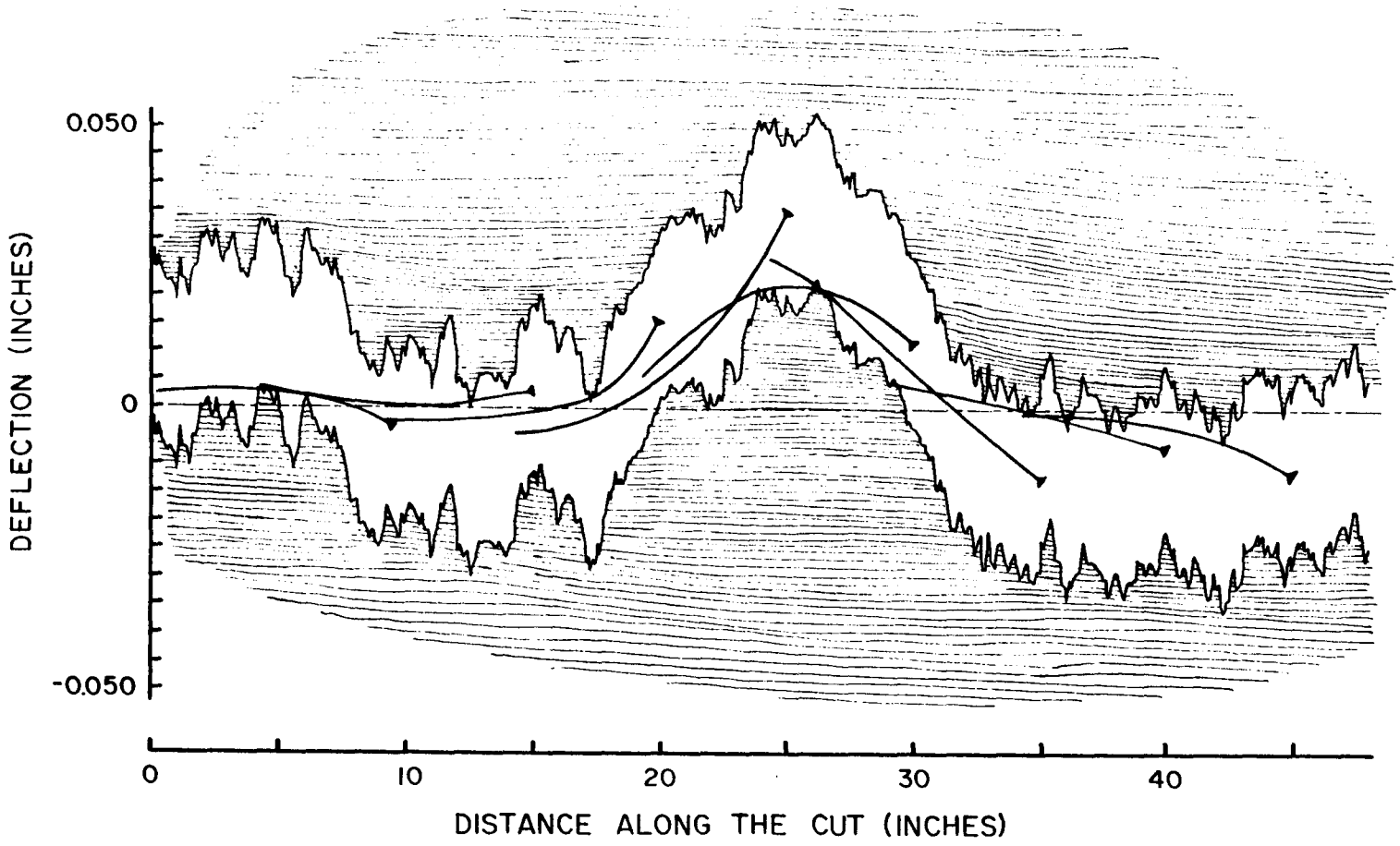

Figure 4-17. The Deflected Shape of the Blade during a Simulated Cut.

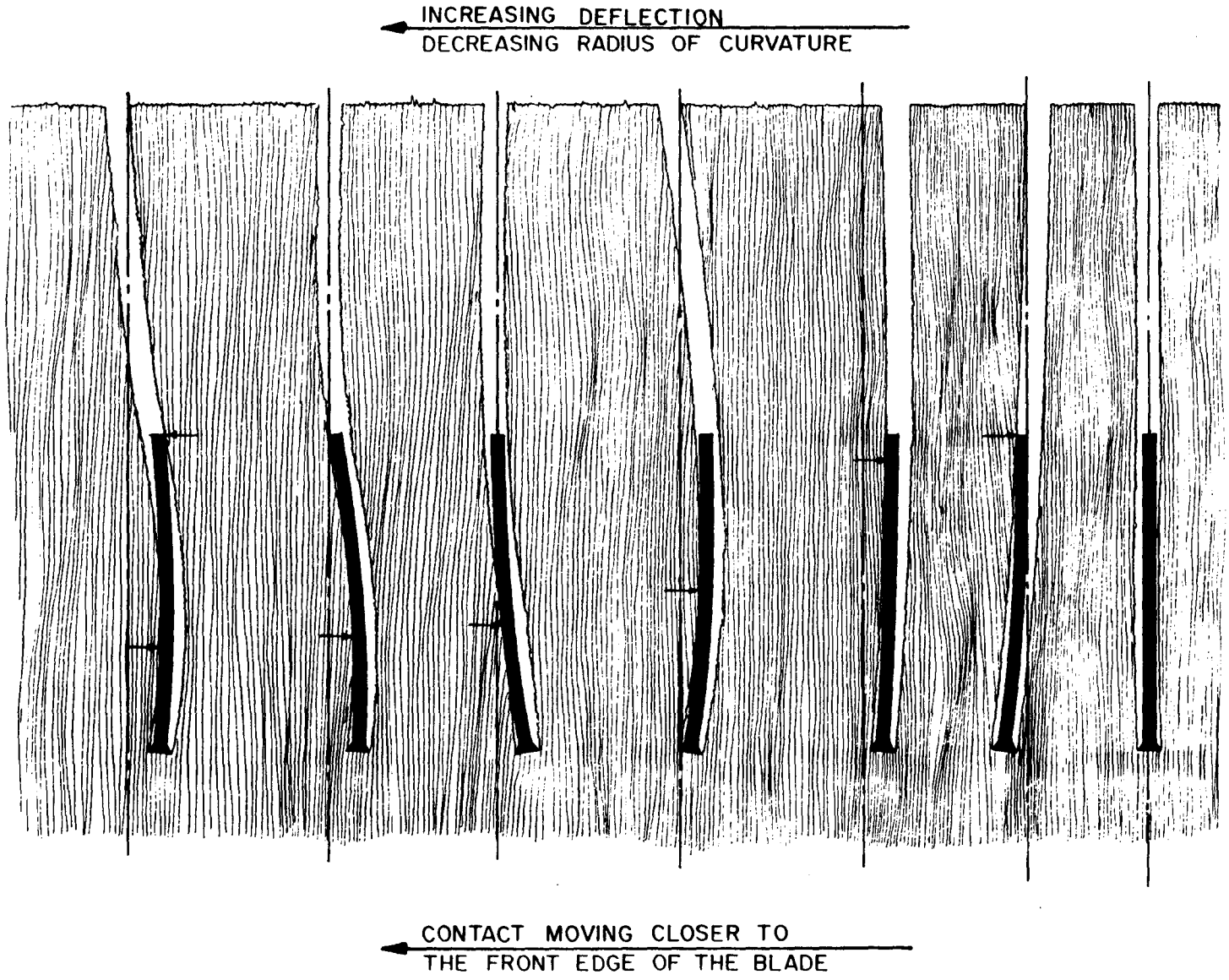

Figure 4-18. Progression of Contact. Markers show where Contact occurs.

blade design.

Effect of Non-uniform Load Patterns

A simple method for investigating the effect of variations in the cutting force through the depth of cut is to calculate how different load patterns affect the blade deflection. The assumed load patterns, which have triangular wave forms, and the resulting tooth deflections are shown in Figure 4-19. The wavelengths of the applied force distribution, λ, are expressed as multiples of the tooth pitch, P, which was 1.75 inches. The peak-to-peak amplitude of the load patterns was 2 lbs. and the mean force of each load distribution was adjusted to be zero. For the case $\lambda=\infty$, a uniform load of 1 lb. on each tooth was used. The blade parameters are specified in Table 4-I.

Clearly, the effect of the mean force ($\lambda=\infty$) will dominate the response of the blade. Variations in the load shorter than $\lambda=6P$ will have to have huge magnitudes to produce deflections comparable to that of the mean force.

General Case of Unequal Forces on the Teeth

Since the deflection caused by the mean cutting force dominates the deflection response of the teeth, it is convenient to separate the force distribution into two components: a mean force and the variant from the mean.

$$f_{it} = m_i + e_{it} \quad ; t = 1,..,N_T \quad ; i = 1,..,N_c \tag{4.7}$$

where f_{it} is the force on the t-th tooth at the i-th increment along the cut; m_i is the mean of the forces on the teeth during the i-th increment; and e_{it} is the variant on the t-th tooth during the i-th increment. It follows that the standard deviation of the cutting force is

$$S_f^2 = S_m^2 + S_e^2 \tag{4.8}$$

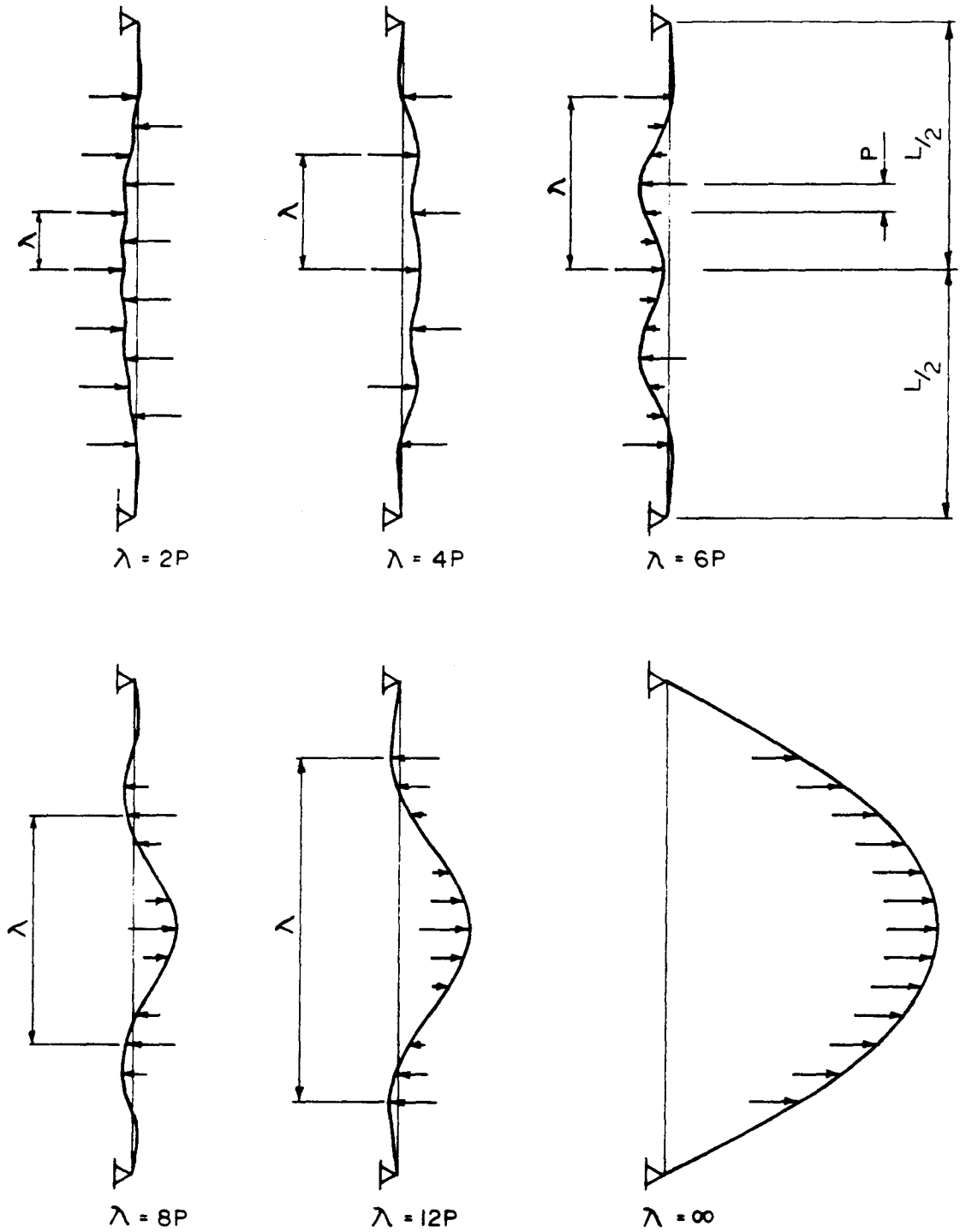

Figure 4-19. Effect of Load Variation Through the Depth of Cut. The Arrows show the Magnitude and Direction of Forces on the Tooth-tips.

where S_m^2 = Var(m) and S_e^2 = Var(e) for all teeth and for all increments. A derivation given in Appendix D shows that the following two equations apply when no contact occurs:

$$S_o^2 = \frac{S_m^2}{K_o^2} + \frac{S_e^2}{Q_o^2} \tag{4.9}$$

$$\bar{x} = \frac{\bar{f}}{K_{eq}} \tag{4.10}$$

where K_o, Q_o and K_{eq} are equivalent blade stiffnesses, $\bar{f}$ is the mean cutting force, and $\bar{x}$ is the mean deflection.

The effect of depth of cut, expressed as the number of teeth in the cut, N_T, on K_o, Q_o and K_{eq} is shown in Figure 4-20. The cutting zone is symmetrical about mid-span. For $N_T = 1$,

$$K_o = Q_o = K_{eq} = K_{tt}$$

so the formulae collapse to the single tooth cutting case presented earlier. For $N_T > 7$ (a 12 inch depth of cut), Q_o levels off and K_o is about one third of Q_o. Assuming $S_e = S_m$, and $3K_o = Q_o$, S_e contributes only five percent to the value of S_o. This result reinforces the earlier conclusion that effect of the mean cutting force, m_i, dominates the cutting deviation.

Consequences of Assuming Equal Forces on the Teeth

The model assumes that the forces on the teeth through the depth of cut are equal (i.e., $S_e = 0$). Although the analysis will not be given here, it can be shown that when S_e is not known S_o can be quite reasonably approximated by S_m/K_o, even if $S_e = 2S_m$. This approximation underestimates S_o. The assumption of Se = 0 does not, therefore, significantly affect the results of the simulation. In any case, S_o remains the parameter for nondimensionalizing S_T and g on the contact graph.

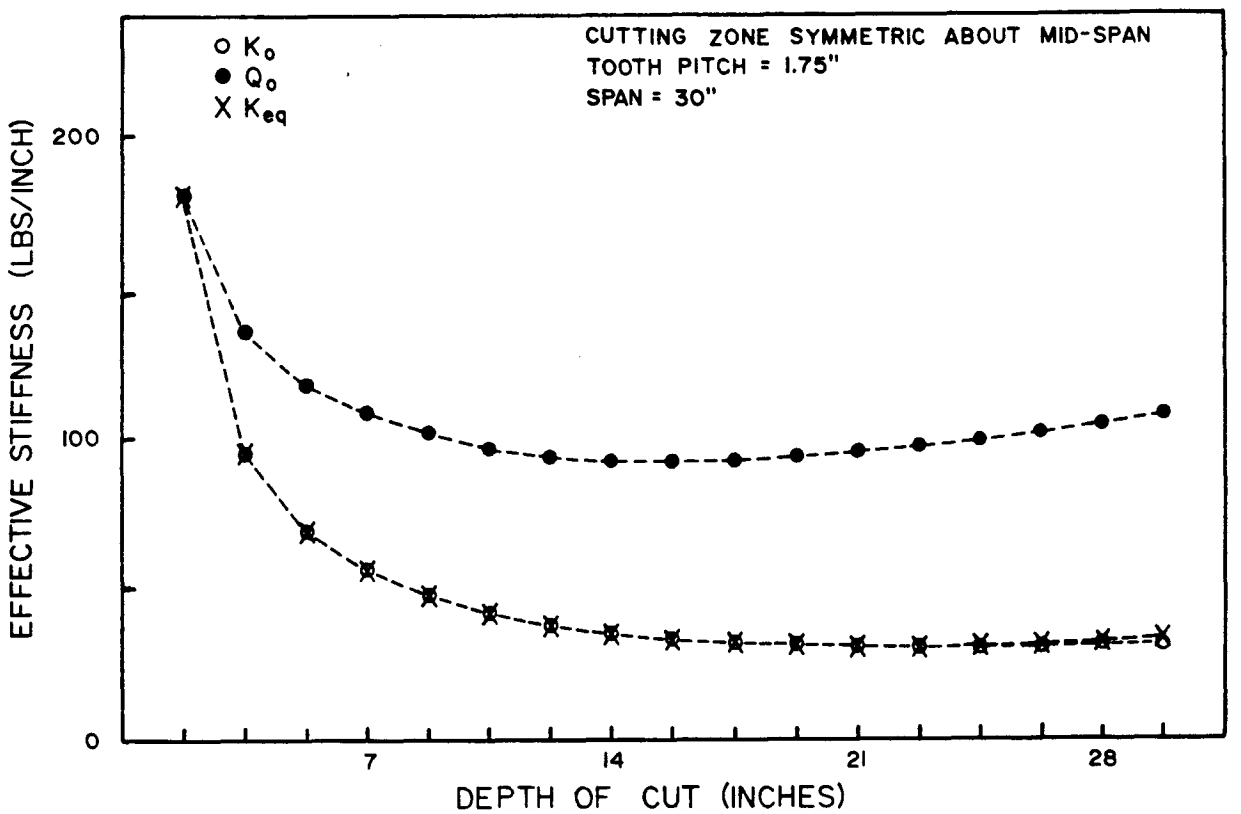

Figure 4-20. Effect of Depth of Cut on the Equivalent Stiffnesses.

The effect of depth of cut on the contact graph is small, as can be seen in Figure 4-21. For values of gK_0/S_f greater than 0.7 the curves for $N_T > 1$ conincide with the curve developed from the single tooth simulation. For values less than 0.7, there is some deviation from the curve, but the simulation is not expected to be that accurate in this region anyway because heating effects are not accounted for.

There are three important conclusions from this analysis of the effect of depth of cut.

1) The variations in the lateral cutting force through the depth of cut, e_{it}, will have to be large compared to the mean, m_i, before their effect will be comparable to that of the mean force. If e_{it} (or S_e) is small in reality, then the shape of the blade between the guides will be bow-shaped, as in Figure 4-19 ($\lambda=\infty$), and will not bend into an S-shape. In experiments [Taylor, 1985; Alexandru, 1967], the bow-shape is always seen, which indicates that the variant force, e_{it}, is small.

2) If the effect of e_{it} is small, as it appears to be, then it is not important to measure it accurately. Variations in the cutting force that have wavelengths less than $\lambda = 6P$ could be ignored.

3) Since the blade always deflects into a bow-shape, the deflections measured by a probe located above the cutting zone will give a good indication of how the blade is deflecting in the wood. Probe data would be useless if the blade bent into an S-shape.

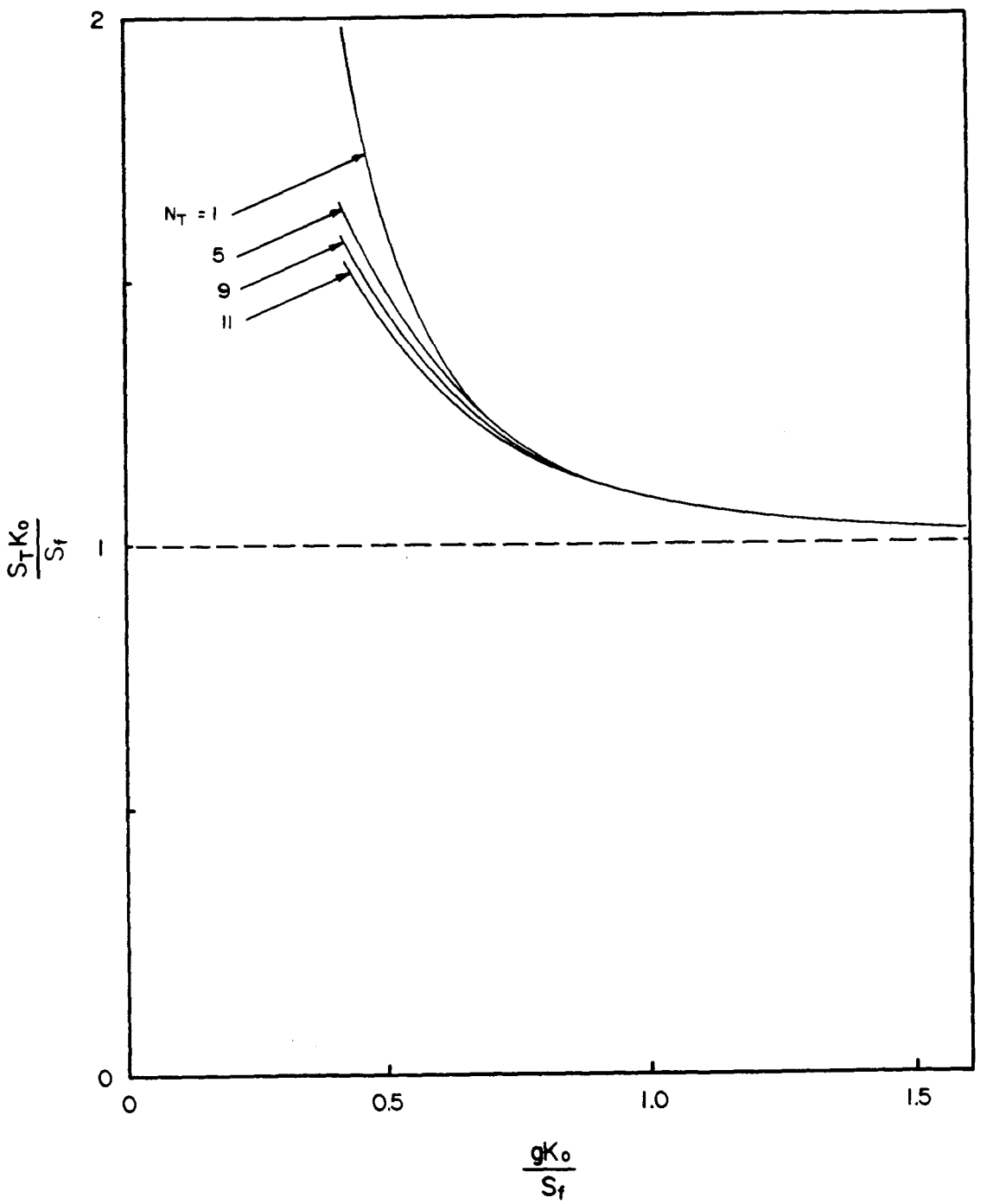

Figure 4-21. Effect of Depth of Cut on the Contact Graph.

An idea, like a ghost, according to the common notion of ghosts, must be spoken to a little before it will explain itself.
Charles Dickens

To know a thing well, know its limits. Only when pushed beyond its tolerance will true nature be seen.
Frank Herbert

CHAPTER 5

DISCUSSION AND APPLICATIONS

A set of variables for quantifying the basic sawing system and a mathematical relationship between these variables has been found. Although the model is an incomplete representation of the sawing process, it provides enough information to explore the optimization of blade design and to better understand the practical aspects of sawing.

MINIMIZATION OF FIBRE LOSS

The fibre loss (the sum of the kerf width and the amount removed by the planer), allowing for five percent planer skip [Brown, ed., 1982], can be written as

$$F = \alpha(1.64)S_T + h + 2(g+d) + p \tag{5.1}$$

where

α = a factor to account for the difference between the board thickness deviation, σ_T, and tooth deflection deviation, S_T.

h = blade thickness

g = clearance gap

d = difference between side clearance and the clearance gap

p = planer allowance

The cutting deviation, S_T, can be expressed by Equation 4.5 so that Equation (5.1) can be written in as,

$$F = \frac{1.64\alpha S_f}{K_o}\left(1 + 0.089\left(\frac{gK_o}{S_f}\right)^{-2.755}\right) + 2g + 2d + h + p \tag{5.2}$$

For a given blade thickness, increasing the tooth stiffness, K_o, always reduces fibre loss. The fibre loss is also sensitive to the ratio $S_o = S_f/K_o$, which means that the factors that affect S_f, such as the tooth sharpness and the characteristics of the wood, need to be monitored as well.

Figure 5-1 shows how the fibre loss varies with side clearance and α. The following values were used: h = 0.065 inches, d = 0.015 inches, p = 0.060 inches, and $S_o = S_f/K_o$ = 0.020 inches. For a given blade thickness there is an optimum side clearance that minimizes the fiber loss. It is important to see that fibre loss is insensitive to changes in the side clearance as long as the value is not smaller that 90 percent and not larger that 120 percent of the optimum side clearance. This is fortunate because this allows for variations in the clearance gap caused by tooth grinding, sawdust spillage and surface roughness.

The optimum side clearance is somewhat sensitive to 'α', so it is important to reduce the between cut (and between-board) variation, which is affected by the repeatability of the setworks, and to

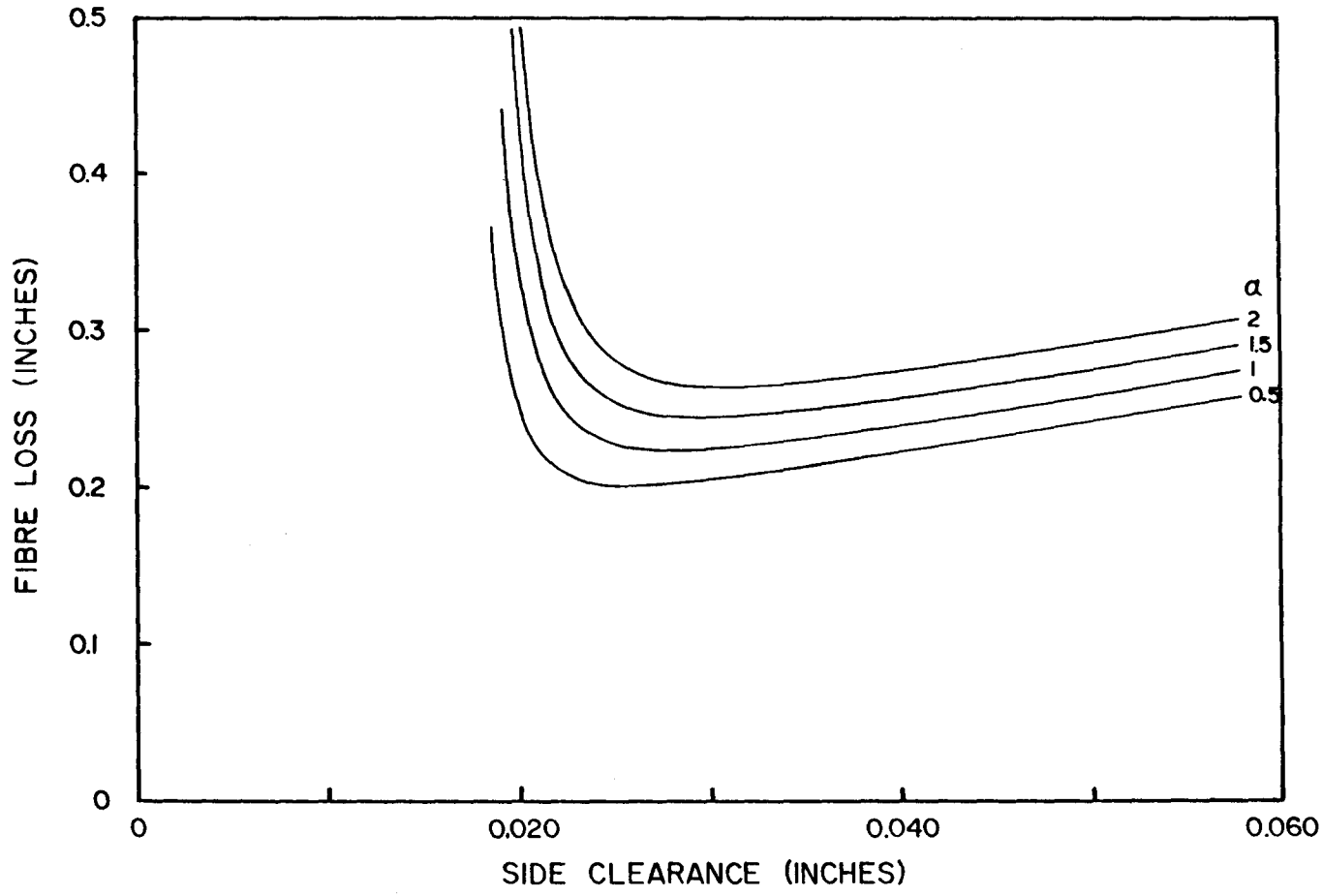

Figure 5-1. Effect of Side Clearance on Total Fibre Loss.

know the relationship between board thickness variation and blade deflection deviation.

The predicted optimum side clearance is close to the clearances used in practice. Typically, the side clearance ranges between 0.025 inches and 0.035 inches. For 'α'=1, the optimum clearance is 0.028 inches. To keep the fibre loss no larger than 2% of the optimal minimum (i.e., within a 1% change in lumber recovery), the clearance would have to be within 0.025 to 0.033 inches. To introduce production costs into the optimization, the effect of bite on S_f and g needs to be known.

THE PRACTICE OF SAWING

The purpose of this section is to discuss, in terms of the principles presented in this thesis, how the sawing process is monitored and controlled in contemporary sawmills.

As described in Chapter 2, blade design is mostly a trial and error process. Given the common emphasis on production volume rather than lumber recovery, the general objectives are typically to:

1) improve blade reliability to minimize production stoppages;
2) increase the feed speed to increase production volume;
3) improve recovery if and only if production volume is not compromised; and
4) improve surface finish.

These goals limit the usefulness of the optimization developed in the previous section.

Whether or not the drive for production volume dominates, the managers and mill personnel affect the design of the saws. Firstly, the type and quality of the logs available or chosen by the managers and/or log buyers affects not only the grade of the lumber, but also the ease or difficulty in processing the logs. Wood properties affect the cutting forces and the straightness of the logs affects how well the feed system can hold the logs. For example, a low grade log will have more

knots so either thicker (i.e., stiffer) blades or slower feed speeds are necessary. Also, since the blade must recover from more disturbances, more side clearance is needed.

The sawfiler controls the stiffness of the blade, and is the only person to do so. The filer influences a) the cutting forces by selecting the tooth geometry, the method of sharpening the teeth and, in consultation with management, the saw replacement schedule; b) the clearance gap, by setting the side clearance and the gullet area; c) the maximum feed speed, by setting the tooth pitch and gullet area; d) the reliability of the blade by preparing consistent quality blades. In cooperation with the millwrights, the filer is also responsible for the condition and alignment of the bandmill and the feed system.

The sawyer, in most cases, controls the feed speed, which is adjusted to account for the depth of cut, the condition of the wood and the quality of the saw. The sawyer watches how the saw responds, directly controlling the sawing deviation. In this way, the sawyer compensates for variations in blade preparation, and in the wood properties. By setting the feed speed the sawyer controls the cutting forces and the amount of sawdust spillage by changing the bite per tooth.

For systems where the feed speed is determined from measurements of the log diameter, the compensating feedback of the sawyer is removed. Consequently, the saw must be oversized to allow for the worst log (worst cutting conditions) and for variations in blade preparations.

COMPLETE DATA SET

The complexity of the sawing system is partly caused by the large number of variables involved. It has been impossible to apply the theories developed in this thesis to published cutting data, other than the comparison of general trends, because important information was not included in the

recorded data. The data were omitted because they were not considered important, or because there is no reliable method of measurement.

To focus the need for measuring and recording the many variables involved in sawing, and for developing measurement procedures, the following is suggested as a complete set of data for cutting tests. The necessary accuracy of the measurements has yet to be determined. Knowing this information not only ensures that experimental results can be repeated, but will also aid in diagnosing problems in the laboratory or sawmill. Experimental repeatability corresponds directly to consistent sawing in the mills.

1) Blade Properties. One should record the blade dimensions, speed, strain, strain system parameter, κ, span, tensioning, backcrown, wheel tilt and crown, tooth dimensions and tooth stiffness, temperature distribution, location of the cutting zone. The equivalent stiffnesses K_o, Q_o and K_{eq} are the minimum parameters that should be measured. Ideally, the flexibility or stiffness matrix of the blade, including the tooth-tips and the probe locations should be measured.

2) Cutting Forces. Record the wood species, and the mean and variation of the density and moisture content. If possible, measure S_f, S_m, and S_e. A good estimate is $S_f = S_o K_o$. Other variables are the bite, the tooth geometry and the sharpness.

3) Clearance Gap. Record the side clearance, gullet area, gullet feed index, the surface roughness, depth of tooth marks, the quantity and location of spilled sawdust, blade flatness and tooth runout, the alignment and the looseness of the feed system. Keep in mind that the wood may deform during cutting and either lean against saw or pinch the blade.

4) Cutting Accuracy. Board thickness data is only an indicator of blade behavior. The more

correct measurement of blade behavior is the shape of the sawn surface, from which a standard deviation of deflection, S_T, can be calculated.

We are not interested in establishing scientific theories as secure, or certain, or probable. Conscious of our fallibility we are interested only in criticizing them and testing them, in the hope of finding out where we are mistaken; of learning from our mistakes; and if we are lucky, of proceeding to better theories.

Sir Karl Popper
Truth and Approximation to Truth

Experience never errs; what alone may err is our judgment, which predicts effects that cannot be produced by our experiments
Leonardo da Vinci

CHAPTER 6

CONCLUSIONS

A model of a bandsaw, subjected to lateral cutting forces on the teeth and restrained by the sawn surfaces of the wood, has been developed. The blade model includes the effects of blade dimensions, bandmill strain, in-plane stresses, tooth (gullet) depth, tooth bending stiffness, blade speed, strain system parameters, and the span between the guides.

The spectrum of the blade deflection during cutting was experimentally found to be inversely proportional to the frequency. From this observation it was argued that lateral cutting forces also have this character. Since the blade motion is dominated by motions at frequencies much lower that the natural frequencies of the blade, it is possible to ignore the effects of the inertia of the blade when calculating the blade deflection during cutting.

The cutting simulation model was used to determine how blade parameters, the cutting forces and the clearance gap affect blade deflection. These simulations showed that any change in the blade that increased the tooth-tip stiffness reduced the deflection amplitude during a cut. A sensitivity study showed that plate thickness, bandmill strain and the guide span had the greatest

effect on tooth-tip stiffness.

Three equivalent tooth-tip stiffnesses, K_O , Q_O, and K_{eq}, define how the cutting deviation and the mean deflection of the blade are affected by blade design, depth of cut, and the location of the cutting zone. The combination of blade parameters used to get these stiffnesses does not have a significant effect on cutting deviation.

The simulations conducted show that reducing the clearance gap hinders the ability of the blade to change direction in the cut. This effect is caused completely by the increased amount of contact between the blade and the sawn surfaces as the clearance gap is reduced. The closer the contact occurs to the front of the blade, the more the cut path is affected. Consequently, reducing the clearance gap amplifies the amplitude of blade deflection and prolongs the length of the recovery stage. Contact, therefore, can have a significantly negative effect on blade behavior during cutting.

Saw behavior can be separated into two broad cases. The first occurs when there is little or no contact between the blade and the sawn surfaces. In this case the blade deflection is determined solely by the magnitude of the cutting forces and the tooth-tip stiffness. The second case occurs when the effects of the contact forces have a significant effect. It was found that the degree of contact is governed by a dimensionless variable, g/S_O.

The cutting deviation can be nondimensionalized as S_T/S_O. A relationship was found between g/S_O and S_T/S_O. This relationship defines how the design and operating parameters and the cutting forces affect the sawing deviation. The relationship between g/S_O and S_T/S_O predicts the existance of a critical side clearance below which cutting deviation increases rapidly.

FUTURE WORK

1) Quantify, in statistical form, the factors that affect the lateral cutting forces. The definitions of S_f, S_m, S_e and $\bar{f}$ provide a rationale for measuring the lateral cutting force. There are five issues to be resolved:

a) the variation of the lateral force along the length of the cut;

b) the variation of the lateral force through the depth of the cut;

c) the effects of wood properties such as density, moisture content, number of knots, and grain direction (and how they can be monitored);

d) the effect of bite per tooth; and

e) the effect of tooth geometry and tooth sharpness.

The use of functions having a 1/f characteristic to model how the lateral force varies along the length of the cut appears to be very promising. A possible experiment is use with a blade with a very large side clearance so that contact does not occur. The shape of the sawn surface can be measured, from which S_0 can be calculated. The variation of the cutting force, S_f, is proportional to S_0. The facts that Q_0 is large compared to K_0 and that the low frequency component dominates the character of the lateral cutting force means that the spatial resolution for measuring the lateral cutting forces can be quite coarse.

2) In the model, the lateral cutting force does not change if the tooth deflects, which is not the case in practice. The change in the lateral cutting force, F, with deflected position, x_T, can be accounted for in the current model by defining a process stiffness $k_p = \partial F/\partial x_T$. Springs of this stiffness can be attached to the tooth-tips in the model. The flexibility matrix can be appropriately modified to account for these springs. The contact algorithm and other aspects of the simulation model do not need to be changed.

3) Determine how the clearance gap is affected by the side clearance, bite, sawdust spillage (gullet shape, depth of cut), springback, and tooth marks. It is expected that the clearance gap will vary along the length and through the depth of the cut.

4) Develop a device for measuring the effective stiffnesses of the blade, or some other measure of blade stiffness that quantifies how well the blade is prepared. A consequence of Q_0 being larger than K_0 means that K_0 has the most influence on blade behavior. Hence, K_0 should be used as a quality control parameter for blade preparation.

5) Determine how much the feed system allows or causes the wood to move during sawing. This would include the effect of pinching caused by the release of residual stresses in the wood.

6) The model does not consider blade heating, which is commonly assumed to be the cause of poor sawing accuracy, yet it does predict the critical side clearance phenomenon. Furthermore, the common assumption of the Gullet Feed Index (GFI) theory is that heat is generated when the sawdust spills from the gullets. The results of this work indicate that the loss in clearance gap that occurs when sawdust is spilled could also be the cause of the poor cutting accuracy. There is some doubt, therefore, whether heat causes sawing problems or heat is generated because of the contact that occurs when blade deflections are large. It is important, therefore, to determine how much blade heating occurs and how much it affects blade stiffness. The rigidity of the feed system and the amount of sawdust packing are expected to have the major influences.

7) Determine how blade stiffness can be increased without causing cracking or reducing the reliability of the blade.

8) Determine the relationship between board thickness variation, σ_T, and the deviation of blade deflection, S_T. Board thickness variation is more relevant to the process and easy to measure,

whereas saw deviation better describes saw behavior.

LIST OF REFERENCES

Axelsson, B., Grundberg, S.A., and Gronlund, J.A., 1991 "The Use of Gray Scale Images when Evaluating Disturbances in Cutting Force Due to Changes in Wood Structure and Tool Shape," Holz als Roh- und Werkstoff, Vol. 49, No.12, pp. 491-494.

Alexandru, S., 1967. "Automatic Regulation of the Feed Speed in Log Bandsaws in Relation to Blade Deviations in the Cutting Plane", Industria Lemnului, Vol. 18, No. 2, pp. 41-48.

Allen, F.E.,"Bandsaw Tooth and Gullet Design", unpublished engineering notes.

Allen, F.E., 1973a. "High-strain/Thin Kerf," Proceedings of the First North American sawmill Clinic, Portland, Oregon.

Allen, F.E., 1973b. "Quality Control in the Timber Industry", Australian Forest Industries Journal, (September).

Alspaugh, D.W., 1967. "Torsional Vibration of a Moving Band," Journal of the Franklin Institute, Vol. 283, No. 4, pp. 328-338.

Breznjsk, M. and Moen, K., 1972. On the Lateral Movement of the Bandsaw Blade Under Various Cutting Conditions, Norsk Treteknisk Insitutt, No. 46.

Brown, T.D. (Ed.), 1982. Quality Control in Lumber Manufacturing, Miller Freeman Publications, San Francisco.

Chardin, A., 1957. "L'Etude du Sciage par Photographie Ultra-rapide," Bois Forets des Tropiques, No. 51, pp. 40-51.

Foschi, R.O., and Porter, A.W., 1970. Lateral and Edge Stability of High-strain Band Saws, Canadian Western Forest Products Laboratory, Report VP-X-68, 17 pages.

Foschi, R.O., 1975. "The Light-Gap Technique as a Tool for Measuring Residual Stresses in Bandsaw Blades," Wood Science and Technology, Vol. 9, pp. 243-255.

Franz, N.C., 1957. An Analysis of the Wood Cutting Process, University of Michigan, Ann Arbor, Mich.

Fujii, Y., Hattori, N. and Noguchi, M. and Okumura, S., 1984. "The Force Acting on Band Saw and the Sawing Accuracy," Bulletin of the Kyoto University Forests, No. 56, (November), pp. 252-260.

Fujii, Y., Katayama, S. and Noguchi, M., 1986. "Measurement of Bandsaw Deformation with Moire Topography, "Journal of the Japanese Wood Research Society, Vol. 32, No. 7, pp. 498-504.

Gröndlund, A. and Karlsson, L., 1980. "Praktiska rad vid Bandsagning", STFI-Meddelande serie A 666. 41 pages.

Hutton, S.G. and Taylor, J., 1991. "Operating Stresses in Bandsaw Blades and their Effect on Fatigue Life," Forest Products Journal, Vol. 41, No. 7/8, pp. 12-20.

Johnston, J.S. and St. Laurent, A., 1975. "Tooth Side Clearance Requirements for High Precision Saws", Forest Products Journal, Vol. 25 No. 11, pp. 44-49.

Jones, D.S., 1965. "Gullet Cracking in Saws," Australian Timber Journal, (August), pp. 22-25.

Jones, D.S., 1968. "A Psychiatric Examination of a Bandsaw...(or Why a Bandsaw Cracks," Australian Timber Journal, (June), pp. 63-69.

Kirbach, E., 1985. A Procedure to Accurately Determine the Minimum Side Clearance for Wood Cutting Saws, FORINTEK Canada Corp., 11 pp.

Kirbach, E. and Stacey, M, 1986. Problems and Solutions in Maintenance and Operation of Band Saws, FORINTEK Canada Corp. 25 pages.

Koch, P. ,1964. Wood Machining Processes, Ronald Press, New York.

McKenzie, W.M., 1961u. Fundamental Analysis of the Wood-Cutting Process , Department of Wood Technology, School of Natural Resources, University of Michigan, Ann Arbor, 151 pp.

Mote, C.D., 1965. "Some Dynamic Characteristics of Band Saws", Forest Products Journal, Vol. 15, No. 1, pp. 37-41.

Mote, C.D., 1968. "Divergence Buckling of an Edge-loaded Axially Moving Band", J. Applied Mechanics, Vol. 33, pg. 463.

Mote, C.D. and Holoyen, S, 1975. "Confirmation of the Critical Speed Theory in Symmetric Circular Saws" ASME, J. of Engineering for Industry, Vol. 97(B), No. 3, pp. 1112-1118.

Okamoto, N. and Nakazawa, M., 1979. "Finite Element Incremental Contact Analysis with Various Frictional Conditions", International Journal for Numerical Methods Engineering, Vol. 14, pp. 337-357.

Pahlitzsch, G. and Putkammer, K., 1976. "Ermittlung der Steifhiet von Bandsageblattern", Holz als Roh- und Werkstoff, Vol. 31 , pp. 161-167.

Pahlitzsch, G. and Putkammer, K., 1974. "Beurteilungskriterien fur die Auslenkungen von Bandsageblattern", Holz als Roh- und Werkstoff, Part 1: Vol. 32 , pp. 52-57; Part 2: Vol. 32, pp. 295-302; Part 3: Vol. 34, pp. 413-426.

Pahlitzsch, G. and Putkammer,K., 1976. "Schittversuche beim Bandsagen", Holz als Roh- und Werkstoff, Part I: Vol. 34 , pp. 17-21, Part II: Vol. 34, pp. 17-21.

Peirgen, H-O, and Saupe, D. (Eds.), 1988. The Science of Fractal Images, Springer-Verlag, New York.

Porter, A.W., 1971. "Some Engineering Considerations of High-Strain Band Saws," Forest Products Journal, Vol. 21, No. 4, pp. 24-32.

Reineke, L.H., 1956. "Sawing Rates, Sawdust Chambering and Spillage", Forest Products Journal, Vol. 6 No. 9, pp. 348-354.

Soler, A.I., 1968. "Vibrations and Stability of a Moving Band," Journal of the Franklin Institute, Vol. 286, No. 4, pp. 295-307.

St. Laurent, A., 1970. "Effects of Sawtooth Edge Defects on Cutting Forces and Sawing Accuracy", Forest Products Journal, Vol. 20 No. 5, pp. 33-40.

St. Laurent, A., 1971. "Influence des noeuds sur les forces de coupe dans le sciage du bois", Canadian Journal of Forest Research, Vol. 1, pp. 43-56.

Szymani, R., 1985. "Wood Properties and Characteristics Which Are of Concern in Machining", Wood Machining News, March/April, pg. 2.

Taylor, J., 1985. "The Dynamics and Stresses of Bandsaw Blades," Master's thesis, Department of Mechanical Engineering, University of British Columbia, Vancouver, British Columbia, Canada.

Taylor, J. and Hutton, S.G., 1991. "A Numerical Examination of Bandsaw Blade Tooth Stiffness," FORINTEK Canada Report, 17 pages.

Tseng, J., 1980. "The Application of the Mixed Finite Element Method to the Elastic Contact Problem." Master's thesis, Department of Civil Engineering, University of British Columbia, Vancouver, British Columbia, Canada.

Ulsoy, A.G., 1979. Optimizing Saw Design and Operation - Vibration and Stability of Band Saw Blades: A Theoretical and Experimental Study, Technical Report 35.01.330, University of California Forest Products Laboratory, Richmond California, 117 pages.

Ulsoy, A.G., Mote, C.D., 1980. "Analysis of Bandsaw Vibration", Wood Science, Vol. 13, No. 1.

Ulsoy, A.G., Mote, C.D. and Szymani, R, 1978. "Principle Developments in Band Saw Vibration and Stability Research", Holz als Roh- und Werkstoff, Vol. 36, pp. 273-280.

Wang, K.D. and Mote, C.D., 1985. "Vibration Coupling Analysis of Bandsaw Systems", Proceedings of the 8th Wood Machining Seminar, Richmond, California, October 7-9, pg. 416.

APPENDIX A

Inertial and Gyroscopic Effects on Blade Behavior

The purpose of this appendix is to show that the inertial and gyroscopic effects are small compared to the effect of the blade stiffness for the range of excitation frequencies encountered during sawing.

During cutting the blade generally deflects to a bowed shape, similar to the lowest vibration mode. Assuming that the Galerkin shape function for the lowest lateral vibration mode is

$$\Psi(x,y) = \mathrm{Sin}(\pi x/L)$$

the terms in the matrices of the Galerkin formulation for the lowest vibration (n=1) mode are

$$M = \frac{\mu bL}{2} \qquad G = \frac{8\mu cb}{3}$$

$$K = \frac{DL}{2}\left(\left(\frac{\pi}{L}\right)^4 - \left(\kappa\mu bc^2 - \frac{T}{2}\left(\frac{\pi}{L}\right)^2\right)\right)$$

For typical values of the blade parameters

b = 10 inches	$\kappa = 0$
h = 0.065 inches	$\rho = 7.34(10^{-4})$ Lb-sec^2/in^4
L = 30 inches	$E = 30.0(10^6)$ psi
T = 15000 lbs.	$\nu = 0.3$
c = 2000 in/sec	

the sizes of the inertial force, $M\omega^2$, the gyroscopic force $G\omega$, and the stiffness, K, for various excitation frequencies are given in Table A-1.

Since the cutting motion is almost entirely below 5 Hz., the stiffness effect dominates the gyroscopic effect by more than an order of magnitude and the inertial effect by more than two orders of magnitude. This result is consistent with those of Taylor [1985], who measured the transfer function for a bandsaw at various speeds. His results, for a blade similar to that considered here, show that the transfer function is constant over the range of 0 to 30 Hz.

Table A-1. Inertial, gyroscopic and stiffness terms

Excitation Frequency (Hz)	Inertial $\frac{(\text{Lbs-sec}^2)}{\text{in}}$	Gyroscopic $\frac{(\text{Lbs-sec})}{\text{in}}$	Stiffness $\frac{(\text{Lbs})}{\text{in}}$
0	0.0	0.0	1234
1	0.3	16.0	1234
5	6.7	73.5	1234
10	27.0	146.9	1234
20	107.9	294.0	1234
30	243.0	441.0	1234
40	431.0	588.0	1234
50	674.0	735.0	1234
60	971.0	882.0	1234
66.1	1234.0	971.0	1234

APPENDIX B

VERIFICATION OF CALCULATION OF BLADE STIFFNESS AND NATURAL FREQUENCIES

COMPARISON TO MOTE'S UPPER AND LOWER BOUNDS FOR NATURAL FREQUENCY

Mote [1965] developed equations for the upper and lower bounds of the first lateral natural frequency of a bandsaw. The lower bound assumes the blade has no bending stiffness, and the upper bound is a solution of limited series Galerkin approximation.

For typical values of the blade parameters

$b = 10$ inches	$\kappa = 0$
$h = 0.065$ inches	$\rho = 7.34(10^{-4})$ Lb.-sec^2/in^4
$L = 30$ inches	$E = 30.0(10^6)$ psi
$T = 15000$ lbs.	$\nu = 0.3$
$c = 2000$ in/sec	

Mote's lower and upper bound frequencies are 59.0 Hz and 60.1 Hz., respectively. The computer program developed for this thesis calculated the natural frequency to be 59.7 Hz., which is between the bounds estimated by Mote. In addition, by setting Young's modulus, E, equal to zero in the program, which is Mote's condition for the lower bound, a frequency of 59.0 Hz was calculated.

BLADE STIFFNESS AND DEFLECTED SHAPE

In this section the model is tested for its ability to predict how a blade deflects in response to lateral loads. A system of weights, cords, pulleys and bars applied a lateral load to a precise point in the blade. The resulting deflections were measured with a dial gauge.

The dimensions and parameters for the blade were:

Blade thickness	0.049 inches	Wheel width	9 inches (crowned)
Blade width	9.47 inches	Tooth pitch	1.75 inches
Span	30 inches	Tooth depth	0.65 inches
Bandmill strain	13,840 lbs.	Tensioning	None
Blade overhang on the wheels: front		1/8 inches	
		back 5/16 inches	

Figure B-1 shows how the stiffness varied across the width of the blade at mid-span. The analytical prediction compares well with the actual stiffness. The most notable difference is the asymmetry of the experimental results. It is likely that this was caused by the crown, which had its highest point about one third of the wheel width from its front edge, thus causing the front portion of the blade to be slightly tighter than the back.

Figure B-2 shows how the blade deflects for a lateral load applied to the tooth-tip. The deflection is normalized to the tooth-tip deflection as is done in Figure 4-16. Again, the correlation between the analytical and experimental results is good, except that the front of the blade is resisting deflection more than the back.

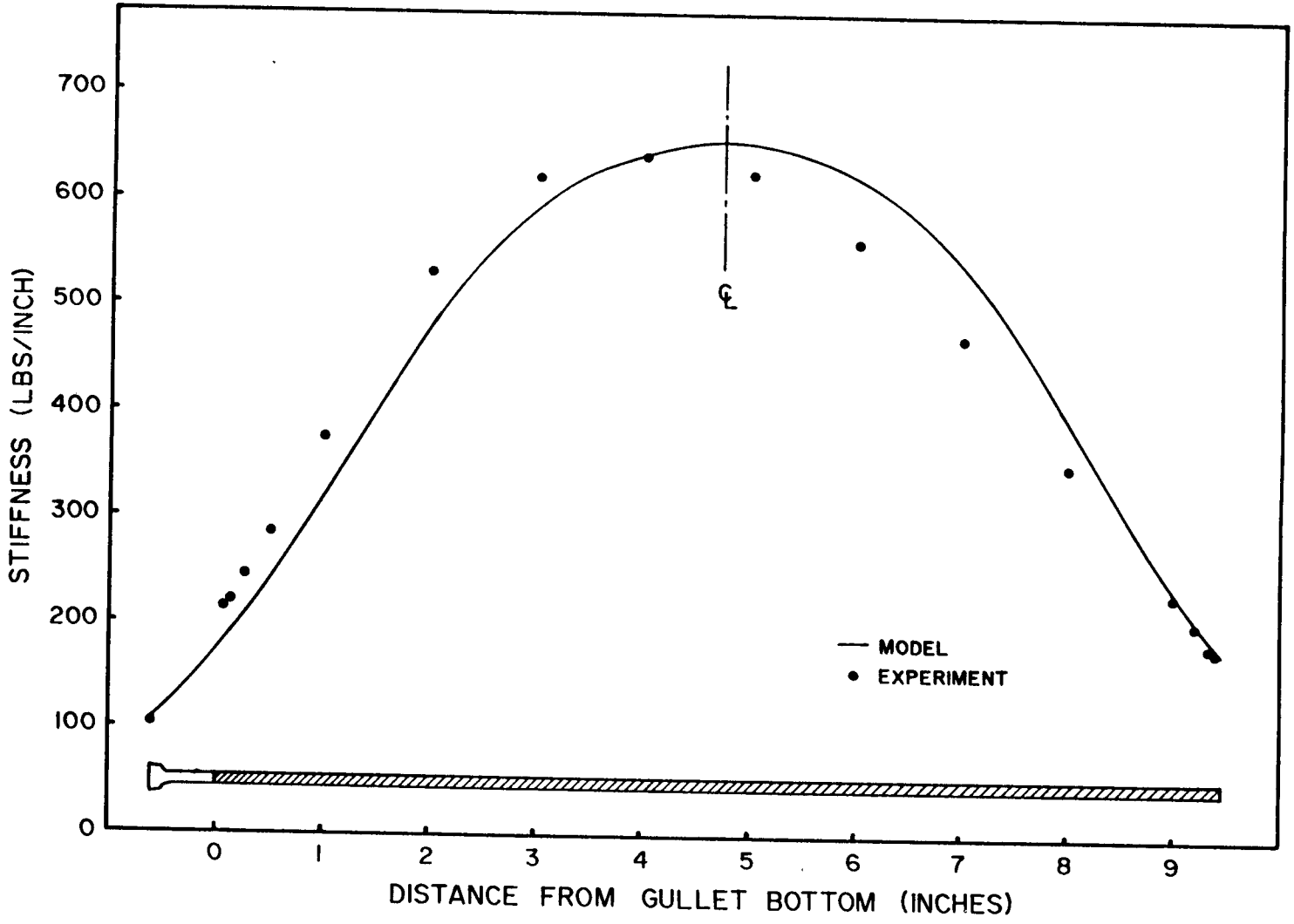

Figure B-1. Analytical and Experimental Blade Stiffness.

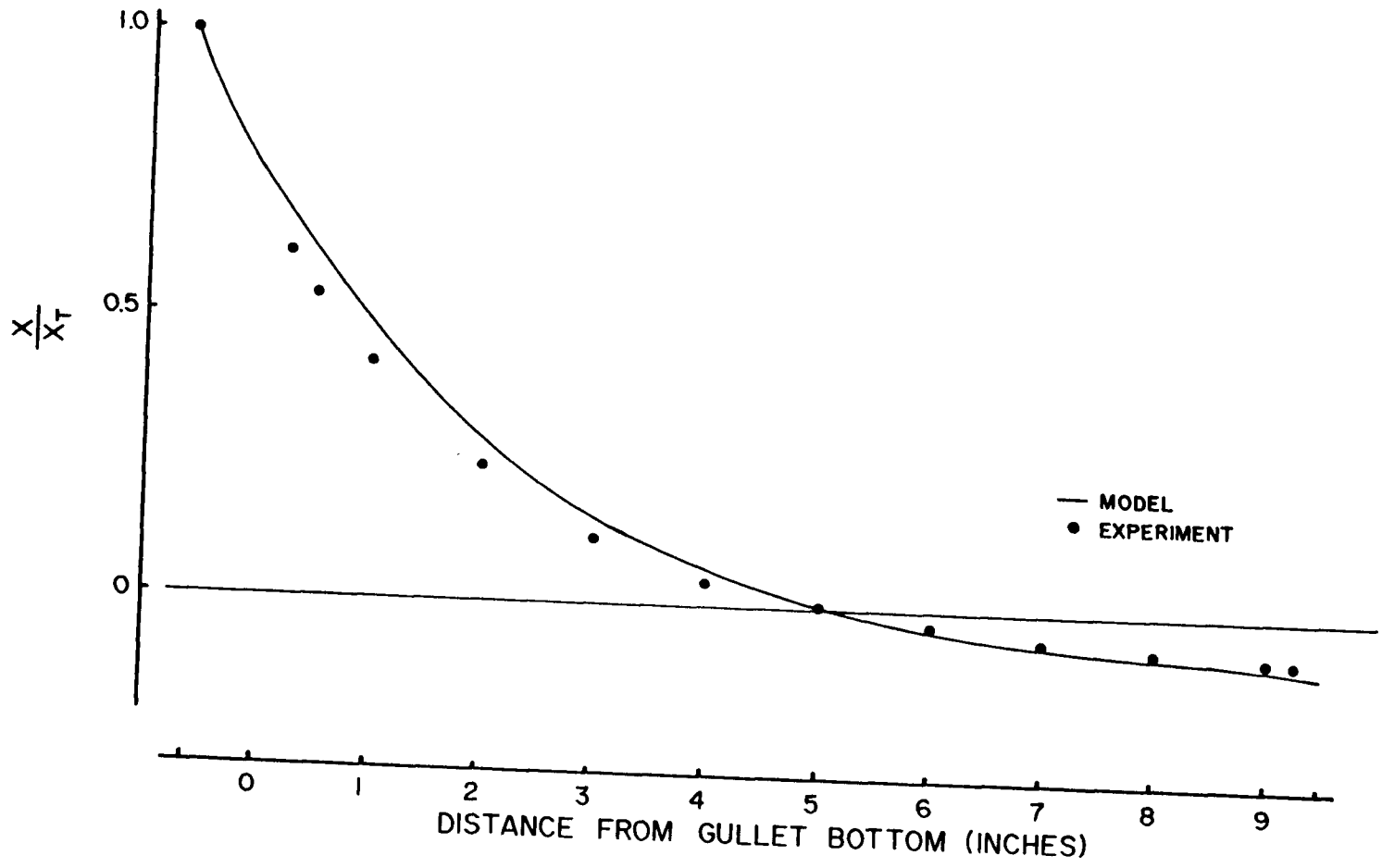

Figure B-2. Analytical and Experimental Normalized Blade Deflection.

APPENDIX C

THE CONTACT ALGORITHM

OVERVIEW

The purpose of this appendix is to describe the theory and structure of the algorithm developed to calculate the constrained deflection of the blade. During sawing, the loads on the blade are applied by both the external loads (i.e., the lateral cutting forces) and the constraints. The problem is to determine which portions of the blade come into contact with the sawn surfaces and the magnitude of the contact forces.

A common method for solving nonlinear problems, such as the contact problem, is to incrementally increase the load, starting from zero, until the full load is attained. However, it is likely that the lateral cutting force could be zero when the body of the blade is in contact with the sawn surfaces. Hence, the load increment method cannot be used. An alternative method is to apply the full external loads to the blade, initially assuming that the constraints are withdrawn, and then incrementally move the constraints towards the deflected blade until they are in their final position. In the case of sawing, the constraints are two parallel sawn surfaces which pinch the blade between them.

The principle of the contact solution algorithm is to determine the order in which the nodes come into contact or lose contact as the constraining surfaces are moved inward. A characteristic of nonlinear problems is that the final solution is dependent upon the order that the loads (or in this case, constraints) are applied to the structure. If the correct order of contact is not found then the algorithm could give an incorrect solution or cyclically fix and free a set of nodes without ever breaking out of the loop. A correct solution is guaranteed only if the order of contact is correct.

The algorithm determines the amount that the constraints should be incremented inward so that

only one node will just come into contact or just lose contact. Between these points where the status of a node (fixed or free) just changes, the system is piece-wise linear because the blade deformation is linear. Hence, between points where the status of a node does not change the changes in the deflections of the structure and in the magnitude of the contact forces will vary linearly with the movement of the constraints. The basis of the algorithm is to use linear interpolation to determine the size of the increment that causes a node to change status.

THE ALGORITHM

The first step is to determine which degrees of freedom of the blade, $\{x\}$, could come into contact with the surface and the location of the constraints, U_n and V_n, for each node. These steps are described in Chapter 3. The algorithm presented here is general in that an external force can be applied to any node on the blade whether or not that node is constrained. In this application, however, the only external forces are those applied to the tooth tips, which are assumed to have no constraints.

Equilibrium Conditions for the Blade

The discrete equilibrium equation is

$$[A]\{F\} = \{x\} \tag{C.1}$$

where [A] is the flexibility matrix of the blade. In the references [Okamoto and Nakazawa, 1979; Tseng, 1980], the contact problem is formulated as a mixed problem, meaning that both displacements and forces can be independent variables. Assume for now that the nodes that are in contact are known. The equilibrium equation can be rewritten as

$$\begin{bmatrix} A_{11} & A_{12} \\ A_{21} & A_{22} \end{bmatrix} \begin{Bmatrix} F_e \\ F_c \end{Bmatrix} = \begin{Bmatrix} X_f \\ X_c \end{Bmatrix} \tag{C.2}$$

where

X_f are the free (unconstrained) degrees of freedom

X_c are the fixed (constrained) degrees of freedom

F_e are the external loads acting on free degrees of freedom.

F_c are the net loads required to enforce the constraint that act on the fixed degrees of freedom.

The external loads $\{F_e\}$ are known. The displacements of the constrained degrees of freedom, $\{X_c\}$ are also known because these nodes are known to be in contact with the constraint. The vectors $\{F_c\}$ and $\{X_f\}$ are unknown, but can be solved by evaluating the following equations:

$$[A_{22}]\{F_c\} = \{X_c\} - [A_{21}]\{F_e\} \tag{C.3}$$

$$\{X_f\} = [A_{11}]\{F_e\} + [A_{12}]\{F_c\} \tag{C.4}$$

Since Equation C.3 is solved with a simultaneous equation routine, this formulation results in faster computer solutions if the number of degrees of freedom in contact is less than half of the total number that could come into contact. However, if most of the degrees of freedom come in contact, then the formulation

$$\begin{bmatrix} K_{11} & K_{12} \\ K_{21} & K_{22} \end{bmatrix} \begin{Bmatrix} X_f \\ X_c \end{Bmatrix} = \begin{Bmatrix} F_e \\ F_c \end{Bmatrix} \tag{C.5}$$

should be used because of the large number of times these equations must be solved. For the contact between the blade and the sawn surfaces, few nodes are expected to come into contact so the flexibility formulation was used.

Note that F_c is not the contact force at the node, but is the net force required to produce a deflection equal to the position of the constraint. The contact force is equal to F_c only if there is

no external load F_n acting on that node. If the contact force, φ, is taken to be positive in compression, then

$$\varphi = \begin{cases} F_n - F_c & \text{contact on the positive x side of body} \\ F_c - F_n & \text{contact on the negative x side of body} \\ 0 & \text{no contact} \end{cases} \tag{C.6}$$

Conditions Consistent with Contact

The conditions that define whether the deflections of the elastic body are consistent with the constraint are:

1) none of the constraints are exceeded

2) where contact occurs, the contact force is compressive (i.e., $\varphi > 0$)

These conditions must apply for each increment of the algorithm. When these conditions and Equation C.2 are satisfied for the imposed constraints, then the contact problem is solved.

Relationships for Piece-wise Linear Contact

In the following derivation the index n is the node number and i is the increment number. The amount that the constraints have been shifted outward is β. For the first increment (i=1), β_1 is set so that only one node is in contact. This situation is shown in Figure C-1.

The algorithm takes advantage of the property of piece-wise linear systems that changes in displacements are proportional to changes in forces. Therefore, when nodes that are fixed to a constraint are moved inward an amount $\Delta\beta$, then the changes in the contact forces at the fixed nodes, $\Delta\varphi$, and the changes in the deflections of the free nodes, Δx, are proportional to $\Delta\beta$.

The proportionality constant between Δx or $\Delta\varphi$ and $\Delta\beta$ must be determined for each node. This

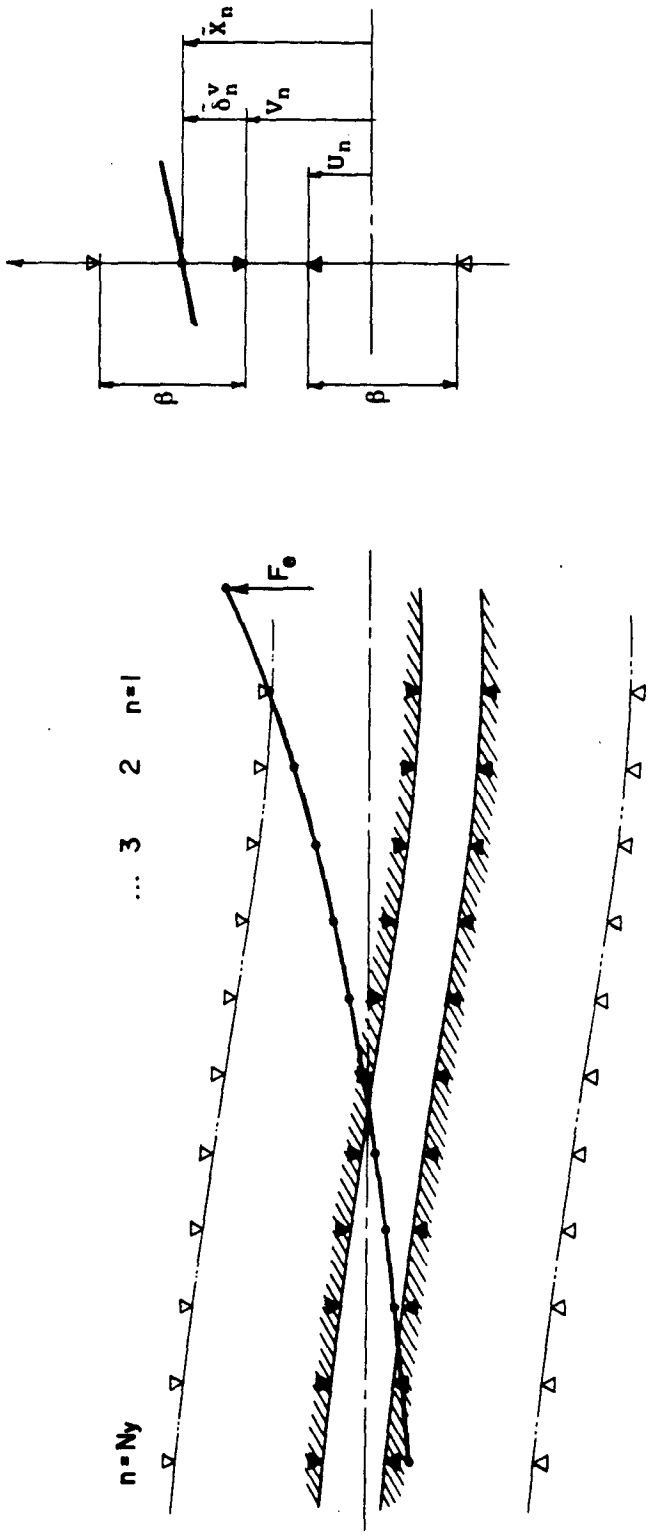

Figure C-1. Geometry of the Constraining Surfaces.

can be done by calculating $\{X_f\}$ and $\{\varphi\}$ for two values of β. Note that status of the nodes must be the same for both calculations. For this algorithm the two values of β are $\beta=\beta_i$ and $\beta=0$. To differentiate the two solutions the variables for $\beta=0$ have a '~' above them (i.e., $\tilde{x}$, $\tilde{\varphi}$, etc.), while the variables for $\beta=\beta_i$ have no mark (i.e., X, φ, etc.).

The amount by which a free node exceeds its constraint is termed the imbedment, which is defined as:

$$\begin{aligned} \delta^v_{ni} &= x_{ni} - v_n - \beta_i \\ \delta^u_{ni} &= u_n - x_{ni} - \beta_i \end{aligned} \tag{C.7}$$

$$\begin{aligned} \tilde{\delta}^v_{ni} &= \tilde{x}_{ni} - v_{ni} \\ \tilde{\delta}^u_{ni} &= u_n - \tilde{x}_{ni} \end{aligned} \tag{C.8}$$

In the following development δ_{ni} is the general variable for δ^u_{ni} and δ^v_{ni}; $\tilde{\delta}_{ni}$ is the general variable for $\tilde{\delta}^u_{ni}$ and $\tilde{\delta}^v_{ni}$.

Because the contact conditions at a node are determined by the imbedment at that node, it is convenient to formulate the algorithm in terms of the imbedments rather than the nodal displacements. This can be done because the imbedments are also proportional to $\Delta\beta$.

The values of δ and φ as a function of β can found by interpolating between their values for $\beta=0$ and $\beta=_i$. See Figure C-2(a) and (b). The relationships are:

$$\frac{\beta_{ni} - \beta}{(\delta_{ni} - \delta)} = \frac{\beta_i}{(\delta_{ni} - \tilde{\delta}_{ni})} \tag{C.9}$$

$$\frac{\beta_{ni} - \beta}{(\varphi_{ni} - \varphi)} = \frac{\beta_i}{(\varphi_{ni} - \tilde{\varphi}_{ni})} \tag{C.10}$$

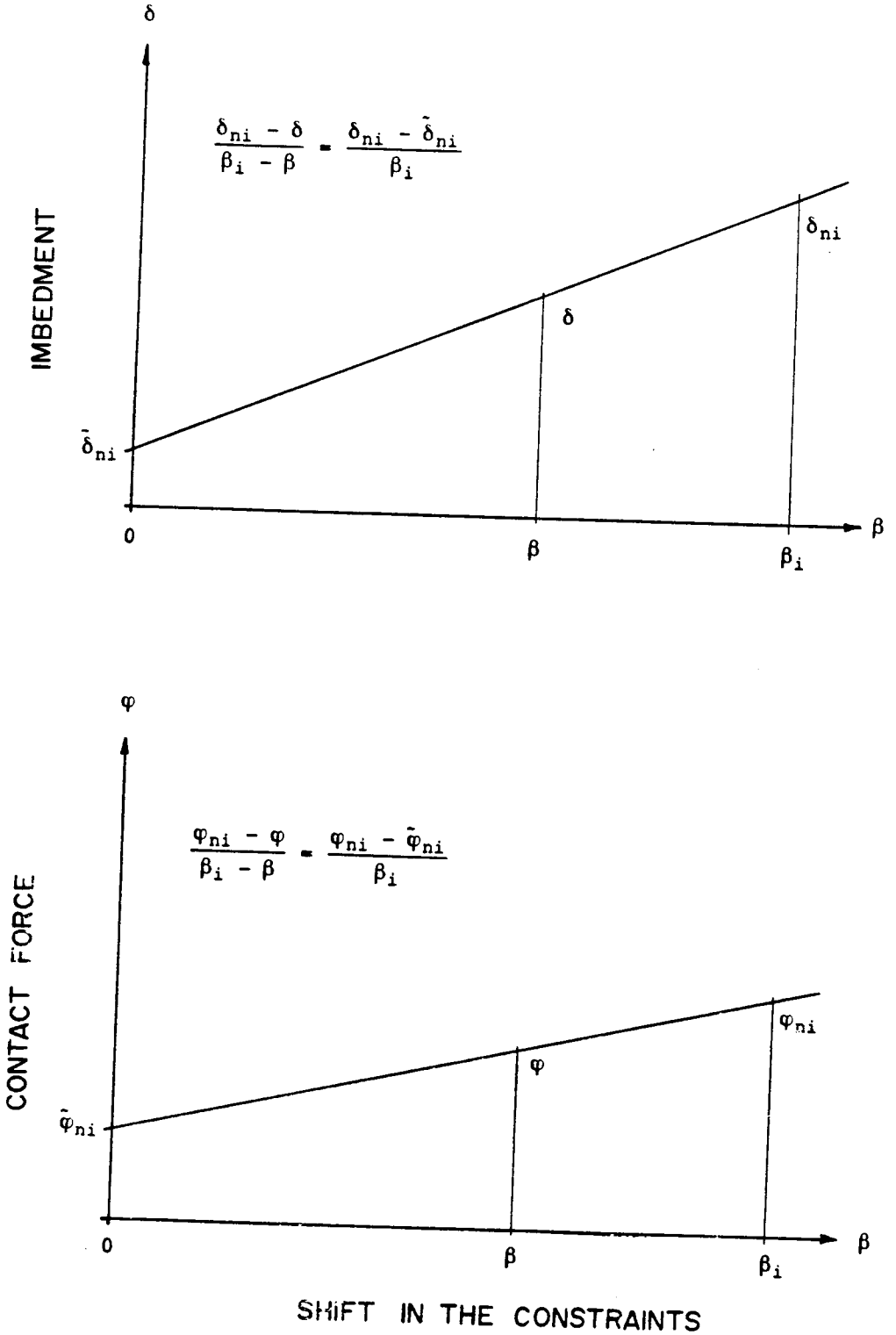

Figure C-2. Geometry of the Interpolation for the Contact Algorithm.

Determining the Size of the Increment

The size of the incremental change in β should be the smallest that causes the status of only one node to change. A change in status occurs when either δ or φ to becomes zero.

1) Free Nodes: When β is reduced so that an imbedment δ_{ni} goes from negative to positive, then that node is a candidate for being fixed. From Equation C.9 the reduction in β_i to have an imbedment, δ, of zero is

$$\Delta\beta_{ni} = \frac{\delta_{ni}\beta_i}{(\delta_{ni} - \tilde{\delta}_{ni})} \tag{C.11}$$

2) Fixed Nodes: When β_i is reduced, so that the contact force φ_{ni} of a fixed node goes from positive to negative, then that node is a candidate for being freed. From Equation C.10 the reduction in β to have a zero contact force, φ, is

$$\Delta\beta_{ni} = \frac{\varphi_{ni}\beta_i}{(\varphi_{ni} - \tilde{\varphi}_{ni})} \tag{C.12}$$

The node corresponding to the smallest value of $\Delta\beta_{ni}$ $(= \Delta\beta_{min})$ is then found. This node, and only this node, is fixed or freed as required.

The value of β for the next increment will be

$$\beta_{i+1} = \beta_i - \Delta\beta_{min} \tag{C.11}$$

The values of $\delta_{n,i+1}$ and $\varphi_{n,i+1}$ can be found by solving equations (C.3) and (C.4), but it is faster to use the interpolations of Equations C.9 and C.10. For the free nodes

$$\delta_{n,i+1} = \delta_{ni} - \frac{\Delta\beta_{min}}{\beta_i}(\tilde{\delta}_{ni} - \delta_{ni}) \tag{C.12}$$

and for the fixed nodes

$$\varphi_{n,i+1} = \varphi_{ni} - \frac{\Delta\beta_{min}}{\beta_i}(\varphi_{ni} - \tilde{\varphi}_{ni}) \tag{C.13}$$

The incrementing procedure given above is carried out until $\beta = 0$ and the contact conditions are consistent.

APPENDIX D

DERIVATION OF THE STATISTICAL REPRESENTATION OF THE CUTTING FORCES

Since the deflection caused by the mean cutting force dominates the deflection response of the teeth, it is convenient to separate the force distribution into two components: and mean force and the variant from the mean.

$$f_{it} = m_i + e_{it} \quad ; t = 1,2,..,N_T \quad ; i = 1,2,...,N_c \tag{D.1}$$

where f_{it} is the force on the t-th tooth at the i-th increment along the cut; m_i is the mean force; and e_{it} is the variant on the i-th tooth.

The deflection of the teeth[1] can be calculated, assuming no contact forces are present, by

$$\{X\} = [A]\{f\}$$

or (D.2)

$$x_{it} = \sum_{j=1}^{N_T} a_{jt} f_{it}$$

where A is the flexibility matrix for the teeth. Substituting Equation D.1 into Equation D.2 results in

$$x_{it} = m_i \sum_{j=1}^{N_T} a_{jt} + \sum_{j=1}^{N_T} a_{jt} e_{it} \tag{D.3}$$

$$= m_i c_t + \sum_{j=1}^{N_T} a_{jt} e_{it}$$

[1] In the following development, x_{it} is equivalent to the cut path S_{it} used in Chapter 3.

The values of c_t are the deflections of the teeth when there is a unit load acting on each tooth.

The cutting force f_{it} has a mean $\bar{f}$ and a standard deviation, S_f, defined as

$$\bar{f} = \sum_{i=1}^{N_c}\sum_{j=1}^{N_T} \frac{f_{ij}}{N_T N_c} \tag{D.4}$$

$$S_f^2 = \sum_{j=1}^{N_T}\sum_{i=1}^{N_c} \frac{\left(f_{ij} - \bar{f}\right)^2}{(N_T N_c - 1)} \tag{D.5}$$

Both of these values depend on tooth geometry, sharpness, wood species and characteristics. There are also variations in m_t and e_{it}, defined as

$$S_m^2 = \sum_{i=1}^{N_c} \frac{(m_i - \bar{f})^2}{(N_c - 1)} \tag{D.6}$$

$$S_e^2 = \sum_{j=1}^{N_T}\sum_{i=1}^{N_c} \frac{e_{it}^2}{(N_T N_c - 1)} \tag{D.7}$$

It can be shown that

$$S_f^2 = S_m^2 + S_e^2 \tag{D.8}$$

The mean deflection of the teeth is then

$$\bar{x} = \frac{\bar{f}}{N_T}\sum_{t=1}^{N_T} c_t = \frac{\bar{f}}{K_{eq}} \tag{D.9}$$

and the standard deviation of the tooth deflection is

$$S_o^2 = \frac{S_m^2}{N_T}\sum_{t=1}^{N_T} c_t^2 + \frac{S_e^2}{N_T}\sum_{j=1}^{N_T}\sum_{t=1}^{N_T} a_{jt}^2$$

$$= \frac{S_m^2}{K_o^2} + \frac{S_e^2}{Q_o^2} \tag{D.10}$$